9950-430

IDENTIFICATION AND ANALYSIS OF FACTORS AFFECTING THERMAL SHOCK RESISTANCE OF CERAMIC MATERIALS IN SOLAR RECEIVERS

Final Report

by

D. P. H. Hasselman
J. P. Singh
K. Satyamurthy

July 15, 1980

Contract No. 955629
Task Order No. RD-152

Department of Materials Engineering
Virginia Polytechnic Institute and State University
Blacksburg, Virginia, 24061

This work was performed for the Jet-Propulsion Laboratory, California Institute of Technology sponsored by the National Aeronautics and Space Administration under Contract NA57-100.

ABSTRACT

An analysis was conducted of the possible modes of thermal stress failure of brittle ceramics for potential use in point-focussing solar receivers. The pertinent material properties which control thermal stress resistance were identified for conditions of steady-state and transient heat flow, convective and radiative heat transfer, thermal buckling and thermal fatigue as well as catastrophic crack propagation. Selection rules for materials with optimum thermal stress resistance for a particular thermal environment were identified. Recommendations for materials for particular components were made. The general requirements for a thermal shock testing program quantitatively meaningful for point-focussing solar receivers were outlined. Recommendations for follow-on theoretical analyses were made.

TABLE OF CONTENTS

LIST OF TABLES

LIST OF FIGURES

IDENTIFICATION AND ANALYSIS OF FACTORS AFFECTING THERMAL SHOCK RESISTANCE OF CERAMIC MATERIALS IN SOLAR RECEIVERS

1. INTRODUCTION

1.1. General

Advances in energy-conversion technology require the improvement in conversion efficiency of existing systems or the development of technically and economically viable new systems. For energy conversion systems currently in use, such as steam-electric power plants, internal combustion and turbine engines, the conversion efficiencies, at least in principle, can be improved simply by increasing their temperature of operation. Unfortunately, such an approach is not practical at this time. This is because of the lack of availability of suitable materials of construction which can render satisfactory service at high temperatures over the time periods required for economic operation with minimum down-time. The successful development of new energy conversion systems such as MHD, nuclear fusion, etc., to large extent if not completely, will depend on whether appropriate materials of construction for critical components are available or can be developed.

Solar energy represents an attractive alternative among the many new sources for energy under consideration at this time, in view of its near unlimited supply. However, for solar energy systems too, the availability of suitable materials of construction will be a major factor which will decide their technical and economic feasibility. Even for solar receivers which operate at relatively low temperatures, such as hot water systems, the durability and reliability of available materials of construction still need to be established for reliable estimates of technical and economic feasibility of such systems.

For solar receivers which operate at much higher temperatures, such as steam-electric or hot air-electric system, potential problems to be encountered with materials are expected to be quite severe. For acceptable conversion efficiencies, such systems may have to operate at temperatures well in excess of 1000°C. At these temperature levels very few, if any, polymeric or metallic materials will be available to provide satisfactory trouble-free service without frequent replacement. Ceramics, for this reason, are the logical (and only) choice of materials of construction.

Ceramic materials have many favorable properties for high-temperature solar receivers such as high melting point, excellent resistance to creep deformation and high resistance to corrosion and erosion. Unfortunately, ceramics, in spite of these favorable properties, also exhibit certain undesirable characteristics which dictate extreme care in their use. These unfavorable properties include a high degree of brittleness, low to moderate tensile strength and low impact resistance. Due to the brittleness and unfavorable combination of other physical properties, ceramic materials also are highly susceptible to fracture when subjected to constrained thermal expansions due to non-linear temperature distributions or rapid temperature variations, commonly referred to as "thermal shock". Such "thermal shock" can result in thermal stresses of magnitude well in excess of the failure stress of a ceramic. Under these conditions fracture can occur in a catastrophic manner, rendering the structure or component completely incapable of providing continued satisfactory service. This aspect of ceramic materials is particularly critical for high-temperature solar receivers which even under normal operating conditions will be subjected to rapid temperature variations. This, for instance, will occur under weather conditions consisting of intermittent cloud

covers, which can cause rapid heating and cooling due to large variations in the intensity of the incident radiant heat flux.

It is the view of the writers of this report that the feasibility of solar receivers made of ceramic materials will critically depend on their ability to withstand the thermal stresses resulting from rapid temperature variation. The possibility of catastrophic failure due to such thermal stresses should be considered in the very preliminary design stages of such solar receivers. Furthermore, materials of construction should be chosen very carefully to reduce the probability of thermal stress failure to an absolute minimum. In order to do so, it is imperative that the factors which affect the thermal stress fracture behavior of brittle ceramics are well understood.

The objective of the present study is to review the current understanding of the factors which govern the failure of brittle ceramics under conditions which generate thermal stresses of high magnitude. This review will provide a general framework for the selection of ceramic materials for solar-energy receivers and associated components with maximum resistance to thermal stress failure.

1.2. Scope of Study

In order to render the results of this study as generally useful as possible, the discussion to be presented will not be design-specific. Nevertheless, a few recommendations will be made appropriate to point-focus solar receivers for which a number of general design features have been developed and for which a number of specific designs are underway. No attempt will be made to develop the basis for thermo-elastic theory, the

principles of heat transfer or the various aspects of materials science and engineering. For these, a vast literature is available.

The role of the various material properties and specifically their interaction as currently available from the literature, will receive major emphasis. Recommendations for further analytical work, material development and physical property measurement appropriate to the thermal stress failure in solar receivers will be made. A number of general design and operating principles which will reduce the incidence of thermal stress fracture of individual components, will be outlined.

For convenience to the reader, the technical discussion of this report will be subdivided into individual sections as follows:

a. General discussion of the sequence of events and relevent material properties associated with thermal stress fracture.

b. Discussion of general approach to analysis of thermal stresses and development of selection rules for materials with optimum thermal stress resistance. The general principles of different philosophies for the selection of material with high thermal stress or shock resistance will be included here.

c. Discussion of role of material properties and other variables for specific heat transfer conditions including steady-state and transient heat transfer for structures or components for which thermal stress failure cannot be allowed.

d. Discussion of general principles of catastrophic crack propagation in brittle ceramics subjected to severe thermal shock and development of selection rules for materials which will undergo a minimum extent of crack propagation.

e. Summary of thermal stress resistance "figures-of-merit" and comments on individual property data.

f. Discussion of geometric and dimensional variables, including spatially non-uniform heating or cooling.

g. Discussion and recommendation for specific materials for solar receivers.

h. Recommendations for thermal shock testing of candidate ceramics materials for solar receivers.

i. Materials-related comments and recommendations for system design and operation.

j. Recommendations for further theoretical work to aid material selection for solar receivers.

For the purpose of efficiency of the reader, the discussion will emphasize the highlights obtained from the literature and minimize the theoretical and experimental details. Whenever appropriate, reprints of the particular literature studies cited, will be included in the report in the form of appendices.

2. MATERIAL PROPERTIES AND OTHER VARIABLES WHICH AFFECT THE THERMAL STRESS FAILURE OF BRITTLE CERAMICS: GENERAL OUTLINE.

In order to establish a framework for the selection of ceramic materials for solar receivers with optimum thermal shock resistance, a general discussion of the material properties and external variables which affect the thermal stress failure of such materials will be presented first. Most conveniently, this can be done by considering thermal stress failure to be result of four independent successive phenomena or stages as follows:

a. generation of temperature distributions.

b. generation of thermal stresses as the result of temperature distributions.

c. the onset of failure due to thermal stresses of high magnitude.

d. the formation of cracks as the result of failure and their effect on subsequent performance.

Each of these stages is controlled by a unique set of material properties and other variables, to be discussed individually in the following section.

2.1. Variables Which Control Temperature Distributions

Temperature changes in a structure are the result of heat conduction through its surface (either inward or outward) or as the result of internal heat generation. Heat transfer by conduction within the solid is controlled by thermal conductivity and diffusivity of the material. Such heat transfer can occur in a steady-state or transient mode. Heat can be transported to or from the surface by convection or radiation or a combination of both.

A large body of literature is available on convective and radiative heat transfer. Convective heat transfer generally is a function of the

properties of the medium surrounding the structure, the geometry of the structure as well as the temperature difference between the structure and the medium. Convective heat transfer, generally, is not a function of the properties of the material being heated, with the possible exception of heat transfer involving nucleate boiling which may be a function of the surface roughness.

Radiative heat transfer on the other hand, in addition to geometric effects, is a function of the optical properties of the material including the reflectivity, absorptivity, emissivity and the absorption coefficient for transmitted radiation. It is important to note that these optical properties are a function of wave-length, temperature, surface condition (finish) and angle of incidence for the incident radiation.

2.2. Materials Properties Which Control the Magnitude of Thermal Stress

From a known temperature distribution, the resulting thermal stresses can be calculated. It is important to point out that such a calculation requires only the distribution of the temperature, without knowing specifically how this temperature distribution was achieved.

A distribution of temperature causes an equivalent distribution of thermal strains directly proportional to the coefficient of thermal expansion. Thermal stresses arise when the thermal expansions cannot occur freely as the result of external or internal constraints. For linearly elastic solids, the thermal stresses are directly proportional to Young's modulus of elasticity, and frequently are a function of Poisson's ratio as well.

Plastic deformation such as by dislocation mechanisms in metallic materials can help reduce the magnitude of the thermal stresses appreciably.

However, plasticity is generally very limited in ceramic materials for solar receivers at normal operating temperatures. At sufficiently high temperatures, however, thermal stress relaxation in ceramics can occur by diffusional creep. For creep rates directly proportional to the stress (i.e., linear creep), the rate of thermal stress relaxation can be described by a stress-independent "viscosity" term. It appears appropriate at this time to point out that thermal stress relaxation by creep or any other type of non-linear deformation may not be desirable. On bringing the structure to thermal equilibrium at ambient temperature, such thermal stress relaxation could result in levels of residual stress of sufficient magnitude that catastrophic failure could occur.

2.3. Materials Properties Which Control Failure Under the Influence of Thermal Stresses

For an assessment of the properties which affect thermal stress failure, three failure modes must be considered.

a. Rapid fracture

b. Fatigue failure

c. Thermal buckling

Rapid fracture occurs when the thermal stresses exceed the failure stress of the material. In brittle materials, such failure usually occurs in tension, because of the high ratio of compressive to tensile strength. Nevertheless, failure under the influence of compressive stresses cannot be ruled out, especially those due to external constraints. Brittle materials generally fail from pre-existing cracks. A knowledge of the crack size and geometry as well as the appropriate thermal stress intensity factor, will permit an assessment of rapid failure in terms of the critical

stress intensity factors for the materials under consideration. For tensile or shear failure (or their combinations), this will involve the critical stress intensity factors, K_{IC}, K_{IIC} and K_{IIIC} for mode I, mode II, and mode III of the crack opening displacement, respectively.

Fatigue failure occurs as the result of sub-critical crack growth at steady-state or cyclic stress levels below those required for fast fracture. At temperatures near room temperature, such crack growth frequently occurs due to a "stress-corrosion" reaction, or is accelerated by the presence of surface-active molecules. In particular, water appears to be very effective in this respect. At high temperatures where the rate of the surface, grain boundary or bulk diffusion becomes appreciable, subcritical crack growth can occur by diffusional phenomena.

In principle, as discussed in detail in a subsequent section, the fatigue-life in terms of time or cycles to failure can be calculated if data on the kinetics of subcritical crack growth are available. A common expression (among many others) to describe the rate of crack growth, V is given by:

$$V = AK_I^n \exp(-Q/RT) \qquad (2.3.1)$$

where A and n are numerical constants, K_I is the stress intensity factor and Q is the activation energy for the process reponsible for the crack growth. Therefore, calculations of fatigue life for a given material require values of A, n and Q.

Thermal buckling, to be described in further detail later, also represents a failure mechanism which should be considered in the design of ceramic solar receivers. Thermal buckling occurs as the result of the mechanical instability of relatively slender structures which are prevented

from expanding against rigid constraints or cooler parts of the structure. Thermal buckling can result in major bending deformations of the structures, which depending on the conditions of constraint can serve as a mechanism of thermal stress relief. On the other hand, the bending stresses induced by such deformations could result in a tensile fracture. As will be shown later, thermal buckling and subsequent possible fracture depends on the coefficient of thermal expansion, Young's modulus, tensile strength or critical stress intensity factor and in some cases on the thermal conductivity as well.

2.4. Material Properties Which Control Crack Propagation Following the Fracture of Brittle Ceramics by Thermal Stresses

Crack propagation following the onset of fracture in brittle ceramics under the influence of thermal stresses can be quite extensive. For this reason, materials selection and design for high-temperature structures is based on promoting rapid crack arrest, rather than avoiding thermal stress fracture altogether, a goal not easily achieved. A design philosophy based on crack arrest requires data on the behavior of crack propagation.

The extent of dynamic (unstable) crack propagation, commonly encountered in high-strength ceramics is governed by the elastic energy at fracture, the energy expended in propagating a crack per unit area of crack surface, γ_f, as well as the total number of cracks participating in the fracture process. The elastic energy at fracture is governed by the Young's modulus, Poisson's ratio, and the failure stress such as the tensile strength.

Stable crack propagation in thermal stress fields is controlled by the coefficient of thermal expansion, Young's modulus, Poisson's ratio

as well as the fracture surface energy.

At this point it is important to mention that the fracture surface energy can also be derived from the critical stress intensity factor, K_{IC}. However, it should be noted that the values of γ_f or K_{IC} for the initiation of fracture may not be identical to the corresponding values observed for the crack propagation or arrest.

Finally, the inertial effects of crack propagation will be assumed to be small for the thermal stress fracture of solar receivers and hence the sound velocity will not be considered as a design parameter.

2.5. Summary

For convenience of the reader, the total number of all material properties referred to in the above discussions are listed in Table I.

TABLE I. Material Properties which Control Thermal Stress Resistance of Brittle Ceramics

Symbol	Property
α	coefficient of linear thermal expansion
A	constant in equation for sub-critical crack growth, $V = AK_I^n \exp(-Q/RT)$
ε	emissivity
E	Young's modulus
η	viscosity
γ_f	fracture surface energy
K	thermal conductivity
K_{IC}	critical stress intensity factor
κ	thermal diffusivity
λ_o	wave-length above which dielectric material is opaque
μ	absorption coefficient
n	constant in $V = AK_I^n \exp(-Q/RT)$
ν	Poisson's ratio
Q	activation energy for sub-critical crack growth
r	reflectivity
S_c	compressive strength
S_t	tensile strength

3. DISCUSSION OF GENERAL APPROACH TO DEVELOPMENT OF SELECTION RULES FOR CERAMIC MATERIALS WITH OPTIMUM THERMAL STRESS RESISTANCE

In order to establish the basic framework for the development of selection rules for ceramics with optimum thermal stress resistance, a discussion is in order to the basic definition of how such thermal stress resistance is defined. For this purpose, it is important to recognize that in the technical community engaged in high-temperature technology, two radically different philosophies have evolved for the designation of thermal stress (or shock) resistance. As will be demonstrated in subsequent sections of this report, failure to appreciate the basic difference in philosophies could lead to major errors in the selection of the appropriate materials, which in turn could lead to spectacular catastrophic failures.

3.1. Material Selection Based on the Avoidance of Thermal Stress Fracture.

The first of the two philosophies referred to above is based on the concept that the thermal stresses be kept sufficiently low that thermal stress failure is not initiated. In other words, the magnitude of thermal stress (or stress intensity factor) is always less than the failure stress (or critical stress intensity factor) of the component or structure. Of course, this philosophy is not unique to high-temperature technology and is universally accepted in the fields of mechanical, civil and other engineering involved in structural design.

For brittle ceramics, this design philosophy is appropriate (if not essential) to structures or components for which the performance would be adversely effected by the formation of cracks. This would be so particularly

for load-bearing structures subjected to tensile or bending stresses such as turbine blades. Also, this philosophy would apply to such items required to maintain atmosphere or pressure control such as automotive spark-plugs, heat exchangers, seals, etc.

Thermal stress resistance of the materials, from which such components are made is defined in terms of the maximum temperature difference, the maximum radiant heat flux, the maximum rate of heating and other similar criteria such that the maximum thermal stress does not exceed the design strength of the material at any instant during the time period over which the material is subjected to thermal stress.

The first step in developing the selection rules for ceramic material with optimum thermal stress resistance as defined by this philosophy, is to obtain information on the temperature distribution for a given thermal environment. This information can be obtained theoretically for the known heating/cooling conditions or can be obtained experimentally. In this respect, it should be noted that particularly for complex geometries, calculations of temperature distributions in a structure from basic principles of heat transfer still can be rather uncertain. Spatially non-uniform heating and cooling and mixed radiative and convective heat transfer introduce further complexities. The reliability of calculated temperature distribution is expected to be no better than the assumptions made. Also, any uncertainties in the temperature distributions will be reflected in the calculated thermal stresses. For this reason, it is strongly recommended that any proto-type solar receiver be instrumented as completely as practically possible to obtain experimental data on the temperature distribution. These data can constitute a more reliable basis for the evaluation of the thermal stresses than calculated temperature

distributions based on simplified assumptions. An additional benefit in obtaining experimental data for the temperature is that a comparison can be made with the calculated data for the validity of the original assumptions on heat transfer conditions. The resulting feed-back will be a major value in the assessment and interpretation of possible thermal stress failures in solar receivers.

The next step is to evaluate the thermal stresses from the temperature distributions. This can be done by analytical or numerical methods. Analytical methods have the disadvantage that they are limited to relatively simple geometries, spatially uniform heat transfer and material properties which are independent of temperature. A major advantage of the analytical method is that it results in analytical expressions for the thermal stresses in which the contributory role of the relevant material properties, heat transfer mechanisms, geometry, etc. are clearly defined.

Numerical methods, such as finite element analysis are more convenient to real-life structures of complex geometry, spatial non-uniform heat transfer and temperature dependent properties. The disadvantage of the numerical method is that it provides a numerical answer for the stresses with little or no direct information of the relative role of individual material properties and other variables which affect the magnitude of the thermal stresses. For this reason, numerical methods are less convenient for the derivation of general selection rules for materials with high thermal stress resistance. Of course, finite element analysis, for instance, is a highly valuable tool for the optimization of a given design. Since the primary purpose of this study is to identify and analyze the individual factors which affect thermal stress resistance, this report will emphasize selection rules obtained by the analytical approach.

The third step in deriving the selection rules is to define a failure criterion. For instance, the magnitude of thermal stress should not exceed some specified value of stress, such as the tensile strength. Or some minimum value of thermal fatigue-life or cycles may be defined. Other criteria may be appropriate to failure by thermal buckling.

The fourth step in obtaining selection rules for materials with high thermal stress resistance is to substitute the failure criterion into the appropriate equation for the thermal stresses. Rearrangement of this equation will result in expressions for the maximum rate of heating, temperature difference, incident radiant heat flux, thermal fatigue-life, etc., to which the structure and component can be subjected without incurring the risk of thermal stress failure. As will be demonstrated, these expressions clearly define the individual effects of the relevant material properties, geometry and dimensions which affect the thermal stress resistance. For a given thermal environment, geometry and defined failure criterion, these expressions will yield so-called thermal stress resistance "parameters" or "figures-of-merit" on the basis of which the optimum material can be selected. This report will review all such expressions which have appeared in the technical literature for a wide variety of thermal conditions and failure criteria. Since a change in geometry involves a change in the numerical value of the geometric constant, for purposes of efficiency, redundancy can be avoided in presenting the equation for a given thermal environment for a single geometry only. Further redundancy is avoided by presenting the equations, whenever appropriate, in terms of the maximum thermal stress value (such as the tensile strength) to which the material can be subjected. For materials with cracks of known size and geometry,

the equations can be expressed in terms of the critical stress intensity factor by simple substitution of the relationship between this latter quantity and the fracture stress.

3.2. Material Selection Based on Limited Crack Propagation

Frequently, in high-temperature structures, the magnitude of thermal stress can be so high that even in the materials with the highest thermal stress resistance, as defined in the previous section, failure cannot be avoided. This situation is common in such structures as various furnaces and crucibles in the metal working industry, various kilns, thermal storage systems, casting nozzles and similar applications. Under such conditions, material selection based on the avoidance of fracture as discussed previously, simply is not relevant. Instead, material selection and design is based on the philosophy that the extent of crack propagation which results from thermal stress failure is kept to a minimum. In this manner, the relevant material properties are affected as little as possible. Also, the material will retain its geometry and will continue to provide satisfactory service in spite of being in a partially fractured condition. This philosophy is applied almost exclusively to materials used in the "refractories" industry. The methods of testing of the thermal stress resistance of such materials also reflect this philosophy. Instead of measuring the maximum heat flux, rate of heating, etc., required for failure, as would be done to establish thermal stress resistance based on the avoidance of thermal fracture, refractories are tested in a different manner. Such testing consists of subjecting the material to a very severe thermal environment such as quenching with a high heat transfer coefficient followed by measuring the effect of the resulting failure on the properties or dimen-

sions of the material. For instance, a measure of thermal stress resistance may be based on the weight lost by the material per unit area due to the complete loss of fragments from the surface. Alternatively, the number of cycles may be measured required for propagation of a crack completely through the material. A favorite method is to measure the tensile (bend) strength retained by the material following the thermal shock. In terms of the latter test, the criterion for good thermal stress resistance is based on the maximum retention of strength.

The development of selection rules for high thermal stress resistance for limited crack propagation must be based on an analysis of crack propagation behavior in thermal stress fields. It should be noted that the theory of crack propagation under thermal stresses is relatively unexplored and is a fruitful area for future work. Nevertheless, for simple mechanical models, a number of selection rules have been developed to be presented in further detail later together with experimental evidence in support of these rules. As will be expected and demonstrated, the selection rules for the avoidance of thermal fracture differ significantly from those appropriate for material selection based on limited crack propagation.

4. DEVELOPMENT OF SELECTION RULES FOR BRITTLE CERAMICS WITH OPTIMUM THERMAL STRESS RESISTANCE

This section will concentrate on presenting an overview of the analytical results for the thermal stresses for a variety of heat transfer conditions and modes of failure. Appropriate selection rules for ceramics with maximum thermal stress resistance will be developed. Unless stated, the pertinent material properties will be assumed to be independent of temperature. Throughout the discussion, the material will be assumed to behave as a continuum. For grossly heterogeneous structures or composite materials, the results obtained may require modification. For instance, caution is advised with regard to selecting values of the fracture stress. Since in composite materials with thermal and elastic discontinuities, the thermal stress concentration factors are expected to differ from those under conditions of mechanical loading, the thermal stress may not necessarily be equal to the mechanical failure stress.

4.1. Steady-State Heat Flow or Isothermal Conditions

4.1.1. Flat plate. Absence of external constraints

The flat plate is located in the y,z-plane and $-a \leq x \leq a$ and is subjected to steady-state heat flow in the x-direction. The thermal conductivity is independent of temperature and position. This condition results in a linear temperature distribution of the form:

$$T = T_o + \nabla x \qquad (4.1.1.1)$$

where ∇ is the temperature gradient. The temperature difference, ΔT, across the plate in the x-direction becomes $\Delta T = 2a\nabla$.

For an unconstrained flat plate, the stresses can be computed from:

$$\sigma_{y,z} = \frac{\alpha E}{1-\nu}\left[-T + \frac{1}{2a}\int_{-a}^{a} T\,dx + \frac{3x}{2a^2}\int_{-a}^{a} Tx\,dx\right] \qquad (4.1.1.2)$$

Substitution of eq. 4.1.1.1 into eq. 4.1.1.2 results in:

$$\sigma_{y,z} = 0 \qquad (4.1.1.3)$$

As shown by Boley and Weiner (1960), this result can be shown to be generally valid for any geometry and temperature distribution which is linear in a rectangular coordinate system (even in three dimensions) as long as the body is free from external constaints.

At first sight, the above result may appear trivial. Nevertheless, it is critical to the understanding of how thermal stresses arise and how the magnitude of such stresses for any design configuration can be minimized. First of all, the result of eq. 4.1.1.3 shows that the existence of a temperature difference within a structure is not a sufficient condition for the existence of thermal stresses. The key-element for the development of thermal stresses is the existence of constraints, either external or internal, which prevent free thermal expansion. The stress-free condition of the above flat plate with linear temperature distribution results from the absence of external constraint so that the non-uniform thermal expansion can be accommodated by bending of the plate. For a linear-temperature gradient, the distribution of the thermal expansions are exactly equal to the displacements in the plane of the plate due to the bending. Under these conditions, the plate is free to deform to a uniform radius of curvature, R given by:

$$R = (\nabla\alpha)^{-1} \qquad (4.1.1.4)$$

If in the above plate under steady-state heat flow, the temperature distribution were non-linear as the result of a spatially or temperature dependent thermal conductivity, the stresses no longer will be zero. In general, in unconstrained materials the magnitude of thermal stress is a function of the non-linearity of the temperature distribution.

4.1.2. Flat plate. Constrained to prevent bending deformations

This flat plate has the identical boundary conditions as those in section 4.1.1, but with the additional constraint that bending deformations are prevented. The linear temperature distribution in this plate will result in a bending moment of such a magnitude that when applied on a free plate will result in a radius of curvature of opposite sign of the curvature of eq. 4.1.1.4. The maximum stress which result from this bending moment equals:

$$\sigma_{y,z} = 0.5\,\alpha E\Delta T/(1-\nu) \qquad (4.1.2.1)$$

The result of eq. 4.1.2.1 can be used to develop a selection rule for materials with optimum thermal stress resistance subjected to steady-state heat flow and constrained from deformation in bending. Brittle ceramics generally exhibit values of tensile strength which are some order of magnitude lower than the compressive strength. In the above plate constrained from bending, the magnitude of tensile stress equals the magnitide of compressive stress. For this reason, failure most likely is to occur in tension. The designer is interested in the maximum temperature difference (ΔT_{max}) or maximum heat flux (q_{max}) to which the constrained flat plate can be subjected. An upper limit on ΔT_{max} or q_{max} can be obtained by setting the value of the stress in eq. 4.1.2.1 equal to the tensile strength, which

upon rearrangement yields:

$$\Delta T_{max} = 2\, S_t(1-\nu)/\alpha E \qquad (4.1.2.2)$$

Note that ΔT_{max} is independent of the thickness of the plate. This effect arises because a thicker plate would require a smaller value of temperature gradient ∇ (and a corresponding smaller value of induced curvature in the unconstrained form) to achieve a given value of ΔT.

An expression for the maximum heat flux (per unit area), q_{max}, can be obtained by noting that the heat flux can be related to ΔT by:

$$q = K\Delta T/2a \qquad (4.1.2.3)$$

where K is the thermal conductivity.

Substitution of eq. 4.1.2.3 into eq. 4.1.2.2 yields:

$$q_{max} = S_t(1-\nu)K/\alpha Ea \qquad (4.1.2.4)$$

Note that q_{max} is inversely proportional to the plate thickness.

It should also be noted that the derivation of the above expressions for ΔT_{max} and q_{max} assumes a safety factor equal to unity. This assumption will be made throughout the rest of this report. Clearly, because of statistical reasons and uncertainties in the degree of constraints imposed and many other design-related reasons, safety factors in excess of unity may well be preferred in order to insure high reliability.

Examination of eqs. 4.1.2.2 and 4.1.2.4 shows that the expressions for ΔT_{max} and q_{max} include a geometric constant (which depends on the degree of constraint), a size factor and a number of material properties. For a given constraint and plate size, the materials engineer or designer can achieve increases in ΔT_{max} or q_{max} only by optimization of the relevant material properties. Accordingly, ΔT_{max} can be optimized by maximizing

the "thermal stress resistance parameter" or "figure-of-merit" given by:

$$S_t(1-\nu)/\alpha E \qquad (4.1.2.5)$$

Similarly, q_{max} can be optimized by maximizing the parameter:

$$S_t(1-\nu)K/\alpha E \qquad (4.1.2.6)$$

4.1.3. Flat plate at uniform temperature, constrained from in-plane expansion

This flat plate located in the y,z-plane is at uniform temperature, but prevented from thermal expansion by rigid constraints at the edges of the plate. The plate will be considered to be sufficiently thick so that failure due to elastic instability (i.e. thermal buckling) is avoided. This mode of failure will be discussed later in this report.

The stresses in the plate due to a uniform temperature rise ΔT are:

$$\sigma_{y,z} = -\alpha E \Delta T/(1-\nu) \qquad (4.1.3.1)$$

For materials with a positive coefficient of thermal expansion, as is the case with most materials, the stresses in the plate are compressive. At sufficiently high values of ΔT, the material in the plate could fail in a compressive mode.

The maximum value of temperature difference, ΔT_{max}, by which the plate can be heated, without incurring compressive failure can be derived by setting the stress in eq. 4.1.3.1 equal to the compressive strength, S_c, which yields:

$$\Delta T_{max} = S_c(1-\nu)/\alpha E \qquad (4.1.3.2)$$

with a corresponding thermal stress resistance parameter identical to the above expression.

4.1.4. Composite structures

High levels of thermal stress even under isothermal conditions can be generated in composites and structures composed of strongly bonded dissimilar materials with mismatches in their coefficients of thermal expansion. Such a composite or structure will be stress-free only at the temperature at which the materials which constitute the composite or structure were fabricated or joined. A change from this value of temperature creates thermal stress, as each individual material is prevented from free expansion by the other material(s). Such stresses usually are undesirable, with the possible exception of the bi-metallic strip for which the resulting deformation can be used to advantage to the operation of a thermostat.

A simple expression can be given for the stresses which result from a mismatch in the coefficients of thermal expansion for a composite structure consisting of a thin coating on an underlying thick substrate. The magnitude of the stresses in the coating equals:

$$\sigma = E\Delta\alpha\Delta T/(1-\nu) \qquad (4.1.4.1)$$

where $\Delta\alpha$ is the difference in the coefficients of thermal expansion of the substrate and the coating and ΔT is the difference in temperature at which the coating was joined to the substrate and the new temperature to which the composite is heated or cooled. For other composite structures such as inclusions (Eshelby, 1961; Selsing, 1961) and concentric rings or cylinders, the expressions for the stresses which result from a mismatch in the coefficients of thermal expansion, are more complex and involve the elastic properties of all individual components or materials. Regardless of the geometry, however, the magnitude of these stresses is proportional

to the quantities $\Delta\alpha$ and ΔT. For this reason, the magnitude of these stresses can be kept to a minimum by choosing $\Delta\alpha$ and ΔT as low as possible.

Examination of eq. 4.1.4.1 shows that the stresses can be positive or negative depending on the sign of $\Delta\alpha$ and ΔT. For this reason, these stresses can be used to advantage by placing the weakest component in a state of compression by means of a judicious choice of the value (and sign) of $\Delta\alpha$.

4.1.5. Cencentric hollow cylinder. Radially outward heat flow

The concentric hollow cylinder infinite in extent with inner and outer radius of a and b, respectively, is subjected to radially outward heat flow. This results in a radial distribution of temperature with a temperature difference ΔT between the inner and outer surfaces. The cylinder is not constrained externally. Thermal stresses will arise from "internal" constrainst because the cooler and hotter sections in the cylinder prevent one another from free thermal expansion.

The maximum tensile stress in the cylinder occurs at the outside surface given by (Timoshenko and Goodier, 1951):

$$\sigma = \frac{\alpha E \Delta T}{(1-\nu)} \left[\frac{1 - \frac{2a^2}{b^2-a^2} \ln\left(\frac{b}{a}\right)}{2\ln(b/a)} \right] \qquad (4.1.5.1)$$

For a cylinder of finite length, the tensile stresses exhibit their maximum value at the end of the cylinder in the tangential direction and is given by the above equation 4.1.5.1 multiplied by the factor (Kent, 1931; Coble and Kingery, 1955):

$$\left[1 + \frac{(1-\nu^2)^{\frac{1}{2}}}{\sqrt{3}} - \nu \right] \qquad (4.1.5.2)$$

By setting the value of the tensile stress in eq. 4.1.5.1, equal to the tensile strength, an expression can be obtained for the maximum value of temperature difference, ΔT_{max} across the cylinder wall, which can be tolerated without tensile failure given by:

$$\Delta T_{max} = \frac{S_t(1-\nu)}{\alpha E}\left[2\ln\left(\frac{b}{a}\right)\right]\left[1 - \frac{2a^2}{b^2-a^2}\ln\left(\frac{b}{a}\right)\right]^{-1} \qquad (4.1.5.3)$$

By noting that the heat flux, q per unit length of the cylinder can be related to the temperature difference, ΔT across the wall, by:

$$q = 2\pi K\Delta T/\ln(b/a) \qquad (4.1.5.4)$$

Eq. 4.1.5.3 for ΔT_{max} can be rearranged to yield an expression for the maximum heat flux per unit length, q_{max}, to which the cylinder can be subjected given by:

$$q_{max} = \frac{4\pi S_t(1-\nu)K}{\alpha E}\left[1 - \frac{2a^2}{b^2-a^2}\ln\left(\frac{b}{a}\right)\right]^{-1} \qquad (4.1.5.5)$$

Expressions for ΔT_{max} and q_{max} for a cylinder of finite length can be obtained by dividing equations 4.1.5.3 and 4.1.5.5 for ΔT_{max} and q_{max} for the infinitely long cylinder by the factor given by eq. 4.1.5.2.

Examination of eqs. 4.1.5.3 and 4.1.5.5 shows that for a hollow cylinder of given inner and outer radii, the quantities ΔT_{max} and q_{max} can be maximized by selecting materials with high values for the thermal stress resistance parameters:

$$S_t(1-\nu)/\alpha E \quad \text{and} \quad S_t(1-\nu)K/\alpha E \qquad (4.1.5.6)$$

identical to these given by eqs. 4.1.2.5 and 4.1.2.6 .

For a hollow concentric cylinder subjected to radially inward heat flow, equations for the thermal stresses, ΔT_{max} and q_{max} equivalent to

those given by eqs. 4.1.5.1, 4.1.5.3, and 4.1.5.5 can be derived. It is important to mention that for radially inward heat flow, the magnitude of the tensile stress exceeds the corresponding value for radially outward heat flow (Hasselman and Youngblood, 1978). The values for ΔT_{max} and q_{max} are correspondingly reduced. This indicates that for hollow cylinders, such as those found in heat exchangers made from brittle ceramics and prone to failure in tension, radially outward heat flow is preferred whenever practical.

From a structural point of view, the results of the present section also indicate that under steady-state heat flow and isothermal conditions, the magnitude of thermal stresses can be reduced by promoting free thermal expansion, by avoiding external constraints, whenever practical.

4.1.6 Uniform internal heat generation

Thermal stresses of high magnitude can be caused by the non-uniform temperature distributions resulting from internal heat generation. This occurs for instance in such components as nuclear fuel elements, in materials subjected to micro-wave heating or materials undergoing a chemical decomposition with a negative heat of reaction. In solar collectors, internal absorption of incident solar radiation also represents a form of internal heat generation. This latter topic, in view of its relevance to solar collectors is treated in a separate extensive section of this report.

For steady-state, spatially uniform internal heat generation, the role of material properties can be obtained from the solutions for a solid circular cylinder (Thermal Stress Techniques in Nuclear Industry, 1965). The maximum tensile stress is:

$$\sigma = \alpha E H b^2 / 8(1-\nu) K \qquad (4.1.6.1)$$

where H is the rate of internal heat generation per unit volume and b is the cylinder radius. Eq. 4.1.6.1 can be rearranged to yield the maximum rate of internal heat generation, which can be tolerated without risking tensile thermal stress fracture:

$$H_{max} = 8S_t(1-\nu)K/\alpha Eb^2 \qquad (4.1.6.2)$$

Eq. 4.1.6.2 indicates that materials which can withstand high rates of internal heat generation should have high values of the thermal stress resistance parameter:

$$S_t(1-\nu)K/\alpha E \qquad (4.1.6.3)$$

Eq. 4.1.6.2 also suggests that in order to reduce the possibility of tensile thermal fracture, the cylinder radius should be kept as small as possible.

4.1.7. Thermal discontinuities

Steady-state heat flow in materials with a linear temperature distribution and absence of external constraints, as related earlier, will result in zero thermal stress. If, however, such materials contain inclusion with heat conduction properties different from the matrix materials, the temperature field near these inclusions will be disturbed to be non-linear. This, as indicated by Florence and Goodier (1959) for a spherical cavity and by Tauchert (1968) for a general inclusion, will result in a thermal stress field in the immediate vicinity around the inclusion.

For the spherical cavity, which represents an extreme case, the magnitude of the maximum tensile stress is:

$$\sigma = 0.5\alpha E\nabla b/(1-\nu) \qquad (4.1.7.1)$$

where ∇ is the temperature gradient in the absence of the cavity and b is the cavity radius.

Eq. 4.1.7.1 can be rearranged to give the maximum temperature gradient, ∇_{max} which can be imposed without incurring the risk of tensile failure, which yields:

$$\nabla_{max} = 2S_t(1-\nu)/\alpha Eb \qquad (4.1.7.2)$$

Eq. 4.1.7.2 can be rewritten to yield the maximum heat flux given by:

$$q_{max} = 2S_t(1-\nu)K/\alpha Eb \qquad (4.1.7.3)$$

Eqs. 4.1.7.2 and 4.1.7.3 show that in order to prevent tensile failure around cavities, materials should be selected with high values of the thermal stress resistance parameters:

$$S_t(1-\nu)/\alpha E \quad \text{and} \quad S_t(1-\nu)K/\alpha E \qquad (4.1.7.4)$$

which are identical in form to these derived earlier for other conditions of steady-state heat flow.

Eqs. 4.1.7.2 and 4.1.7.3 also indicate that if such thermal discontinuities are required for functional or other purposes, they be kept as small as possible.

4.2 Thermal Buckling

4.2.1. General

The thermal expansion of structures or components subjected to an increase in temperature can be prevented by external constraints. Under these conditions, equi-dimensional structures or components will be placed in a state of compression. Failure occurs when the compressive stresses exceed the compressive strength, as discussed earlier in section 4.1 of this report.

For slender columns or plates with a length much greater than their thickness, axially (in plane) constrained thermal expansions can be accommodated by bending deformations, in a direction perpendicular to the direction of constraint. This phenomenon is referred to as thermal buckling.

Thermal buckling in straight column (and flat plates) is characterized by a thermo-elastic instability consisting of a sudden deflection at a critical temperature difference ΔT_c. It should be noted that bending as the result of a thermo-elastic instability does not necessarily involve fracture. Fracture in tension may occur during "post-thermal buckling" as the result of bending moments induced at temperature differences, $\Delta T > \Delta T_c$.

Thermo-elastic instability does not occur for slender columns and plates with initial curvature or a curvature due to a transverse temperature gradient. Nevertheless, such columns or plates can exhibit failure if the tensile stresses due to the induced bending moments exceed the tensile strength.

Thermal buckling can involve significant changes in geometry, which must be taken into account in the design of any structure or component subject to this mode of deformation.

The following sections discuss a number of cases of thermal buckling for which selection rules for materials with high thermal buckling resistance have been derived.

4.2.2. Boundary conditions

For all thermal buckling cases to be considered, the column will be assumed to have a large length/thickness (i.e., slenderness) ratio, with a uniform cross-section along the total length. Furthermore, the temperatures are assumed to be independent of time and position along the length of the column.

Thermal buckling is strongly affected by the nature of the constraints

which permit or prevent rotation of the ends of the column. These conditions of constraint will be noted for each case of thermal buckling to be analyzed.

4.2.3. Straight column - uniform temperature - thermo-elastic instability

For a straight column with ends free to rotate, Fridman (1964), and Burgemeister and Steup (1957) showed that the column remains straight upto a critical temperature difference, ΔT_c at which it exhibits instability which is given by:

$$\Delta T_c = C_1 \pi^2 I / L^2 \alpha A \qquad (4.2.3.1)$$

where I is the cross-sectional moment of inertia, L is the length of the column, α is the coefficient of thermal expansion and A is the cross-sectional area.

The value of constant C_1 depends on the boundary conditions and is equal to unity in this case. For a column where the ends are not permitted to rotate the value of C_1 is 4.0 and for a column with one end free and the other end restrained from rotation its value is 0.25.

Eq. 4.2.3.1 reveals that the critical temperature is an inverse function of the coefficient of thermal expansion α. So a thermal buckling resistance parameter can be defined as:

$$\alpha^{-1} \qquad (4.2.3.2)$$

This parameter controls the critical temperature ΔT_c, if the dimensions of the column are constant. To maximize ΔT_c, one should choose a material with lowest value of α.

If the cross-section of the column is rectangular of width b and depth d, eq. 4.2.3.1 can be written as:

$$\Delta T_c = C_1 \pi^2 / 12 \alpha (L/d)^2 \qquad (4.2.3.3)$$

From eq. (4.2.3.2) it is clear that the slenderness ratio plays an important role in the buckling phenomenon. The higher the slenderness ratio is, the lower is the critical temperature. Columns with very low slenderness ratio (short columns) will normally fail in compression rather than in buckling.

4.2.4. Straight column - uniform temperature - post-buckling behavior

When the temperature rise in a straight column with ends free to rotate, exceeds the critical temperature ΔT_c, it will not fail immediately, but exhibits post-thermal buckling analyzed by Boley and Weiner (1960). It will fail only when the maximum bending stresses in the column exceed its tensile strength. Under this condition, the maximum temperature difference, ΔT_{max} over which a column with square cross-section can be heated, is given by Hasselman, 1979 (appendix 4.2.4.A)

$$\Delta T_{max} = \Delta T_c + S_t^2 L^2 / \pi^2 \alpha E^2 d^2 \qquad (4.2.4.1)$$

where S_t is the tensile strength of the column.

Eq. 4.2.4.1 leads to another thermal buckling resistance parameter which is given by:

$$S_t^2 / \alpha E^2 \qquad (4.2.4.2)$$

Again to maximize ΔT_{max}, one should choose a material with high value of $S_t^2/\alpha E^2$. It is important to note that in the second term of eq. 4.2.4.1, the slenderness ratio has an opposite effect to that of the first term given by eq. 4.2.3.3. So high values of ΔT_{max} can be achieved by choosing either very high or low values of L/d. Some basic calculations are necessary here to obtain the right value of L/d.

4.2.5. Column with slight initial curvature - uniform temperature

A column with initial curvature of the form $w = (x^2 - Lx)/2R$ and ends free to rotate is held at a uniform temperature. The geometry at the ends of the column are such that on rotation, the column length remains invariant. Solving the differential equation associated with this situation and applying the necessary boundary conditions, the total deflection y_t, for a ΔT rise in temperature can be found to be equal to (Hasselman, 1979):

$$Y_t = - 5k^2L^4/384R - L^2/8R \qquad (4.2.5.1)$$

where $k^2 = \alpha\Delta TA/I$ and R is the radius of curvature. The maximum tensile stress, σ_{max} is the algebraic sum of the bending stress caused by the total deflection and the compressive stress $\sigma_c = \alpha E\Delta T$, caused by the thermal load.

$$\sigma_{max} = \frac{C_1\alpha^2(\Delta T)^2EA^2L^4C}{RI^2} + \alpha E\Delta T\{\frac{AL^2C}{8RI} - 1\} \qquad (4.2.5.2)$$

where C is the neutral axis-to-outer fiber distance. The term linear in ΔT corresponds to the bending stress caused by the deflection of the column due to initial curvature which is independent of ΔT and is the major contribution to the stress in slender columns. The additional deflections produce stresses that are quadratic in ΔT. The compressive stresses are expected to be minor only.

The maximum temperature difference ΔT_{max} to which the column can be heated without fracture is obtained by substituting in eq. 4.2.5.2 S_t for σ_{max} and solving the following quadratic equation.

$$\frac{C_1\alpha^2(\Delta T)^2_{max}\ E\ A^2L^4C}{RI^2S_t} + \frac{\alpha E\Delta T_{max}}{S_t}\{\frac{AL^2C}{8RI} - 1\} - 1 = 0 \qquad (4.2.5.3)$$

Because of the relatively complex form of eq. 4.2.5.3 a convenient expression for ΔT_{max} is not easily derived. Instead, two simple limiting cases will be discussed:

(i) If the bending stresses linear in ΔT are equal to the compressive stresses, then

$$\Delta T_{max} = (S_t/\alpha^2 E)^{1/2}(RI^2/C_1 A^2 L^4 C) \qquad (4.2.5.4)$$

(ii) If the bending stresses quadratic in ΔT are equal to the compressive stresses, then

$$\Delta T_{max} = (S_t/\alpha E)(8RI/AL^2 C) \qquad (4.2.5.5)$$

Based on eqs. 4.2.5.4 and 4.2.5.5 the following two thermal buckling resistance parameters are defined.

$$(S_t/\alpha^2 E)^{1/2} \text{ and } (S_t/\alpha E) \qquad (4.2.5.6)$$

These two parameters control the maximum temperature difference ΔT_{max}, over which an initial curved column can be heated and their relative merit is decided by the geometry of the column. Again the designer choose a material with high values of $(S_t/\alpha^2 E)^{1/2}$ and $(S_t/\alpha E)$ to achieve a maximum ΔT.

Equation 4.2.5.4 can be rewritten for a rectangular column as:

$$\Delta T_{max} = (S_t/\alpha^2 E)^{1/2} (R/C_2(L/d)^4 C) \qquad (4.2.5.7)$$

Again note the influence of the slenderness ratio on the magnitude of ΔT_{max}. Whenever possible, the designer should always avoid very slender columns. The same thing can be said about equation 4.2.5.5.

It is mentioned earlier that the value of C_1 depends on the end conditions. For a simply supported column the value of $C_1 = 5/384$ and for a column with fixed end $C_1 = 1/384$.

4.2.6. Straight column- transverse heat flow

An initially straight column with end conditions described in section 4.2.5, when subjected to uniform heat flow perpendicular to its length and parallel to the direction of the shortest dimensions under steady-state conditions, and temperature independent properties will exhibit a linear temperature distribution through its thickness. If the constant temperature gradient is $\nabla = dT/dy$, then the radius of curvature R, can be expressed as $R = (\alpha\nabla)^{-1}$. This analysis is identical to the one described in section 4.2.5 if R is replaced by $(\alpha\nabla)^{-1}$. Then the maximum tensile stress can be written as:

$$\sigma_{max} = \frac{C_1\alpha^3E(\Delta T)^2\nabla A^2L^4C}{I^2} + \alpha E\Delta T\{\frac{\alpha\nabla AL^2C}{8I} - 1\} \qquad (4.2.6.1)$$

The maximum temperature difference ΔT_{max} is obtained by the substitution of S_t for σ_{max} and solving the quadratic equation:

$$\frac{C_1\alpha^3(\Delta T)^2_{max}E\nabla A^2L^4C}{I^2S_t} + \frac{\alpha E\Delta T_{max}}{S_t}\{\frac{\alpha\nabla AL^2C}{8I} - 1\}-1 = 0 \qquad (4.2.6.2)$$

In analogy to eqs. 4.2.5.4 and 4.2.5.5, two limiting conditions are:

(i) If the bending stresses linear in ΔT are equal to the compressive stresses, then:

$$\Delta T_{max} = (S_t/\alpha^3E)^{1/2}(I^2/C_1A^2L^4\nabla C)^{1/2} \qquad (4.2.6.3)$$

For a given ΔT, the maximum temperature gradient ∇_{max} can be written as:

$$\nabla_{max} = (S_t/\alpha^3E)\{I^2/(\Delta T)^2C_1A^2L^4C\} \qquad (4.2.6.4)$$

Eq. 4.2.6.4 can also be expressed in terms of maximum heat flux q_{max}, knowing $q_{max} = K\nabla_{max}$, where K is the thermal conductivity.

$$q_{max} = (S_tK/\alpha^3E)\{I^2/C_1(\Delta T)^2A^2L^4C\} \qquad (4.2.6.5)$$

From eq. 4.2.6.3 through 4.2.6.5 the following parameters can be defined.

$$(S_t/\alpha^3E)^{1/2},\ (S_t/\alpha^3E) \text{ and } (S_tK/\alpha^3E) \qquad (4.2.6.6)$$

These parameters control the maximum difference in temperature, maximum temperature gradient and maximum heat flux in a straight column subjected to transverse heat flow. Depending upon the situation one can maximize ΔT, ∇ or q by choosing a higher value of the appropriate parameter.

If the bending stresses quadratic in ΔT are equal to the compressive stresses, then

$$\Delta T_{max} = (S_t/\alpha^2E)(8I/AL^2\nabla C) \qquad (4.2.6.7)$$

Similarly, for a given value of ΔT, ∇_{max} becomes:

$$\nabla_{max} = (S_t/\alpha^2E)\{8I/AL^2(\Delta T)C\} \qquad (4.2.6.8)$$

which for the maximum transverse heat flux, yields:

$$q_{max} = (S_tK/\alpha^2E)\{8I/AL^2(\Delta T)C\} \qquad (4.2.6.9)$$

The parameters (S_t/α^2E) and (S_tK/α^2E) are the governing factors in eq. 4.2.6.7 thru 4.2.6.9. They should be maximized appropriately to have maximum ΔT, ∇ or q.

The constant C_1 used in this section depends on the boundary conditions. Eqs. 4.2.6.3 thru 4.2.6.9 can also be rewritten in terms of the L/d ratio and its effect can also be studied easily.

4.2.7. Column with slight initial curvature - transverse heat flow

For a column with a slight initial curvature R and subjected to conditions of heating as explained in section 4.2.6, the effect of heat adds an additional component $\nabla\alpha$ to the original curvature such that the final radius R_f

can be written as:

$$R_f = R(1 + \alpha \nabla R)^{-1} \qquad (4.2.7.1)$$

Depending upon the direction of heat flow (towards the concave or convex side) the value of ∇ will be either positive or negative and so will cause either an increase or decrease in the maximum stress values. This analysis is identical to the one done in section 4.2.5 if we replace R by R_f as expressed in eq. 4.2.7.1.

4.2.8. Poisson's ratio

In the analysis of two dimensional structures the effect of Poisson's ratio should be taken into consideration. For simple cases it is always possible to extend the one dimensional solutions to these problems by suitable modifications. For example, we have seen for a column in which the ends are free to rotate and subject to a uniform temperature, the critical temperature ΔT_c is given by:

$$\Delta T_c = \pi^2 I / L^2 \alpha A \qquad (4.2.8.1)$$

For a thin plate of dimensions a x b and thickness h, the above solution can be extended by replacing the moment of inertia I by the flexural rigidity $D = bh^3/12(1-\nu^2)$ and multiply by a factor k. Thus for thin plates,

$$\Delta T_c = k\pi^2 h^3 / 12(1-\nu^2) b \alpha A \qquad (4.2.8.2)$$

The constant k depends on the aspect ratio a/b of the plate and for a plate with edges free to rotate it is equal to:

$$k = (a/b + b/a)^2 \qquad (4.2.8.3)$$

For a detailed discussion on this, the reader is referred to Timoshenko and Gere (1961).

Based on eq. (4.2.8.2) another thermal buckling resistance parameter can be defined as:

$$[\alpha(1 - \nu^2)]^{-1} \qquad (4.2.8.4)$$

This parameter controls the critical temperature in thin plates and should be maximized to achieve maximum ΔT_c. All the thermal buckling resistance parameters developed in sections 4.2.3 through 4.2.8 can be applicable for two-dimensional structures if the modulus of elasticity E is replaced by $E/(1 - \nu^2)$.

4.2.9. Effect of creep on thermal buckling

Failure by thermal buckling is due to the presence of external constraints which prevent free thermal expansion. Removal of such constraints will automatically prevent the possibility of thermal buckling. Such constraints can be removed by creep deformation in the column (or plate) or in the external constraints. Such creep will cause a permanent change in the geometry and size of the component subject to thermal buckling as well as the constraints. Once this creep deformation has occurred, the possibility of thermal buckling is eliminated, unless the operating temperatures, purposely or by accident are raised significantly.

For these reasons, at least qualitatively it can be concluded that creep deformation can have a beneficial effect on thermal buckling resistance. No quantitative rules for the selection of materials subject to creep thermal buckling for brittle materials, as far as these authors are aware, have appeared in the literature. The analysis of such selection rules is the subject of a study currently underway under sponsorship by the Office of Naval Research.

4.2.10. Effect of geometry on thermal buckling behavior

The discussions presented so far concentrated on columns or plates which are straight or exhibit slight curvature only. This type of geometry exhibits minimum compliance in the axial and in-plane directions of the column and plate respectively. This low compliance is directly responsible for the thermo-elastic instability in straight columns and the high bending moments in columns with slight curvature.

For this reason, a major increase in thermal buckling resistance can be achieved by increasing the compliance in the direction of the external constraints. Support for this conclusion is provided by the results of Ganeeva (1956) and Shapovalov (1964), which showed that for highly curved plates the critical temperature for buckling instability increases rapidly with the degree of curvature.

It appears that from the design point of view, thermal buckling failure can be avoided by designing components with high curvature rather than straight or low degree of curvature.

4.2.11. Conclusions

(i) Selection of materials with high thermal buckling resistance can be based on a number of different thermal buckling resistance parameters. It is important to note that these parameters presented in this report are appropriate to a specific geometry, thermal environment and failure mode. For this reason, it is critical that prior to material selection, a careful analysis is conducted of the mode of buckling failure. Important to note also is that relevant material properties can exhibit a strong temperature dependence. For this reason, the buckling failure mode and the relevant "thermal buckling resistance parameter" will also depend on the temperature level of operation.

(ii) Failure by thermal buckling can be minimized by avoiding external constraints. For solar receivers this implies that all components subject to large total thermal expansion, be assembled with sufficient free space between them, such that differences in thermal expansions can be accommodated easily.

(iii) Thermal buckling failure can be controlled by the careful choice of geometry. For straight columns, low slenderness ratios are preferred. For initially straight column subject to large post-thermal buckling deformation or for columns with initial curvatures high slenderness ratios will permit excessive bending without risking tensile failure. Conversely, high initial curvature increases the compliance and thereby increase thermal buckling resistance.

(iv) Creep deformation can be beneficial in improving thermal buckling resistance. For ceramic materials this effect is expected to be beneficial at high temperatures near the anticipated upper operating temperatures of solar receivers.

4.3. Transient Heating and Cooling

4.3.1. Convective heat transfer

In practice structures or components initially at thermal equilibrium can experience a sudden change in ambient temperature. In an extreme case, this occurs in a turbine engine experiencing a flame-out condition. A similar situation is encountered in the physical removal of an object from a high temperature structure such as a furnace. Changes in the heat transfer coefficient or heat transfer mechanism in a structure at thermal equilibrium such as a nuclear reactor also involves a change in level of operating temperature.

Regardless of the details, such changes require that the structure or component must achieve new thermal equilibrium at a higher or lower temperature. This involves transient temperature changes, inevitably accompanied by transient thermal stresses. The transfer of heat to or from the structure or component undergoing a change in ambient temperature can occur by natural or forced convection. For Newtonian heat transfer, in which the heat flux at any instant is directly proportional to the difference in temperature of the surface and the ambient atmosphere, solutions for the transient thermal stresses for simple geometries can be derived analytically. The results for the solid circular cylinder (Jaeger, 1945) will be presented in detail, which are qualitatively similar to those for flat plates (Boley and Weiner, 1960) and spheres (Crandall and Ging, 1955).

Figure 4.3.1.1 shows the magnitude of the transient tensile thermal stresses encountered in the center of a solid circular cylinder of infinite length subjected to heating by an instantaneous increase (ΔT) in ambient temperature (Jaeger, 1945). It is common practice in thermal stress analysis to present the results in terms of a non-dimensional stress, $\sigma^* = \sigma(1-\nu)/\alpha E \Delta T$ and non-dimensional time $\kappa t/a^2$ where t is the real time and a is the radius of the rod. The stresses go through a transient maximum and are zero at $t = 0$ and $t \to \infty$. The magnitude of the stresses at any instant of time is a function of the Biot number, $\beta = ah/\kappa$, where h is the heat transfer coefficient. Note that the magnitude of the maximum stress is not governed by the thermal diffusivity. Differences in the thermal diffusivity for different materials only affect the time at which a given stress value is reached.

For design purposes, the maximum value of the tensile stresses are of interest. Over the range of $0.1 < \beta < 20$ the stresses to a very good

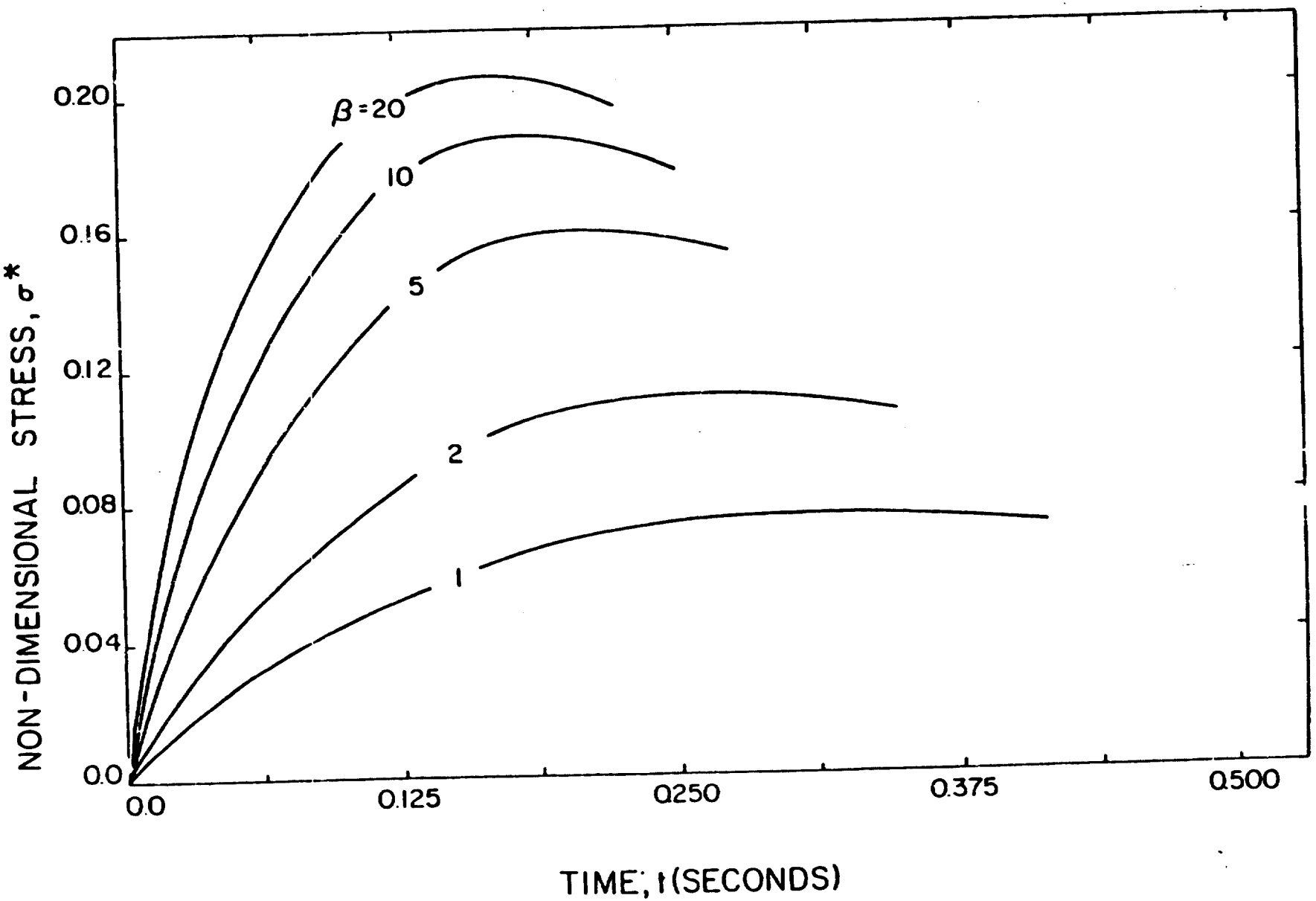

Fig. 4.3.1.1. Time dependence of maximum tensile thermal stress at the center of solid circular cylinder subjected to sudden convective heating for various values of Biot's number, β.

approximation can be expressed by:

$$\sigma^{*-1}_{max} = 1.451(1 + 3.41/\beta) \qquad (4.3.1.1)$$

By setting the value of maximum tensile stress, equal to the tensile strength an expression can be obtained for the maximum change in ambient temperature ΔT_{max} to which the cylinder can be subjected:

$$\Delta T_{max} = \frac{1.451\ S_t(1-\nu)}{\alpha E}\ (1 + 3.41/\beta) \qquad (4.3.1.2)$$

For the higher values of Biot number, eq. 4.3.1.2 can be simplified to:

$$\Delta T_{max} = 1.451\ S_t(1-\nu)/\alpha E \qquad (4.3.1.3)$$

Similarly for low values of the Biot number ($\beta < 1$), eq. 4.3.1.2 becomes:

$$\Delta T_{max} = 4.95\ S_t(1-\nu)K/\alpha Ebh \qquad (4.3.1.4)$$

The above results indicate that the thermal stress resistance of brittle materials, as measured by ΔT_{max}, strongly depends on the numerical value of the Biot number. For high values of β, as indicated by eq. 4.3.1.3 the thermal stress resistance is independent of the thermal conductivity as well as the heat transfer coefficient and cylinder size. In contrast, at low values of the Biot number, the thermal stress resistance is strongly affected by the values for the thermal conductivity, heat transfer coefficient and radius of the cylinder. In fact, for a cylinder of given thermal conductivity, subjected to a given convective heat transfer condition, any desirable value of ΔT_{max} can be achieved simply by decreasing the cylinder size.

From the point of view of selection of materials, high values of ΔT_{max} require high values of the thermal stress resistance parameters, obtained from Eqs. 4.3.1.3 and 4.3.1.4 given by:

$$S_t(1-\nu)/\alpha E \qquad (\beta >> 1) \qquad (4.3.1.5)$$

$$S_t(1-\nu)K/\alpha E \qquad (\beta < 1) \qquad (4.3.1.6)$$

The above parameters are of the same dimensional form as those derived previously for steady-state heat flow, but of course, appropriate to a completely different measure of thermal stress resistance.

It is important to note that due to the role of the Biot number, the relative thermal stress resistance of two different materials depending on their relative value of thermal conductivity may well be interchanged for conditions of high or low values of Biot number. This latter observation is critical in assessing the relative thermal stress resistance of materials by experimental methods and the use of these results for design purposes. Experimental comparisons of the relative thermal stress resistance frequently use relatively small laboratory specimens. For these, the specimens size and thermal conductivity play an important part in establishing the measured values of ΔT_{max}. However, these experimental results are no longer appropriate for larger sized structures scaled-up from laboratory models. Lack of appreciation of this fact, can (and has) led to major errors in the design and selection of materials for high-temperature structures.

Expressions, identical in form, but differing only in their values of the numerical constants, can be derived for other geometries such as plates and spheres. For this reason, the above conclusion for the solid cylinder, should be generally applicable to other geometries as well.

Predictions of values of ΔT_{max} for thermo-elastic theory have shown reasonable agreement with experimental data (Glenny and Royston, 1958), (Hasselman and Crandall, 1963; Hasselman, 1970). Any discrepancies between calculated and observed values most likely can be attributed to uncertainties in the values of the heat transfer coefficient and the magnitude of the failure stress.

It should be noted that the above discussion and results assumed the existence of Newtonian heat transfer (i.e. a constant heat transfer coefficient for the total period over which the material comes to thermal equilibrium). Under conditions of natural convection, however, heat transfer coefficients generally decrease as the thermal equilibrium is approached. Preliminary results obtained by the present writers, by finite element analysis, show that under these conditions the thermal stresses are less than those given by eq. 4.3.1.1 especially at the higher values of heat transfer coefficients. For this reason, under conditions of natural convection, eqs. 4.3.1.2, 4.3.1.3 and 4.3.1.4 for ΔT_{max} represent conservative estimates.

4.3.2. Transient heat transfer. Controlled rate of heating

In principle, thermal stress failure can be avoided by controlling the rate of heating such as placing an upper limit on the rate of change of surface temperature. In practice, this could be done by careful control of the heat transfer coefficient in convective heat transfer or controlled filtering or masking of incident radiant energy. This latter approach may possibly provide a solution to the severe thermal shock expected for components of solar collectors under intermittent cloud cover conditions.

The role of the pertinent material properties which control the thermal stress resistance of brittle ceramics is indicated by the solution for the maximum thermal stress in a flat plate cooled by a constant rate of change of surface temperature (Buessum, 1960):

$$\sigma = - \frac{\alpha E b^2}{3(1-\nu)\kappa} \frac{dT}{dt} \qquad (4.3.2.1)$$

where b is the total thickness of the plate.

By setting the thermal stress equal to the tensile strength, the maximum permissible rate of cooling becomes:

$$\left(\frac{dT}{dt}\right)_{max} = \frac{3\, S_t (1-\nu)\kappa}{\alpha E b^2} \qquad (4.3.2.2)$$

Eq. 4.3.2.2 indicates that materials which can be subjected to high rates of cooling should have high values of the thermal stress resistance parameter:

$$\frac{S_t (1-\nu)\kappa}{\alpha E} \qquad (4.3.2.3)$$

Furthermore, for a given material, high cooling rates can be tolerated by keeping the plate thickness as low as possible.

On dimensional grounds, these conclusions should also be valid for controlled heating rates.

4.3.3. Radiation heat transfer

Radiation is a principal mode of heat transfer in solar collection system and an important possible source of thermal stress failure. The functional response to the incident solar radiation and corresponding thermal

stress state for any design of solar collection system depends upon the particular component under consideration. Mirrors, which concentrate the solar radiation, should absorb little or no part of the incident radiation and should have high reflectivity. On the other hand, the window, which permits the concentrated solar flux to be incident on the solar receivers, should have low reflectivity and should transmit as much radiation as possible. In contrast, the receiver, which converts the radiation flux into heat energy, should have high absorptivity. It is expected that these three components should exhibit different thermal responses to the incident radiation, with each having different material requirements. As will be shown, the material requirements for high efficiency in converting solar energy into another form may not be necessarily compatible with other performance criteria such as high thermal stress resistance. Therefore, an optimization of material properties will have to be made in order to achieve high conversion efficiency in addition to high thermal stress resistance.

The assessment of the magnitude of thermal stresses in material subjected to radiation heating or cooling can be quite complex. Heat transfer in radiation mode is proportional to the fourth power of the absolute temperature. In addition, spectral and temperature dependence of the pertinent material properties combined with the internal absorption and re-emission of the incident radiation introduces further complexities. For this reason, the evaluation of thermal stress in radiation environments, in general, requires numerical techniques. As stated before, such numerical techniques are useful and essential in practice for a specific component design with known spectral and temperature dependence of material properties and heat transfer environment. However, the analytical solutions

necessary to indicate the general role of the pertinent material properties must be based on a number of simplifying assumptions.

A number of such solutions were obtained by the present authors and co-workers (Hasselman, 1963, 1966; Hasselman et al., 1980; Thomas et al., 1980; Singh et al., 1980a,b) for materials subjected to incident radiation heating. These studies included materials which are opaque, semi-transparent and partially absorbing. The semi-transparent materials were assumed to be transparent below a given wavelength and opaque above this wavelength. In partially absorbing materials, the incident radiation gets absorbed, while being transmitted through them. Depending upon the external cooling conditions, the internal absorption of the incident radiation can result in a temperature distribution such that the interior of the structure may be at higher temperature than the surface known as "thermal trapping" effect. A simplifying assumption common to these solutions was that the temperature of the material was kept sufficiently low that the effect of any re-emitted radiation could be neglected. This assumption permitted to regard the incident radiation, for all practical purposes, to consist of a constant heat flux. This assumption was found to be valid in all cases because the thermal stresses reach their maximum value at or near the initial stage of thermal history before the material becomes hot. It was also assumed that the optical properties of the material are "grey", i.e., independent of wavelength. However, the spectral dependence of the material properties can be easily taken into account by superposition of a number of analytical solutions for appropriate wavelengths.

The highlights of these analytical and numerical results pertinent to different components in a solar collecting system and the role of the material properties will be given below. For convenience, the reprints or the copies of the studies cited are presented in appendices 4.3.3(A-F).

A. Opaque sphere subjected to symmetric radiation heating

This analysis by Hasselman (1963) involved the evaluation of thermal stresses in a cylinder, sphere and flat plate subjected to radiation heating all around without any cooling taking place. Such heat transfer environment is pertinent to the solar receivers when they are subjected to radiant heat flux without any circulating fluid around them due to a malfunction of the circulating pump.

The maximum steady state ($t \to \infty$) tensile thermal stress in a sphere occurs in the center of the sphere and is given by:

$$\sigma_{max} = \frac{1}{5} \frac{\alpha E \varepsilon q_o a}{(1-\nu)K} \qquad (4.3.3.1)$$

where q_o is the intensity of the radiant heat flux, K is the thermal conductivity, E is the Young's modulus of elasticity, α is the ccefficient of thermal expansion, $\varepsilon=1-r$ is the emissivity, r is the reflectivity, ν is the Poisson's ratio and a is the radius of the sphere.

As can be seen in equation 4.3.3.1, the magnitude of the maximum stress depends upon the intensity of heat flux in addition to many other physical and optical properties of the material. Therefore the maximum permissible heat flux should be such that the thermal stresses developed do not exceed the allowable stress for the material in order to avoid failure. Thus, to examine the effects of various material and geometric parameters on the magnitude of the maximum permissible heat flux, the analytical expression for the maximum permissible heat flux, q_{max}, was obtained from equation 4.3.3.1 by equating the maximum tensile stress to the strength of the material, S_t, which resulted in:

$$q_{max} = \frac{5\, S_t (1-\nu) K}{\alpha E \varepsilon a} \qquad (4.3.3.2)$$

The maximum heat flux due to black-body radiation can also be represented by:

$$q_{max} = \rho(T_{max}^4 - T_1^4) \qquad (4.3.3.3)$$

where ρ is Boltzmann's constant, T_1 is the temperature of the sphere and T_{max} is the maximum permissible temperature of the incident radiation.

It is assumed that $T_1^4 << T_{max}^4$. Therefore, equation 4.3.3.3 becomes

$$q_{max} = \rho\, T_{max}^4 \qquad (4.3.3.4)$$

From equations 4.3.3.2 and 4.3.3.4, the expression for maximum permissible temperature for radiant heat flux without causing any failure can be given as:

$$T_{max} = \left[\frac{5}{\rho a}\right]^{1/4}\left[\frac{S_t(1-\nu)K}{\alpha E\varepsilon}\right]^{1/4} \qquad (4.3.3.5)$$

In order to formulate the selection rules for the optimum material, thermal stress resistance parameters were obtained from equation 4.3.3.2 and 4.3.3.5 as follows:

$$\frac{S_t(1-\nu)K}{\alpha E\varepsilon} \quad \text{and} \quad \left[\frac{S_t(1-\nu)K}{\alpha E\varepsilon}\right]^{1/4} \qquad (4.3.3.6)$$

Thus, high thermal stress resistance requires high values of tensile strength and thermal conductivity in combination with low Poisson's ratio, coefficient of thermal expansion, Young's modulus and the emissivity.

B. Semitransparent sphere subjected to symmetric radiation heating

In this study by Hasselman (1966), the material was assumed to be transparent below a given wavelength and opaque above this wavelength.

Similar to section 4.3.3.A, the sphere was subjected to radiation heating all around with no cooling. This analysis is quite pertinent to materials for windows in solar receivers. A typical window material, such as quartz, has very low absorptance for the radiation in the range of 1-2.6μ while the absorptance increases rapidly above this wavelength.

The maximum permissible heat flux, q_{max}, for a sphere is given by:

$$q_{max} = \frac{5\, S_t(1-\nu)K}{\alpha E \varepsilon a} \qquad (4.3.3.7)$$

and the maximum permissible temperature of the radiant heat flux is given by:

$$T_{max} = \left[\frac{5}{\rho a}\right]^{1/4}\left[\frac{S_t(1-\nu)K}{\alpha E \varepsilon (1-F_{\lambda o})}\right]^{1/4} \qquad (4.3.3.8)$$

where $F_{\lambda o}$ is the fraction of total radiant energy at a wavelength shorter than λ_o and λ_o is the wavelength below which the material is completely transparent.

Equations 4.3.3.7 and 4.3.3.8 result in the following two thermal stress resistance parameters:

$$\frac{S_t(1-\nu)K}{\alpha E \varepsilon} \text{ and } \left[\frac{S_t(1-\nu)K}{\alpha E \varepsilon (1-F_{\lambda o})}\right]^{1/4} \qquad (4.3.3.9)$$

In addition to the requirements for the opaque material in section 4.3.3.A, the high thermal stress resistance requires high value of cut off wavelength $F_{\lambda o}$ for semitransparent materials.

C. Semi-absorbing flat plate subjected to radiation heating at the front surface and cooled by convection at the rear surface

This kind of thermal environment is very common to the solar receivers where the radiation is incident on only one side and cooling takes place at

the other side by convection. Figure 4.3.3.1 shows the schematic of a plate (thickness = 2a) assymmetrically heated by radiation and cooled by convection with heat transfer coefficient, h. The expressions for the maximum tensile stress are lengthy (appendix 4.3.3.C) due to assymmetric nature of heat transfer and, therefore, only the numerical results will be presented for the general case. However, for limiting values of optical thickness, μa, the expressions will be simplified and the results will be presented in analytical form. Results for three cooling conditions are presented below.

Heat transfer coefficient, h = finite

Figure 4.3.3.2 shows the time dependence of the maximum tensile thermal stress for $\mu a = 3$ and various values of heat transfer coefficient, h. It can be noted that the value of steady state ($t \to \infty$) stress is independent of h whereas the maximum transient stress is an inverse function of h. The steady state stress does not depend on h because the temperature profile in this case is independent of h even though the magnitude of temperature is an inverse function of h. This conclusion can be shown to be true for any value of μa. The value of the maximum tensile stress as a function of μa for steady state ($t \to \infty$) condition is shown in figure 4.3.3.3. The plot shows a peak at an optical thickness (μa) of 2.0 with zero values of stress at $\mu a = 0$ and ∞. The stresses are zero for $\mu a = 0$ because no heat is absorbed at all in the material. Although, for $\mu a = \infty$, all the heat is absorbed in the surface, the distribution of temperature at steady state ($t \to \infty$) is linear resulting in zero stress. The peak in the steady state stress is due to the maximum thermal trapping effect at $\mu a = 2.0$.

The analytical expressions for thermal stress for finite h is too complex (appendix 4.3.3.C) to derive simple expressions for the maximum permissible heat flux and thermal stress resistance parameter in order to discuss the role of material properties. Therefore, two separate analyses were per-

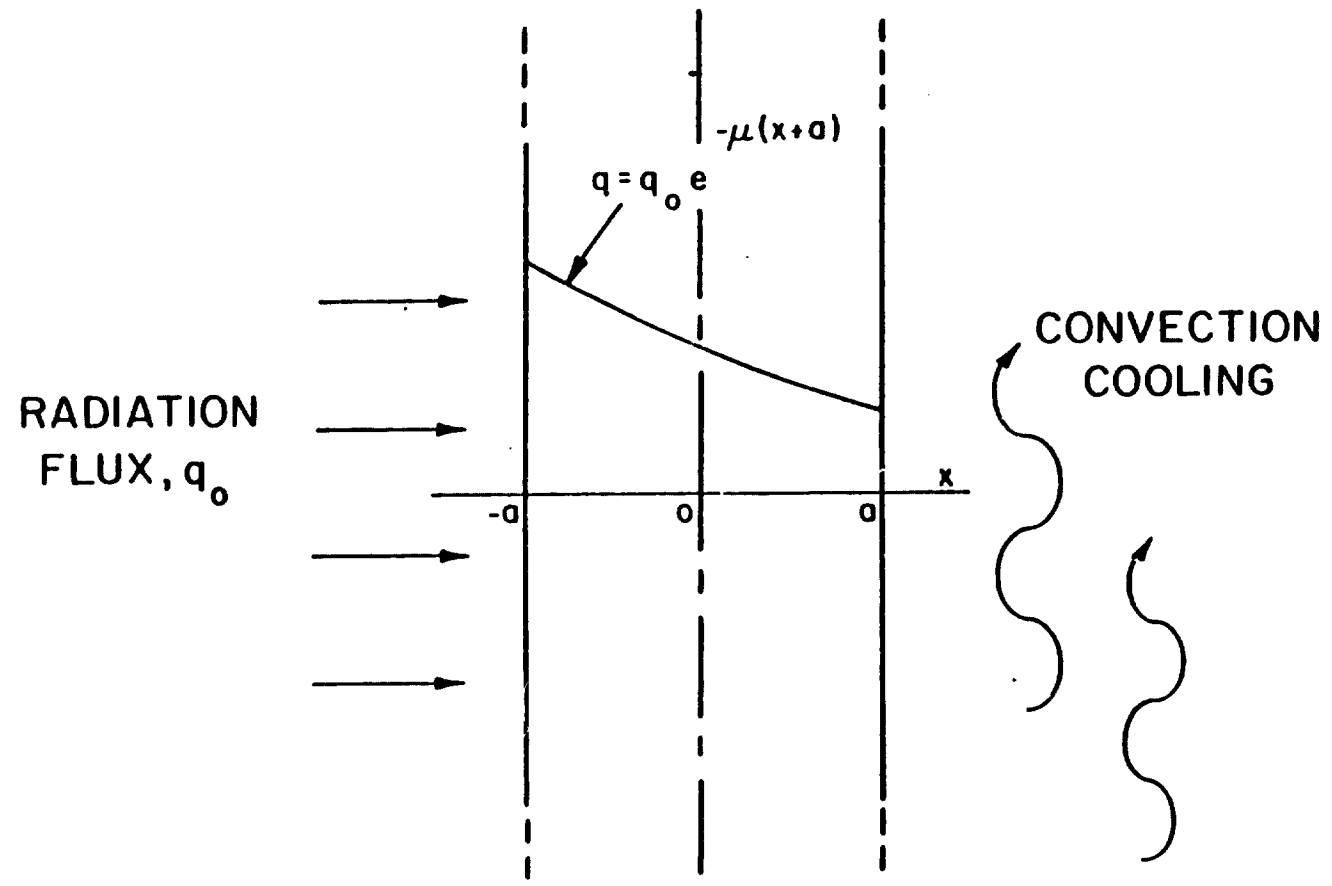

Fig. 4.3.3.1. Schematic diagram of a flat plate subjected to radiation heating on one side and convection cooling on the other side.

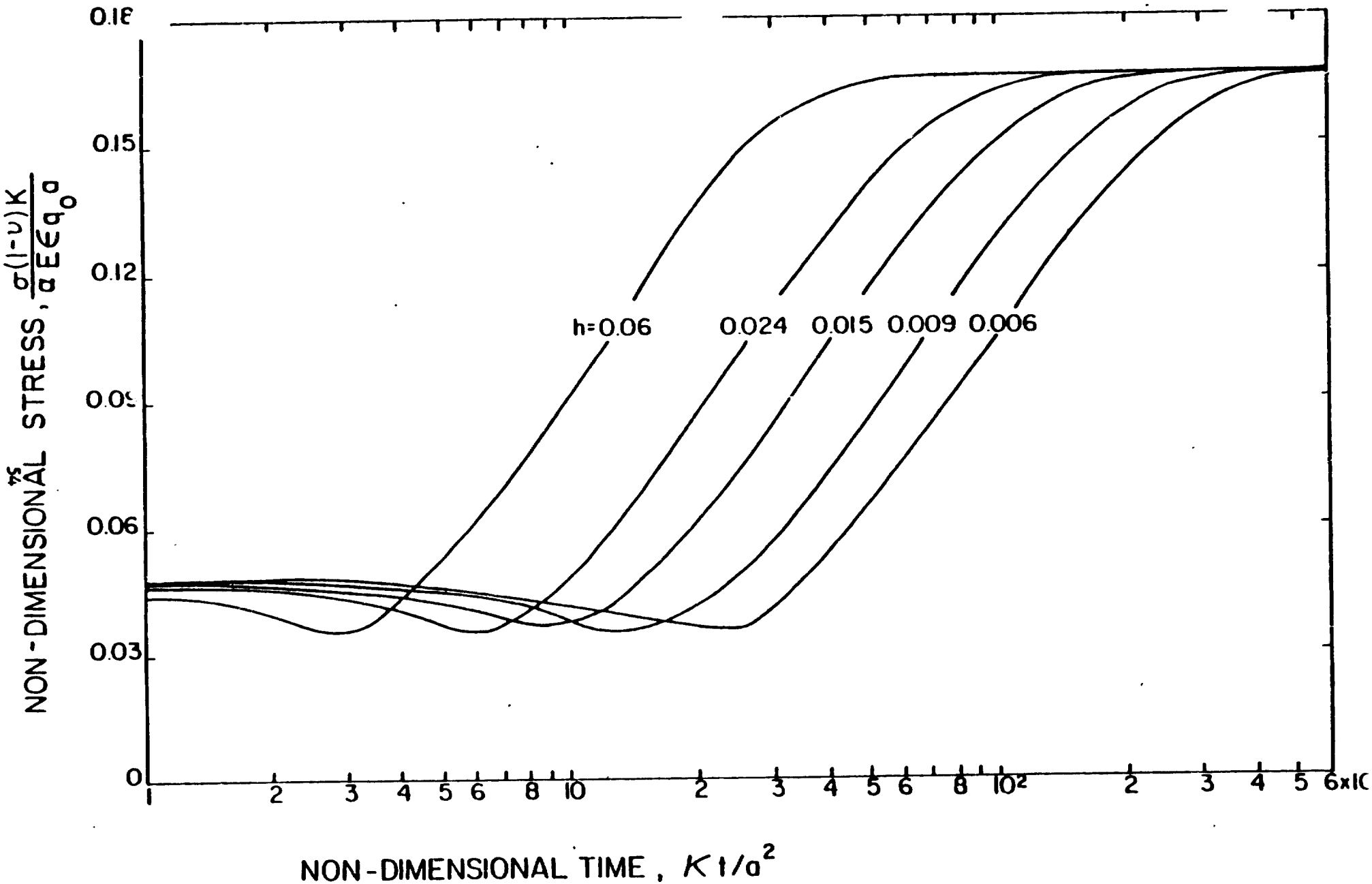

Fig. 4.3.3.2. Time dependence of maximum tensile thermal stress in a partially absorbing flat plate with $\mu a = 3$, assymmetrically heated in front by normally incident radiation and cooled at the rear surface by convection for various values of heat transfer coefficient, h (watts. cm^{-2}. $^{\circ}c^{-1}$) with K = 0.3 watts. cm^{-1}. $^{\circ}c^{-1}$ and a = 1 cm.

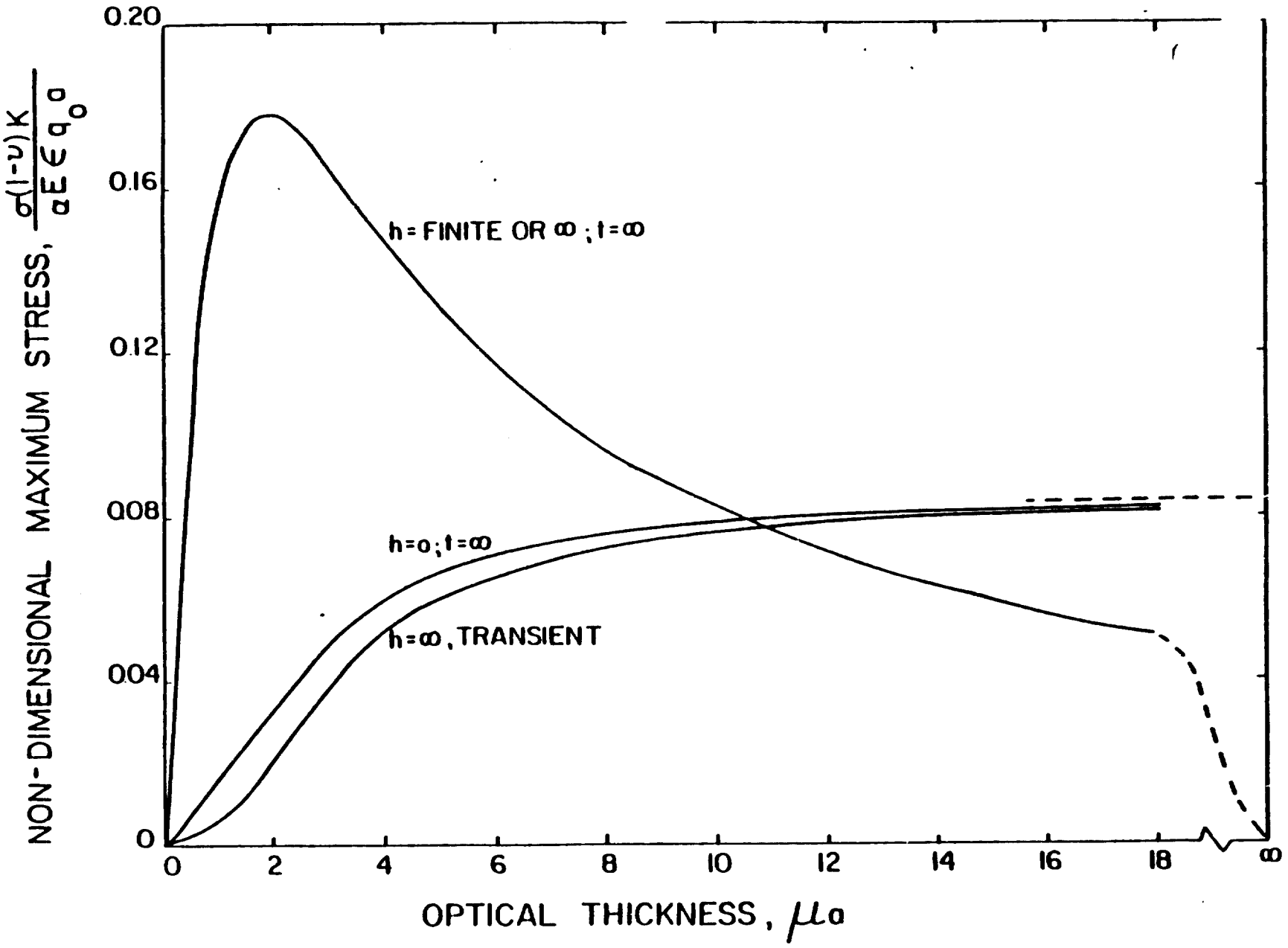

Fig. 4.3.3.3. Maximum tensile thermal stresses in partially absorbing flat plate assymmetrically heated in front by normally incident radiation and cooled at the rear surface by convection with heat transfer coefficient, h = 0, ∞ and finite, K = 0.3 watts. cm^{-1}. $^{\circ}c^{-1}$ and a = 1 cm.

formed for h = 0 and ∞ which resulted in simple expressions for the maximum permissible heat flux and thermal stress resistance parameters for the limiting values of optical thickness, μa as shown below.

Heat transfer coefficient, h = 0

Figure 4.3.3.3 shows the value of the maximum tensile stress at steady state ($t \to \infty$) as a function of the optical thickness, μa (appendix 4.3.3.C). The stresses are zero at μa = 0, monotonically increases with μa and plateau at high values of μa.

Since there is no cooling (h = 0), the temperature of the plate increases with time. However, as mentioned before, the stresses reach their maximum value in the initial part of transient state before the plate gets very hot. This permits the assumption of constant heat flux for stress calculations.

It is interesting to point out that the maximum tensile thermal stress, at least for small values of μa, occurs in the front face of the plate which is at the high temperature (appendix 4.3.3.C, figure 6). This result has significant engineering implication to be discussed later.

The expressions for maximum permissible heat flux were obtained by simplifying the stress equation for optically thick ($\mu a \to \infty$) and optically thin ($\mu a << 1$) plates as follows.

For optically thick plate, the maximum steady-state tensile stress occurs in the center (x = 0) of the plate and is given by:

$$\sigma_{max} = (0,\infty) = \alpha E q_o \varepsilon a/12(1-\nu)K \quad (\mu a \to \infty) \qquad (4.3.3.10)$$

For optically thin plate, the maximum steady-state tensile stress occurs in the front fact (x = -a) of the plate and is given by:

$$\sigma_{max}(-a,\infty) = \alpha E q_o \varepsilon \mu a^2/(1-\nu)K \quad (\mu a << 1) \qquad (4.3.3.11)$$

Equating the maximum stress to the tensile strength S_t, the expressions for the maximum permissible heat flux, q_{max} can be given by:

$$q_{max} = \frac{12\ S_t(1-\nu)K}{\alpha E\epsilon a} \qquad (\mu a \to \infty) \qquad (4.3.3.12)$$

$$q_{max} = \frac{S_t(1-\nu)K}{\alpha E\epsilon\mu a^2} \qquad (\mu a \ll 1) \qquad (4.3.3.13)$$

From the point of view of solar collectors, the expressions will be limited to the maximum stress σ_{max} and maximum permissible heat flux q_{max}. However, the expressions for maximum permissible temperature for incident radiation can be obtained simply by substituting $\rho\ T_{max}^4$ for q_{max} as shown in equation 4.3.3.5.

Heat transfer coefficient, $h = \infty$

The values of the maximum steady state ($t \to \infty$) and transient stress are included in figure 4.3.3.3 as a function of optical thickness, μa. It can be seen that the steady state stress for $h = \infty$ or finite exceeds the transient stress for $0 < \mu a < 10.7$ and the converse is true for $10.7 < \mu a < \infty$.

The value of the maximum permissible heat flux, q_{max}, was obtained by simplifying the expression for thermal stress for the limiting values of μa, viz., $\mu a \ll 1$ and $\mu a \to \infty$. The maximum steady state tensile stress, which occurs at $x = -a$, is given by:

$$\sigma_{y,z}(-a,\infty) = 0 \qquad (\mu a \to \infty) \qquad (4.3.3.14)$$

$$\sigma_{y,z}(-a,\infty) = \frac{0.2719\alpha E q_o \epsilon \mu a^2}{(1-\nu)K} \qquad (\mu a \ll 1) \qquad (4.3.3.15)$$

and the maximum permissible heat flux can be given by:

$$q_{max} \to \infty \qquad (\mu a \to \infty) \qquad (4.3.3.16)$$

$$q_{max} = \frac{3.677\ S_t(1-\nu)K}{\alpha E\epsilon\mu a^2} \qquad (\mu a \ll 1) \qquad (4.3.3.17)$$

In order to formulate the selection rules for the optimum material, thermal stress resistance parameters were obtained from the expressions for q_{max}. From equations 4.3.3.12, 4.3.3.13 and 4.3.3.17, thermal stress resistance parameters can be obtained as:

$$\frac{S_t(1-\nu)K}{\alpha E c} \quad , \quad \frac{S_t(1-\nu)K}{\alpha E c \mu} \qquad (4.3.3.18)$$

Equation 4.3.3.18 indicates that in order to obtain high thermal stress resistance, high values of tensile strength and thermal conductivity in combination with low values of coefficient of thermal expansion, Poisson's ratio, Young's modulus, emissivity and absorption coefficient are required. Furthermore, equations 4.3.3.12, 4.3.3.13 and 4.3.3.17 clearly indicate that high thermal stress resistance is always associated with smaller component size.

At this point, it is important to mention that in this case, the heat absorbed in the plate has to be conducted through the total plate thickness before it can be removed at the rear surface. This effect results in a high temperature difference in the plate especially for high values of the optical thickness, μa.

D. Semi-absorbing flat plate subjected to radiation heating and convection cooling at the front surface

This kind of thermal environment (appendix 4.3.3.D) is another likely design configuration for solar receivers. A qualitative evaluation of the two systems, viz., front and rear cooling suggests that the maximum temperature difference in the plate at steady state in case of front heating with rear cooling will exceed that encountered in the case where heating and cooling both occurs in the front face. This is because, as mentioned before, in case of heating in the front and cooling in the rear surface, the heat ab-

sorbed in the plate has to be conducted through the total plate thickness before it can be removed at the rear surface. However, in case of front cooling, the heat is immediately removed from the surface with little or no heat absorbed inside the plate resulting in more uniform temperature in the plate. For high incident heat flux, this may result in higher front surface temperature in case of rear cooling than that in case of front cooling for a given temperature of the cooling environment. The uniformity of temperature distribution in a plate subjected to heating and cooling in the front face has important implication for the design of solar receivers to be discussed later.

The results for the thermal stresses for three cooling conditions are discussed below.

Heat transfer coefficient, h = finite

Figures 4.3.3.4 and 4.3.3.5 show the plots for the maximum stress as a function of time and optical thickness respectively. A comparison of these results with those for the case of assymmetric heating with cooling at the rear surface (figures 4.3.3.2 and 4.3.3.3) indicates that the stress plots are qualitatively similar in nature in both cases. However, a comparison of stress profiles indicates that the stress distributions are different. In addition, the transient stress and the times to reach the transient peak are different in two cases (See appendices 4.3.3.C and 4.3.3.D).

Heat transfer coefficient h = 0

For h = 0, the thermal environments for flat plate subjected to radiation heating and convection cooling in front surface is identical to the previously discussed case where the cooling takes place at the rear surface. Consequently, the results will be identical and the reader is referred to section 4.3.3.C.

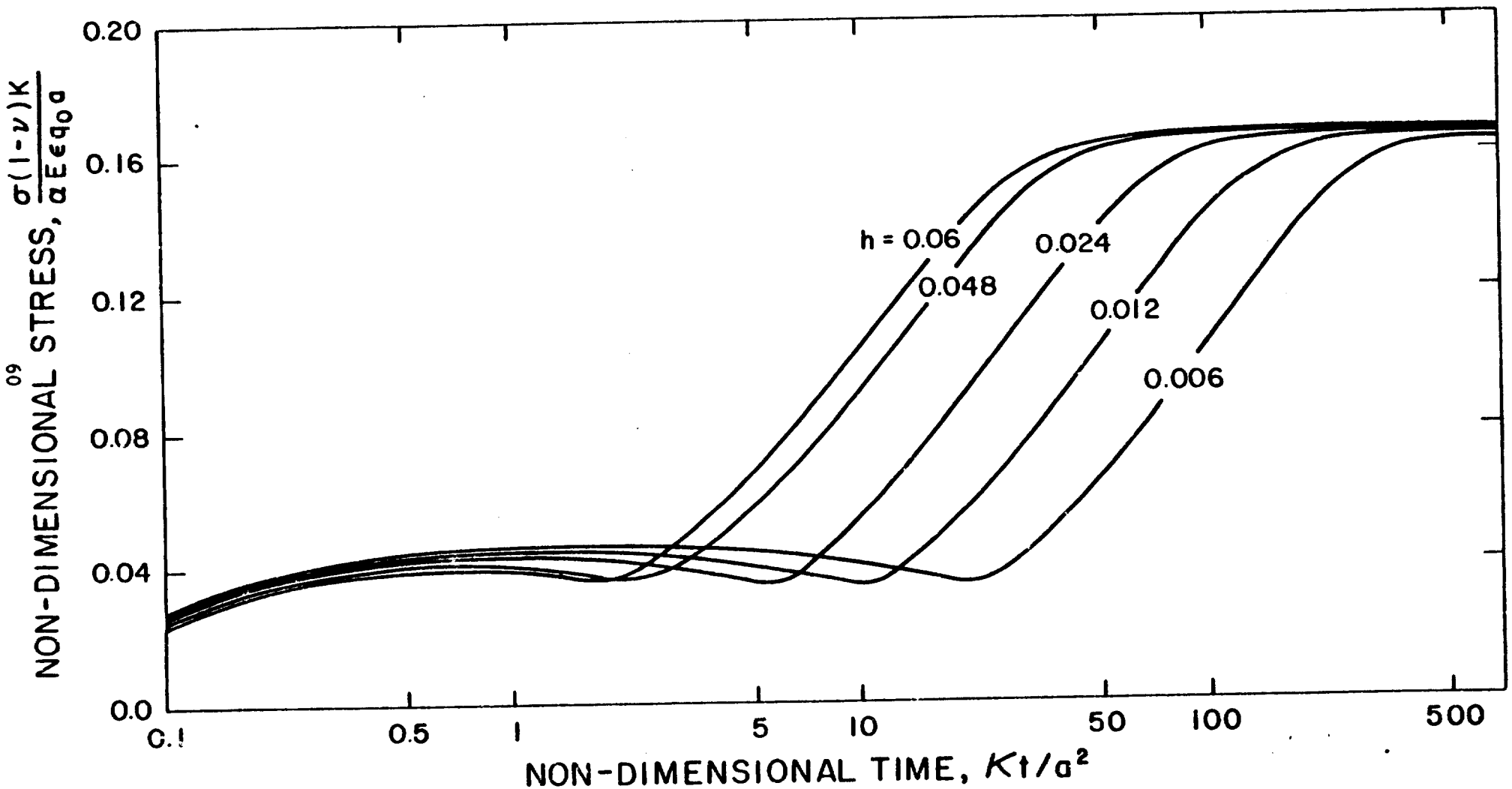

Fig. 4.3.3.4. Time dependence of the maximum tensile thermal stress in a partially absorbing flat plate subjected to radiation heating and convection cooling at the front face for various values of heat transfer coefficient, h (watts. $cm.^{-2}$ $^oC^{-1}$) with K = 0.3 watts. $cm.^{-1}oC^{-1}$, μa = 3.0 and a = 1 cm.

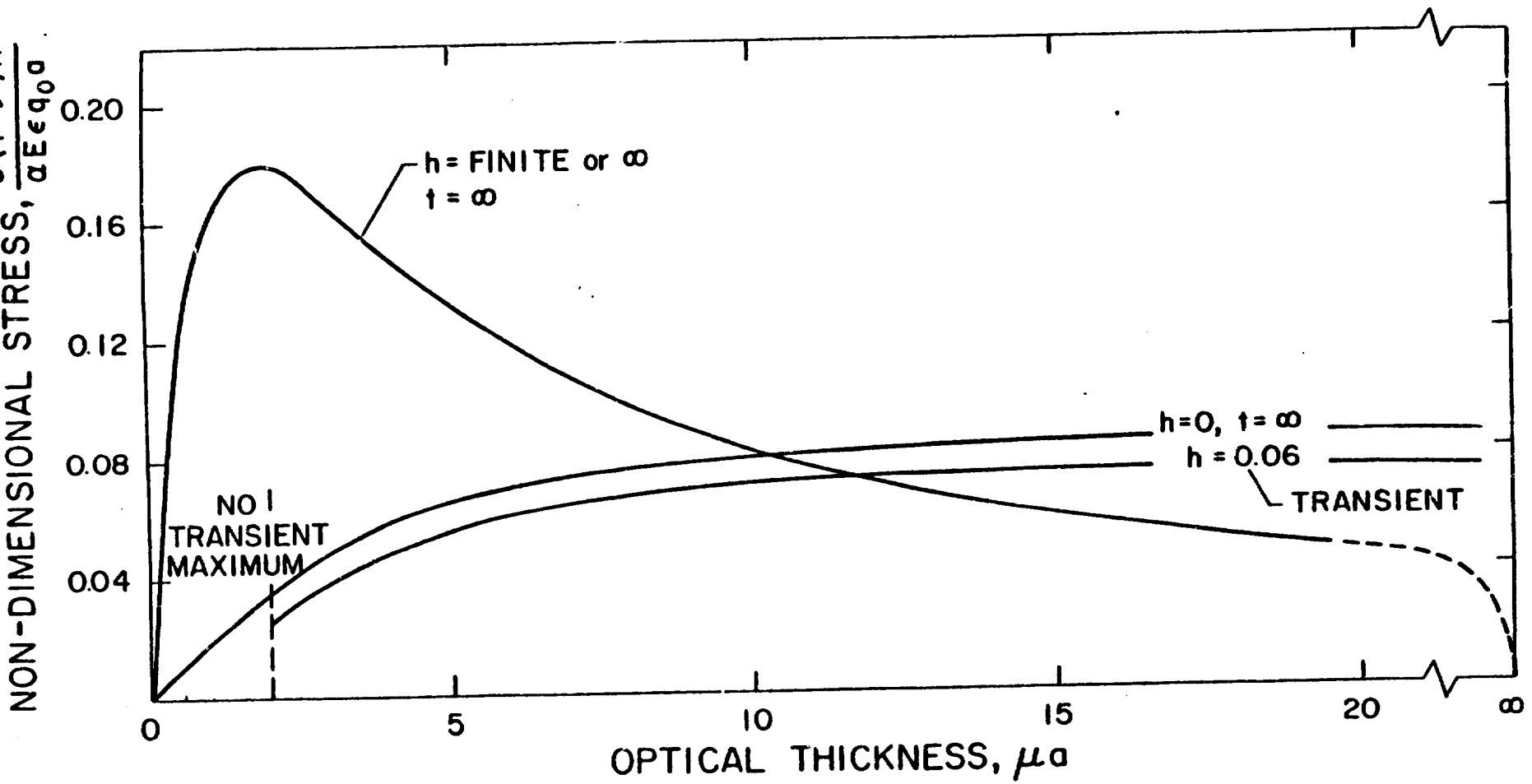

Fig. 4.3.3.5. Variation of maximum tensile thermal stresses as a function of μa in a partially absorbing flat plate subjected to radiation heating and convection cooling at the front face with heat transfer coefficient, h = 0, ∞ and finite, K = 0.3 watts. cm.$^{-1}$C^{-1} and a = 1 cm.

Heat transfer coefficient h = ∞

The values of the maximum steady state and transient stress are shown in figure 4.3.3.5. In this case, there is no transient peak. Since for h = ∞, the front face is always at ambient temperature, whereas the inside temperature increases monotonically with time resulting in a monotonic increase in stress with time and therefore, no transient peak occurs.

The maximum steady state stress occurs in the front face and can be simplified for the optically thick ($\mu a \to \infty$) and the optically thin ($\mu a \ll 1$) plates as follows:

$$\sigma_{max}(-a,\infty) = 0 \qquad (\mu a \to \infty) \qquad (4.3.3.19)$$

$$\sigma_{max}(-a,\infty) = \frac{\alpha E \varepsilon \mu a^2 q_o}{3K(1-\nu)} \qquad (\mu a \ll 1) \qquad (4.3.3.20)$$

and the maximum permissible heat flux can be given by:

$$q_{max} \to \infty \qquad (\mu a \to \infty) \qquad (4.3.3.21)$$

$$q_{max} = \frac{3\, S_t (1-\nu) K}{\alpha E \varepsilon \mu a^2} \qquad (\mu a \ll 1) \qquad (4.3.3.22)$$

For selection rule, thermal stress resistance parameters can be obtained from equation 4.3.3.22 and is given by:

$$\frac{S_t (1-\nu) K}{\alpha E \varepsilon \mu} \qquad (4.3.3.23)$$

It can be seen that thermal stress resistance parameter given by equation 4.3.3.23 is identical to the one in equation 4.3.3.18 and therefore, the property dependence will be similar to those explained before.

E. Semi-absorbing flat plate subjected to symmetric radiation heating and convection cooling

Depending upon the design configuration of the solar receiving system, solar receivers may be subjected to symmetric heating and cooling. As explained in section 4.3.3.D, the symmetric cooling is expected to result in a uniform temperature in the plate. The thermal stresses for three cooling conditions are discussed below (see appendix 4.3.3.E).

Heat transfer coefficient, h = finite

Figure 4.3.3.6 shows the plot for the stresses in the surface and the center of the plate as a function of time. Two interesting features can be noted here. First, similar to assymmetric heating, the steady-state stress is independent of h whereas the maximum transient stress is an inverse function of h. Second, the maximum stress reverses its sign between the transient and steady-state conditions. This results from the effect of non-uniform internal heat generation and associated thermal trapping effect (Singh et al, 1980, appendix 4.3.3.F).

For finite values of heat transfer coefficient, h, the variation of the maximum transient and steady-state tensile thermal stress as a function of the optical thickness, μa is shown in figure 4.3.3.7. Similar to the assymmetric heating case, the magnitude of the transient tensile stress increases with μa and finally approaches an equilibrium value whereas the steady-state tensile stress shows a peak at an optical thickness of ~ 1.3 with zero values at $\mu a = 0$ and ∞.

Heat transfer coefficient, h = 0

In contrast to assymmetric heating case, thermal stresses in this case monotonically increases with time till the steady state ($t \to \infty$) stress is reached. The maximum value of steady-state stress occurs in the center of the plate ($x = 0$) which is given by:

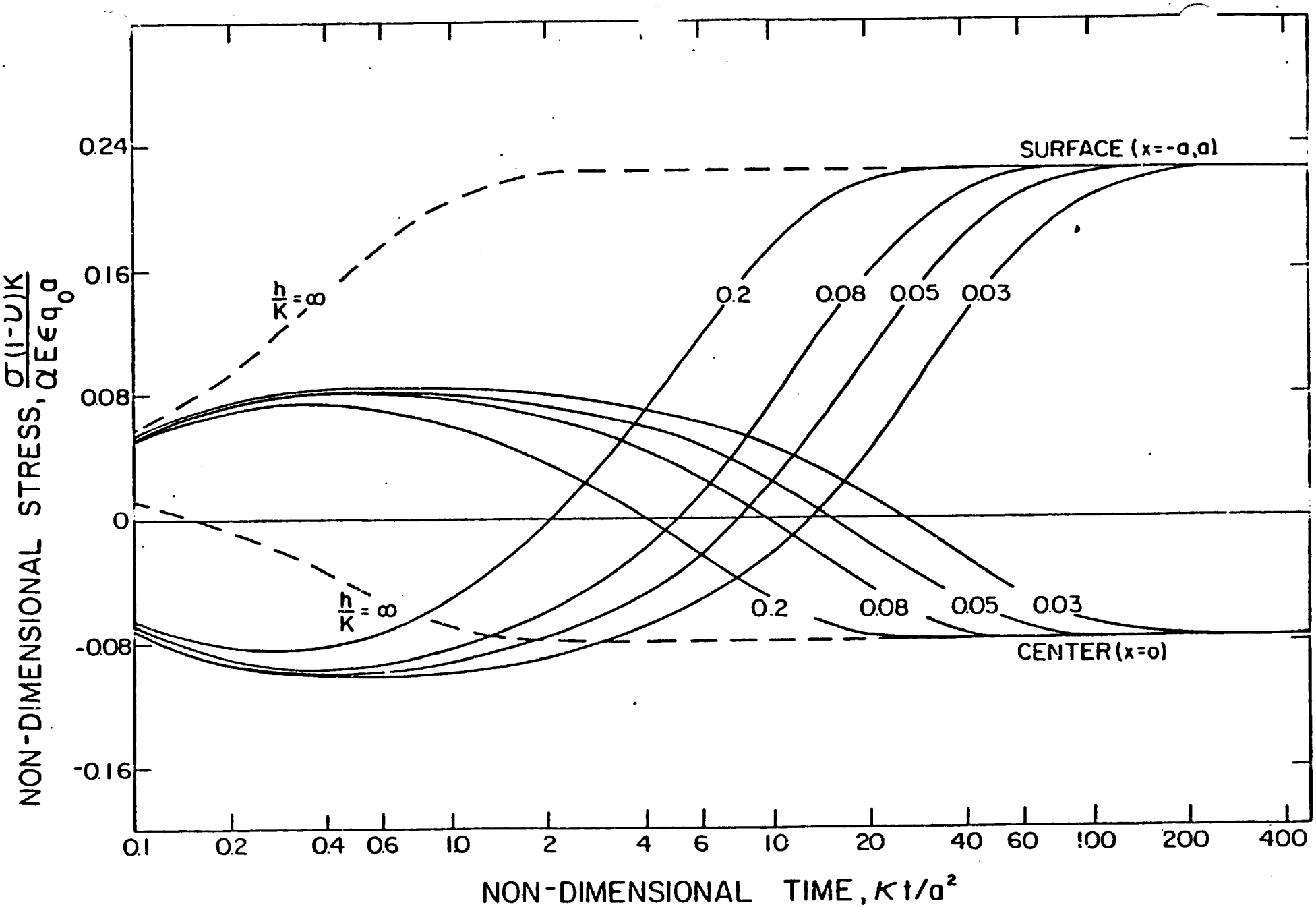

Fig. 4.3.3.6. Time dependence of maximum thermal stress in a partially absorbing flat plate symmetrically heated by normally incident radiation and cooled by convection for various values of h/k (cm.$^{-1}$) with optical thickness, μa = 3 and a = 1 cm.

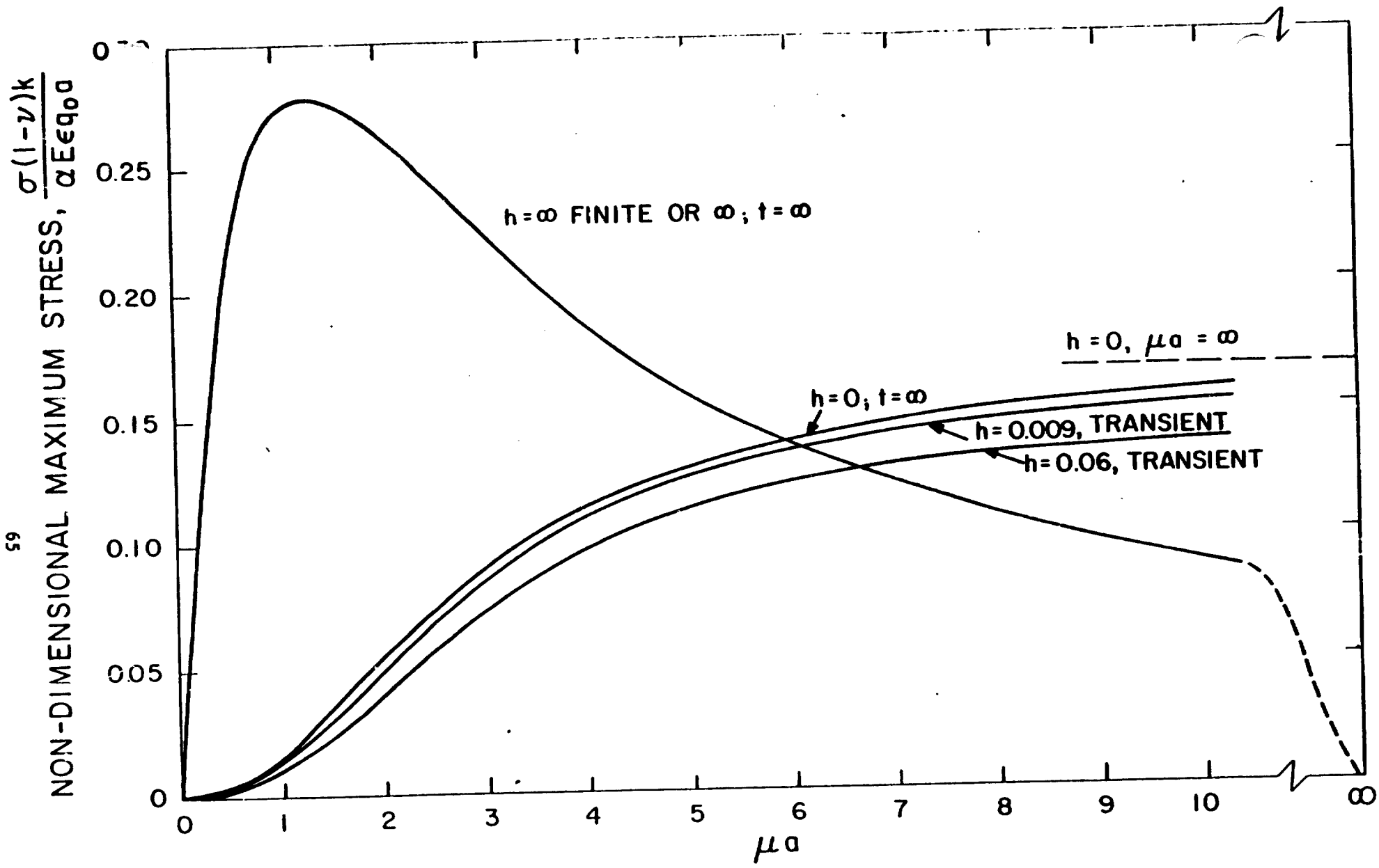

Fig. 4.3.3.7. Maximum tensile thermal stresses in a partially absorbing flat plate symmetrically heated by normally incident radiation and cooled by convection with heat transfer coefficient, h=0, ∞ and finite, k=0.3 watts. $cm^{-1}.{}^{o}C^{-1}$ and a = 1 cm.

$$\sigma_{max}(0,\infty) = \frac{\alpha E \varepsilon q_o e^{-\mu a}}{(1-\nu)K} \{\frac{2}{\mu} + (\frac{a}{3} - \frac{2}{a\mu^2}) \sin h(\mu a)\} . \quad (4.3.3.24)$$

The maximum tensile thermal stress as a function of the optical thickness, μa for the heat transfer coefficient, $h = 0$ is shown in figure 4.3.3.7. Similar to assymmetric heating (figure 4.3.3.3), the stresses are zero at $\mu a=0$, monotonically increases and plateau at high value of μa. Equating σ_{max} in equation 4.3.3.24 with tensile strength S_t, the expression for the maximum permissible heat flux can be given by:

$$q_{max} = \frac{(1-\nu)K S_t e^{-\mu a}}{\alpha E c} \{\frac{2}{\mu} + (\frac{a}{3} - \frac{2}{a\mu^2}) \text{Sin } h(\mu a)\}^{-1} \quad (4.3.3.25)$$

For the two limiting values of the optical thickness μa, equation 4.3.3.25 can be simplified to:

$$q_{max} = \frac{6S_t(1-\nu)K}{\alpha E \varepsilon a} \qquad (\mu a \to \infty) \qquad (4.3.3.26)$$

$$q_{max} = \frac{180 S_t(1-\nu)K}{7\alpha E \varepsilon \mu^3 a^4} \qquad (\mu a << 1) \qquad (4.3.3.27)$$

Heat transfer coefficient, $h = \infty$

For this case, the maximum steady state tensile thermal stress occurs at the surface and is given by:

$$\sigma_{max}(a,\infty) = \sigma_{max}(-a,\infty) = \frac{4\alpha E(\mu a)\varepsilon q_o e^{-\mu a}}{(1-\nu)Ka^2} \cosh(\mu a) \sum_{n=0}^{\infty} \{(\mu^2 + \lambda_n^2)(a\lambda_n^2)\}^{-1} \quad (4.3.3.28)$$

Variation of the maximum steady-state tensile stress as a function of the optical thickness is shown in figure 4.3.3.7. It is important to note in

the figure that the values of the maximum steady-state tensil. stress for heat transfer coefficient, h = ∞ are identical to those for h = finite. As explained before, this is so because the steady-state temperature profile within the plate is independent of h eventhough the absolute magnitude of temperature is an inverse function of h.

To obtain the expressions for the maximum permissible heat flux, q_{max}, two limiting values of the optical thickness were considered namely $\mu a \to \infty$ and $\mu a << 1$. The stresses are given as:

$$\sigma_{max}(a,\infty) = 0 \qquad (\mu a \to \infty) \qquad (4.3.3.29)$$

$$\sigma_{max}(-a,\infty) = \frac{64\alpha E\mu\varepsilon a^2 q_o}{(1-\nu)K\pi^4} \qquad (\mu a << 1) \qquad (4.3.3.30)$$

From equations 4.3.3.29 and 4.3.3.30, the expressions for the maximum permissible heat flux, q_{max} in terms of the tensile strength, S_t can be given as:

$$q_{max} = \infty \qquad (\mu a \to \infty) \qquad (4.3.3.31)$$

$$q_{max} = \frac{\pi^4 S_t(1-\nu)K}{64\alpha E\varepsilon\mu a^2} \qquad (\mu a << 1) \qquad (4.3.3.32)$$

The expressions for q_{max} (equations 4.3.3.26, 4.3.3.27 and 4.3.3.32) result in thermal stress resistance parameters as follows:

$$\frac{S_t(1-\nu)K}{\alpha E\varepsilon} \quad , \quad \frac{S_t(1-\nu)K}{\alpha E\varepsilon\mu^3} \text{ and } \frac{S_t(1-\nu)K}{\alpha E\varepsilon\mu} \qquad (4.3.3.33)$$

It is clear from equation 4.3.3.33 that the analysis of the symmetrically heated and cooled plate results in a new thermal stress resistance parameter $\frac{S_t(1-\nu)K}{E\varepsilon\mu^3}$ in addition to two other parameters $\frac{S_t(1-\nu)K}{\alpha E\varepsilon}$ and $\frac{S_t(1-\nu)K}{\alpha E\varepsilon\mu}$ obtained for assymmetric heating.

F. Summary of the highlights of the results for the thermal stresses in semi-absorbing plate subjected to radiation heating and convection cooling

Due to the importance of thermal stresses in semi-absorbing plate and their relevance to the solar receiving systems, the results for thermal stresses are summarized for the convenience of reader, as follows:

1. For h = finite or ∞, the steady state stresses are minimum for highly transparent ($\mu a \to 0$) and opaque ($\mu a \to \infty$) materials with high values of thermal stress for intermediate values for μa for both symmetric and assymmetric heating cases. On the other hand, for h = 0, steady state ($t \to \infty$) stresses increase monotonically with μa so that semi-transparent materials develop higher values of stress than the transparent ($\mu a \to \infty$) materials.

2. For highly transparent materials ($\mu a \to 0$) with assymmetric heating, the maximum steady state stress is proportional to μ and a^2 for h=finite, 0 and ∞, whereas for symmetric heating, the maximum steady state stress is proportional to μ and a^2 for h=finite and ∞ and to μ^3 and a^4 for h=0.

3. For opaque materials ($\mu a \to \infty$), the maximum steady state stress approaches zero for h=finite and ∞ for both assymmetric and symmetric heating. In contrast, the stress reaches a constant finite value for h = 0.

4. The peak values for steady state stress with h=finite or ∞ occurs at $\mu = 2$ for assymmetric heating, whereas it occurs at $\mu a = 1.334$ for symmetric heating.

5. Although, the magnitude of steady state ($t \to \infty$) stresses in case of assymmetric heating for high values of μa are almost identical for both front and rear cooling, the steady state stresses for lower values of μa as well as the transient stresses for both cases are different. In addition, time to reach the maximum transient stress is smaller in case of front cooling than that in case of rear cooling with a more uniform temperature distribution in case of front surface cooling than that in case of rear surface cooling.

6. Although, the nature of the maximum steady-state stress plots are qualitatively very similar for both assymmetric and symmetric heating cases, the magnitude of the peak stress in assymmetric heating case is smaller than that in symmetric heating case. This is, at least in part, due to the fact that in case of assymmetric heating, the differential thermal strain can be accommodated by bending which is not the case for symmetric heating.

G. General comments

Based on the above mentioned analyses and discussion, the following general comments are made with regard to material properties, component size as well as the system design and operation:

(a) For the high collection efficiency, the reflector and the window should absorb the least amount of radiation whereas the receiver should absorb most of the radiation. Since, for a given intensity of incident radiation, the amount of radiation absorbed in the surface and the interior increases with increasing value of $\varepsilon=1-r$ and μ respectively, high collection efficiency will require:

low ε and μ for reflectors and windows
and high ε and μ for receivers

A close look at these results indicates that the requirements of low ε and μ for reflectors and windows in order to achieve high collection efficiency is compatible with those for high thermal stress resistance. In contrast, the high collection efficiency requires high values for ε and μ for receivers which is incompatible with the requirements of low ε and μ for high thermal stress resistance. However, as $\mu a \to \infty$, the value of steady-state thermal stress approaches zero. Therefore, in order to achieve high collection efficiency and low thermal stresses, the receivers should have practically highest possible value of μa.

(b) Since the peak values of steady state stress with h = finite and = occurs at $\mu a=2$ for assymmetric heating and at $\mu a=1.334$ for symmetric heating, the intermediate values of μa should be avoided in order to minimize thermal stress failure.

(c) For high thermal stress resistance for materials in solar receivers, the component size should be as small as practically possible.

(d) In case of assymmetric heating with cooling at the rear surface, the maximum tensile thermal stress, for small values of optical thickness, μa, occurs in the front face of the plate which is at the highest temperature. This could be very critical for environments which promote fatigue by slow crack growth discussed in a separate section. Slow crack-growth which could occur by stress corrosion or other mechanism, is a thermally activated process and is enhanced by high temperature and stress. Therefore, it is desirable to keep the critical regions (highly stressed) at low temperature in order to minimize the slow crack growth.

(e) A close comparison of the results for two cases of assymmetric heating clearly indicates that the temperature distribution in case of front cooling is more uniform that that in case of rear cooling. Therefore, for a given temperature of the cooling environment the temperature of the front surface will be higher in case of rear cooling than that in case of front cooling. High temperature may result in deleterious effects such as thermal fatigue and melting, etc. In addition, a more uniform temperature distribution in case of front cooling will result in smaller deformation of the plate. Therefore, from design point of view, system with heating and cooling on the same side may be preferred over the one where heating and cooling take place on opposite sides of the plate.

(f) The fact that transient stresses in a partially absorbing plate due to internal heat generation is inversely proportional to the heat transfer coefficient, h, suggests that during the transient heating period of the solar receivers, the working fluid must be circulated at a faster rate to induce high h value. On the other hand, during a sudden decrease of radiant heat flux such as during cloud cover, the value of the heat transfer coefficient, h should be reduced by lowering the circulation rate of working fluid in order to minimize the severity of thermal shock.

(g) The steady-state stress for high values of μa is very small and approaches zero. However, the transient stresses may be of high magnitude even for very high values of μa. These stresses are directly proportional to the radiant heat flux. Therefore, to minimize the thermal stress failure, the transient stresses can be reduced by gradually increasing the incident heat flux towards the final steady-state value rather than subjecting the plate to full value of heat flux at t=0.

(h) Thermal stress resistance parameters for different heat transfer environments can be summarized as:

$$\frac{S_t(1-\nu)K}{\alpha E\varepsilon} \quad , \quad \left[\frac{S_t(1-\nu)K}{\alpha E\varepsilon}\right]^{1/4} \quad , \quad \left[\frac{S_t(1-\nu)K}{\alpha E\varepsilon(1-F_{\lambda_o})}\right]^{1/4}$$

$$\frac{S_t(1-\nu)K}{\alpha E\varepsilon\mu} \qquad \frac{S_t(1-\nu)K}{\alpha E\varepsilon\mu^3}$$

H. Recommendations for future theoretical work

(a) An important situation where the solar receivers will be subjected to thermal shock is the incidence of intermittent cloud cover. The

intermittent cloud cover will cause high thermal stresses inside the structure as a result of thermal shock. These stresses are very complex to evaluate due to the mixed nature of radiation and convection cooling. To date, such stress solutions are not available in the literature. However, it is very important to analyze these stresses for the selection of suitable material and the optimum design.

(b) In the above analyses, the optical properties have been assumed to be independent of temperature and wavelength of the incident radiation. However, it is expected that these properties will vary with temperature and wavelength of the incident radiation. It is, therefore, recommended that the thermal stress analyses should be extended to include these spectral and temperature dependence of the optical properties of the material.

4.4. Thermoviscoelastic Stress Relaxation

4.4.1. General

Under conditions of mechanical stress, materials can exhibit slow deformation by creep. Such creep deformation also is expected to occur under conditions of thermal stress. Ceramic materials will exhibit creep by diffusional processes at levels of temperature at which vacancy concentration and mobility become appreciable. These temperatures correspond to about one half to two thirds of the melting point of the material. Temperature levels in point-focus solar receivers may well reach levels at which creep deformation could be appreciable. For this reason, creep under conditions of thermal stress should be considered in the design and selection for materials of construction of solar receivers.

Creep deformation under conditions of thermal stress, generally is favorable as it leads to stress relaxation. For this reason, the occurrence of creep reduces the probability of failure by thermal stresses. The magnitude of thermal stresses due to external constraints will decrease with increasing time. Therefore, thermal stress relaxation by creep leads to an increase in the thermal condition (i.e. ΔT_{max}, q_{max}, etc.) to which a material can be subjected without thermal stress failure, to a value greater than if no stress relaxation occurred.

In general, the higher the creep rate, the more rapid thermal stress relaxation will occur, with a corresponding greater thermal stress resistance. The derivation of analytical expressions for the magnitude of thermal stress affected by creep is highly complex, if possible at all. In general, the kinetics of creep is a function of the temperature as well as stress. For this reason, in a body subjected to non-isothermal conditions, thermal stress relaxation can occur by a multitude of mechanisms. Complex, numerical methods based on finite element principle are required for such calculations (Poritsky and Fend, 1958). Only for thermal stresses which occur under isothermal conditions due to external constraints such as encountered during thermoelastic instability (buckling), analytical expressions for the stresses and stability condition can be derived for linear creep behavior, i.e., a creep rate which is directly proportional to the stress. For these reasons, derivations of expressions for the purposes of obtaining thermal stress resistance parameters for thermal stress relaxation, in general cannot be obtained unless grossly simplifying assumptions are introduced.

4.4.2. Steady-state heat flow

In such an analytical study, reproduced in Appendix 4.4.2.A, one of the authors of this report (Hasselman, 1967) noted that the rate of creep in a thermal stressed structure corresponding to the stress at the position of lowest temperature, represents a lower bound on the rate of thermal stress relaxation. This concept was applied to a hollow circular cylinder undergoing steady-state heat flow, treated in section 4.1 of this report. It was pointed out that as thermal stress relaxation occurred, the values of the maximum temperature difference or heat flux across the wall could be increased, at a rate such that the maximum value of tensile thermal stress remained constant.

On this basis, the maximum rate of rise of the temperature difference across the cylinder wall for a ceramic material undergoing linear creep was derived to be:

$$\frac{d(\Delta T_{max})}{dt} = \frac{S_t(1-\nu)}{C\alpha\eta} \qquad (4.4.2.1)$$

where

$$C = [2\ln(\frac{b}{a})]^{-1}[\ 1 - \frac{2a^2}{b^2-a^2}\ \ln\ (\frac{b}{a})] \qquad (4.4.2.2)$$

Similarly, the heat flux per unit length can be increased at a rate

$$\frac{d(q_{max})}{dt} = \frac{S_t(1-\nu)K}{C'\alpha\eta} \qquad (4.4.2.3)$$

where

$$C' = [1 - \frac{2a^2}{b^2-a2}\ \ln\ \frac{b}{a}]/4\pi \qquad (4.4.2.4)$$

and η is the viscosity relating the creep rate $\dot{\varepsilon}$ to the stress by:

$$\dot{\varepsilon} = \sigma/\eta \qquad (4.4.2.5)$$

Eqs. 4.4.2.1 and 4.4.2.3 suggest that materials which exhibit maximum thermal stress relaxation should be selected on the basis of the thermal stress resistance parameters:

$$\frac{S_t(1-\nu)}{\alpha\eta} \quad \text{and} \quad \frac{S_t(1-\nu)K}{\alpha\eta} \tag{4.4.2.6}$$

It is of interest to note that the above parameters do not contain Young's modulus as a material property. The reason for this is that the amount of creep strain required for a degree of stress is an inverse function of Young's modulus of elasticity. Since the magnitude of the thermal stresses is directly proportional to Young's modulus, the rate of change of ΔT_{max} or q_{max} are independent of Young's modulus.

Important to note is that these equations represent lower bounds on the rate of rise of ΔT_{max} or q_{max}. As time progresses and the changes in ΔT and q involves changes in the absolute temperature, these rates can be modified.

4.4 3. Remarks

Although to first appearance, thermal stress relaxation appears favorable from the point of view of reducing the magnitide of stress, two unfavorable effects will occur. First, as pointed out previously, thermal stress relaxation under non-isothermal condition, can result in unacceptably high values of residual stress, whenever the material is brought to thermal equilibrium at lower temperature. For most engineering structures or materials, with the exception of tempered glass, the formation of such residual stresses generally is unfavorable for continued satisfactory performance. In addition, thermal stress relaxation can lead to considerable deformation of the component or structure, which also could have an adverse

effect on subsequent performance. It is the view of the writers of this report, that materials for solar receivers should be chosen to keep thermal stress relaxation to an absolute minimum. Conversely, operating temperatures should be kept sufficiently low that creep deformation is prevented.

4.5. Thermal Fatigue ($K_I < K_{Ic}$)

4.5.1. General

Brittle ceramic materials under conditions of static or cyclic stress can exhibit the growth of cracks at levels of stress intensity factor below the critical stress intensity factor (i.e. for $K_I < K_{Ic}$). This phenomenon is referred to as sub-critical crack growth. If for a given stress value or history, the total extent of crack growth is sufficient for the crack to become critical, failure will ensue. For constant or cyclic stress, this mode of failure is referred to as static or cyclic fatigue, respectively.

Subcritical crack growth can also occur under conditions of steady-state or cyclic thermal stress. The resulting failure is referred to as "thermal fatigue." Solar receivers, because of wide temperature excursions and/or non-linear steady-state temperature distributions will be subjected to thermal stress and should be susceptible to failure by "thermal fatigue." In order to take this effect into consideration in the design and selection of materials for solar receivers, the role of the individual factors which effect thermal fatigue behavior, as well as their interaction needs to be well understood.

A framework by which such understanding can be developed is provided by the methodology for the prediction of fatigue behavior of brittle ceramics

based on fracture-mechanical principles. Basically, this methodology requires a knowledge of the size and geometry of the propagating crack, the kinetics of crack growth as well as the stress and temperature history to which the material is being subjected. In principle, with this information, the time required for the propagating crack to become critical (i.e. the time to failure) can be calculated for any stress and temperature history. For constant and cyclic stresses under iso-thermal conditions, expressions in analytical form are easily derived. For transient temperatures and thermal stresses, the time or number of cycles to failure are more conveniently obtained by numerical methods. The results obtained by these latter techniques, however, are less useful for the specific identification of the variables which control thermal fatigue behavior. For this reason, analytical expressions for the time-to-failure t_f for an isothermal steady-state stress, following the approach of Hasselman and Zdaniewski (1978), (Appendix 4.5.1.A), will be presented below:

As shown by Evans (1972), the time-to-failure (t_f) for a brittle material subjected to an isothermal constant tensile stress (σ) is given by:

$$t_f = [2/\sigma^2 Y^2] \int_{K_{Ii}}^{K_{Ic}} [K_I dK_I/V] \qquad (4.5.1.1)$$

where Y is a geometric constant which relates the value of tensile stress to the mode I stress intensity factor, K_I by:

$$K_I = \sigma Y a^{1/2} \qquad (4.5.1.2)$$

where a is the crack size. $K_I = K_I(t = 0)$ and V is the crack velocity which for many materials can be expressed as:

$$V = AK_I^n \exp(-Q/RT) \qquad (4.5.1.3)$$

where A and n are constants and Q is the activation energy for the particular mechanism responsible for the crack growth.

4.5.2. Steady-state heat flow

For steady state-heat flow, substitution of the expression for the maximum tensile stress for any configuration due to an imposed temperature difference, heat flux or other thermal condition in eq. 4.5.1.1, will yield an expression for the time-to-failure in terms of the variables which affect the magnitude of thermal stress as well as those which affect the subcritical crack growth. One should be careful to note that this approach is based on the implicit assumption that the thermal stress intensity factor can be calculated from the value of thermal stress obtained from thermoelastic principles for a continuum and the crack size and geometry as given by eq. 4.5.1.2. This assumption is expected to lead to reliable results as long as the crack size is small (say $\leq$ 1%) relative to the size of the component or structure. For crack sizes, however, which are an appreciable fraction of the body size, the above approach will lead to an over-estimate of the thermal stress intensity factor, due to the effect of the crack on the effective compliance. For this case, the dependence of the thermal stress intensity factor on crack size needs to be established. For this, analytical or numerical techniques are available such as those employed by Stahn et al., (1977a,b), Stern (1979) and Emery and co-workers (1969a,b). Since the present approach neglects the effect of the crack on the compliance, the expressions for the time-to-failure, in fact, are conservative.

For the derivation of the time-to-failure, Hasselman and Zdaniewski (1978) used an expression for the thermal stress of the form:

$$\sigma = C\alpha E\Delta T/(1-\nu) \qquad (4.5.2.1)$$

where C is a geometric constant, which, for instance, for a hollow circular cylinder subjected to steady-state radial heat flow, can be obtained from eq. 4.1.5.1 presented in an earlier section of this report.

Substitution of eq. 4.5.2.1 into eq. 4.5.1.1, and assuming that $K_{Ii} << K_{Ic}$, results in:

$$t_f = [2(1-\nu)^2 \exp(Q/RT)]/[C\alpha E\Delta T)^2 Y^2 A(n-2) K_{Ii}^{(n-2)}] \qquad (4.5.2.2)$$

where K_{Ii} can be obtained (equation 4.5.1.2) knowing the initial stress σ, geometric constant Y and the initial crack length a.

Examination of eq. 4.5.2.2, indicates that a calculation for the time-to-failure for steady-state heat flow, expressed in terms of an imposed temperature difference, involves a total of twelve different variables, including material properties, environmental conditions as well as geometric and dimensional variables.

Eq. 4.5.2.2 can be rewritten in terms of a given value of heat flux q, related to ΔT by $q = C'K\,T$ where C' is another geometric constant. Substitution of this relation for ΔT in eq. 4.5.2.2 results in:

$$t_f = 2(1-\nu)^2 (KC')^2 \exp(Q/RT)/(C\alpha Eq)^2 Y^2 A(n-2) K_{Ii}^{(n-2)} \qquad (4.5.2.3)$$

This equation involves a total of thirteen variables with $(C'/C)^2$ being considered as a single geometric constant.

Additional variables can be introduced by substitution for σ the expression for the maximum tensile thermal stress at steady state ($t = \infty$) for the semi-absorbing flat plate subjected to normally incident radiation. This specific case introduces the reflectivity, the absorption coefficient and the plate thickness as additional variables, bringing the grand total of sixteen independent variables which must be known before a thermal fatigue calculation can be made. For the time-to-failure for a semi-absorbing material subjected to time-dependent incident radiation, the thermal diffusivity must be taken into account as well, bringing the total number of independent variables to seventeen.

The designer may be interested in the maximum temperature difference, heat flux, etc. to which a given component can be subjected to assure a minimum time-to-failure. Such expressions can be obtained by a simple rearrangement of eqs. 4.5.2.2 and 4.5.2.3. For instance, eq. 4.5.2.2 for t_f in terms of ΔT can be rearranged to yield:

$$\Delta T_{max} = [2(1-\nu)^2 \exp(Q/RT)]^{1/2} [(C\alpha E t_f)^2 Y^2 A(n-2) K_{Ii}^{(n-2)}]^{1/2} \qquad (4.5.2.4)$$

and a similar expression for the maximum heat flux:

$$q_{max} = [2(1-\nu)^2 (KC')^2 \exp(Q/RT)]^{1/2} [(\alpha E q)^2 Y^2 A(n-2) K_{Ii}^{(n-2)}]^{1/2} \qquad (4.5.2.5)$$

The present authors are not aware of experimental data which substantiate the equations for t_f or equations for ΔT_{max} and q_{max}.

4.5.3. Thermal cycling

The validity of the above mentioned general approach is provided by the results of Badaliance et al., 1974 and Hasselman et al., 1976 (appendices 4.5.3.A and 4.5.3.B) who studied the effect of sub-critical crack growth on the thermal fatigue behavior of soda-lime-silica glass subjected to a single or multi-cycle quench from a higher temperature into a water bath at lower temperature. The number of thermal cycles required for the onset of fast fracture were obtained by a numerical procedure which takes into account the continuous variation of stress and temperature. Good agreement was found between the experimental and calculated data as shown in fig. 4.5.3.1. It is important to note, however, that the prediction of thermal fatigue behavior also requires an analysis based on the statistical nature of brittle fracture. This statistical effect causes a dependence of the fracture on the magnitude and distribution of the stress leading to differences in fracture probabilities. For this reason, the fracture stress (or critical flaw size) under conditions of thermal stress can differ appreciably from the fracture stress (critical flaw size) determined in a tensile or other type of test. This implies that a statistical analysis of the fracture behavior of brittle ceramics is essential in order to predict the failure in thermal fatigue conditions. For isothermal, constant stress conditions, a number of such statistical studies have appeared in the literature (Fracture Mechanics of Ceramics, 1974, 1978).

In terms of eqs. 4.5.2.2 and 4.5.2.3 for t_f as governed by an imposed temperature difference or heat flux, the following two parameters can be defined for the selection of the brittle ceramic with highest thermal fatigue resistance:

$$[(1-\nu)^2 \exp(Q)]/\alpha^2 E^2 (n-2) A \qquad (4.5.3.1)$$

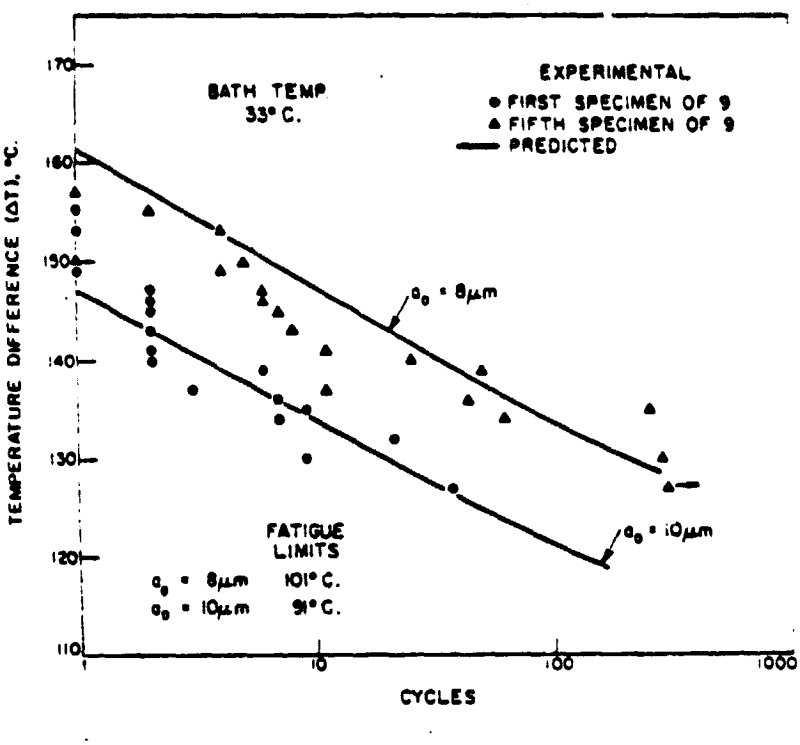

Fig. 4.5.3.1. Predicted and experimental cycles-to-failure of soda-lime-silica glass rods (initial flaw depth = 8.6 μm) subjected to thermal fatigue by quenching into water bath at 33°C.

and

$$K^2[(1-\nu)^2\exp(Q)]/\alpha^2 E^2(n-2)A \qquad (4.5.3.2)$$

Point-focus solar receivers are expected to be susceptible to thermal fatigue because of the high heat fluxes involved in addition to the rapid variation in heat flux as the result of variable cloud cover. It should be evident from the above discussion that for reliable predictions of the thermal fatigue behavior, a great deal of data need to be generated. The magnitude of thermal stresses and operating temperatures must be known quite accurately. In addition, numerous material properties, the size and geometry of the failure initiating flaws as well as the parameters which describe the statistical nature of fracture need to be evaluated. The parameters which control the sub-critical crack growth are a function of environmental conditions which can be highly variable. Furthermore, because of the wide temperature ranges at which solar receivers are expected to operate, it is conceivable that the crack growth may proceed by a number of different mechanisms simultaneously. This is particularly true under conditions of rapid heating and cooling. At the present time, it is quite likely that complete information required for thermal fatigue calculations is not available for even one brittle ceramic.

Establishing a data base for the prediction of thermal fatigue behavior of all possible designs and candidate materials represents a task of considerable magnitude, not only in terms of technical effort, but also in terms of time.

For these reasons, it is recommended that thermal fatigue analysis be limited to final design configurations and only for those materials which are likely to give satisfactory service.

4.6. Critical Crack Propagation ($K_I \geq K_{Ic}$)

4.6.1. General

As discussed in an earlier section of this report, thermal environments can be encountered in practice, for which even in the best materials available, the onset of thermal stress fracture cannot be avoided. Under these conditions, thermal stress resistance of brittle ceramics is based on their ability to undergo minimum crack propagation. In this manner, the ceramic will undergo a minimum change in its physical characteristics, such as strength and its geometry, so that it still can continue to satisfy the performance criteria of its specific application. As pointed out earlier, this particular philosophy for material selection is common in the refractories industries.

It is clear that derivations of selection rules based on a minimum change in physical characteristics and geometry following thermal stress failure requires analyzing the variables which affect the propagation of cracks in brittle materials for thermal stress conditions such that $K_I \geq K_{Ic}$.

Literature studies for crack propagation in thermal stress fields are far less in number than those concerned with the analysis of thermal stresses and the onset of crack propagation. Nevertheless, a small number of such studies related to the fracture-mechanics of crack propagation have been published (Hasselman 1969, 1971a,b; Stahn and co-workers 1977a,b; Bazant and co-workers 1979; Emery and co-workers 1966, 1969b). In general, these studies indicate that the analysis of crack propagation in thermal stress fields is relatively complex. One of the reasons for this complexity is that the propagation of cracks affects the magnitude and distribution of the thermal stresses due to the change in compliance of the structure or material undergoing fracture. Crack interaction introduces a further

degree of complexity. For these reasons, at present, analysis of crack propagation in thermal stress fields must rely on numerical methods. As described earlier, such numerical methods are less convenient for assessing the individual variables which control crack propagation in thermal stress fields. However, analytical solutions for the stability and propagation of cracks in simple mechanical models were obtained in studies by Hasselman (1969, 1971a) reproduced as appendices (4.6.1A and 4.6.1B) to this report. These analytical approaches were permitted by the judicious choice of models consisting of a material tri-axially or uniaxially constrained from shrinking on cooling. From a continuum point of view, these constraints assure spatial uniformity of the thermal stress field regardless of the extent of crack propagation. The material was assumed to contain a uniform density of cracks of equal size. The complexity of the details of the stress distributions was circumvented by expressing the elastic response of the material in terms of an effective bulk or Young's modulus, expressed in terms of Young's modulus of the crack-free material and the density and size of the cracks. Crack interaction effects were assumed to be absent. In respect to this latter assumption, it should be noted, as indicated by preliminary results of studies currently underway by the present writers, that as long as co-planar crack propagation is avoided, crack interaction has a beneficial effect on both the onset as well as the extent of crack propagation in thermal stress fields.

4.6.2. Analytical results

The analytical studies for the two different mechanical models resulted in the same conclusions with regard to the nature of crack propagation and the role of the pertinent material properties. For this reason, the principal results for only one of the models will be presented

here. Reprints of the two analytical studies (Hasselman, 1969, 1971a) presented as appendices to this report contain further information on the assumptions and mathematical details.

For the thin flat plate, with a uniform density N of cracks of equal length ℓ, uniaxially prevented from shrinkage on cooling by rigid constraints, the critical temperature difference on cooling, ΔT_c, required for crack instability is (Hasselman, 1971a):

$$\Delta T_c = (2\gamma_f/\pi\alpha^2 E_o \ell)^{1/2}(1 + 2\pi N\ell^2) \qquad (4.6.2.1)$$

where E_o is Young's modulus of the crack-free plate.

Figure 4.6.2.1 shows the dependence of ΔT_c on ℓ in dimensionless form for two values of crack density, indicated by two solid lines. These curves show that high values of ΔT_c can be achieved for either small or large crack sizes. This latter effect arises bacause at the large values of crack size the compliance of the plate is affected significantly. A minimum in ΔT_c occurs at a crack size, $\ell = \ell_m$.

From the point of view of the relevant material properties, for a given crack size and density, ΔT_c can be increased by selection of a material with a higher value of the parameter:

$$(\gamma_f/\alpha^2 E_o)^{1/2} \qquad (4.6.2.2)$$

It is important to note that this latter conclusion could also be obtained from the previous discussion on the criteria for the onset of thermal fracture, simply by expressing the fracture stress in terms of the appropriate fracture-mechanical parameters.

The validity of the fracture-mechanical approach is demonstrated further by an additional fracture phenomena of major importance to the

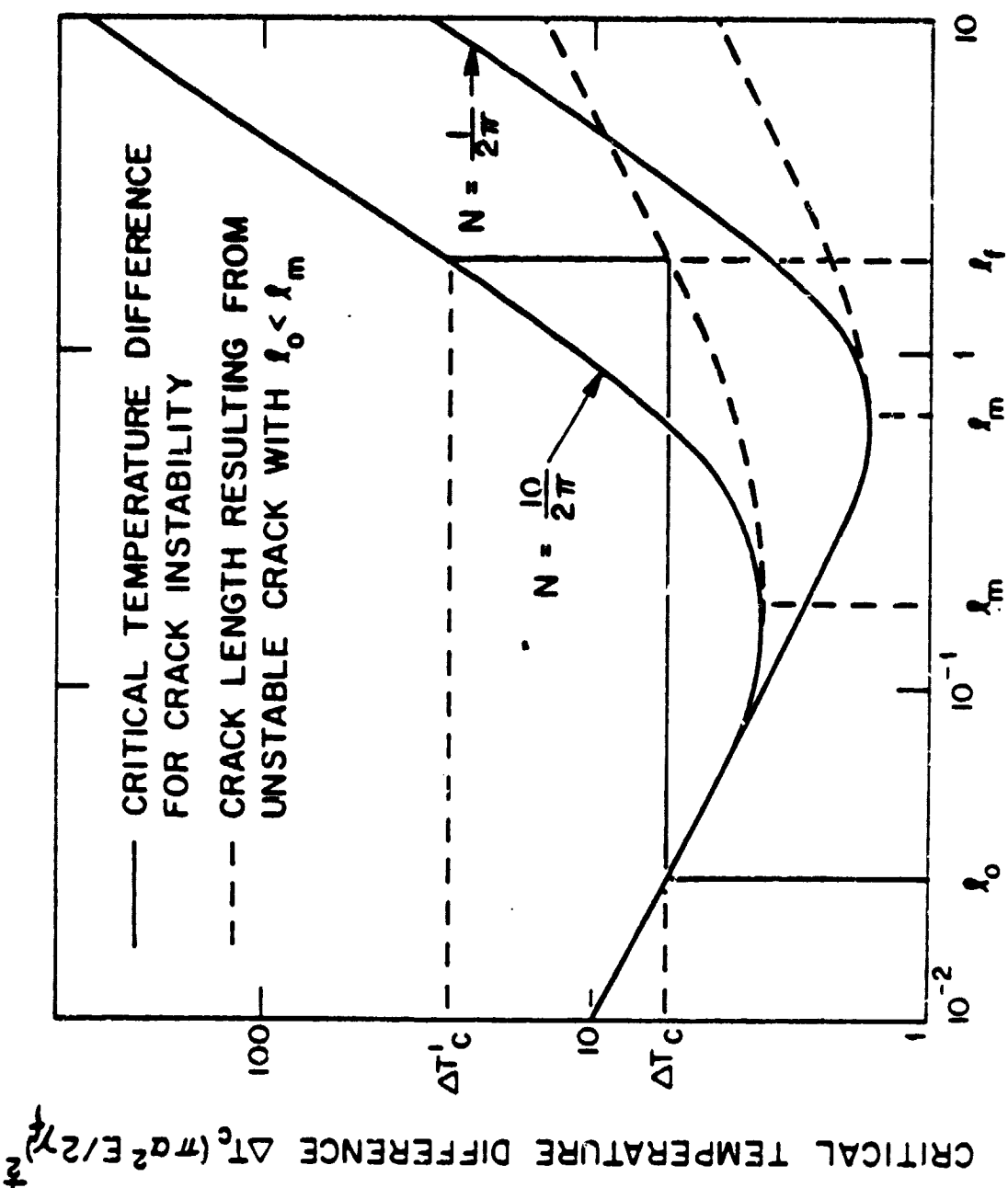

Fig. 4.6.2.1. Crack stability and propagation behavior for a rigidly held thermally stressed flat plate with two crack densities (Hasselman, 1971a)

selection or development of materials and the interpretation of fracture data as follows:

Referring to fig. 4.6.2.1, it is important to note a very basic difference in the propagation behavior of cracks with initial crack size $\ell_o \lesssim \ell_m$, at the onset of instability at ΔT_c. For $\ell > \ell_m$, at $\Delta T \gtrsim \Delta T_c$, the relation between crack length and ΔT is given by eq. 4.6.2.1. This mode of crack extension is referred to as a "stable" crack propagation. For $\ell_o < \ell_m$, however, after the onset of crack propagation at ΔT_c, the elastic energy released exceeds the energy required to create the new crack surfaces. This excess energy is converted to kinetic energy of the propagating crack assuming no other losses. This is referred to as dynamic or unstable crack propagation. The crack will cease propagation at a final crack length ℓ_f, when all the kinetic energy and additional released elastic energy is transformed into surface fracture energy. For $\ell_o << \ell_m$, this value of final crack length can be derived to be

$$\ell_f = (4\pi N \ell_o)^{-1} \qquad (4.6.2.3)$$

This expression indicates that for a given crack density, the crack length which results from unstable crack propagation is inversely proportional to the initial crack length and crack density and <u>independent</u> of other material properties. Low values of ℓ_f can be achieved only by <u>increasing</u> the initial crack length and the crack density. The implications of this conclusion for materials for which the initial crack length, ℓ_o is not easily ascertained, can be examined by substituting into eq. 4.6.2.3 the Griffith relation between crack size, tensile fracture stress, fracture surface energy and Young's modulus (for a single crack in a thin flat plate) which yields:

C-2

$$\ell_f = \sigma_f^2/8N\gamma_f E \qquad (4.6.2.4)$$

This expression indicates that dynamic crack propagation is expected to be extensive in materials with high initial fracture stress, and low values of crack density, fracture surface energy and Young's modulus.

Materials with least dynamic crack propagation should be selected on the basis of the high values of the ratio:

$$N\gamma_f E/\sigma_f^2 \qquad (4.6.2.5)$$

This conclusion can be illustrated further by deriving the tensile fracture strength (σ_a) retained by a material following dynamic crack propagation. With the aid of the Griffith relation (in terms of surface fracture energy) this value of strength can be expressed by:

$$\sigma_a = (\gamma_f E/\sigma_f)(16N/\pi)^{1/2} \qquad (4.6.2.6)$$

This expression also indicates that high strength retention requires high values of fracture surface energy, Young's modulus and low values of original fracture stress. Specifically, it indicates that the strength retained after fracture is inversely proportional to the original strength of the material before fracture. Similar conclusions can also be derived for different mechanical models; dimensional analysis can be used to establish their general validity.

4.6.3. Discussion

From the point of view of the selection of materials with optimum thermal shock resistance, it is critical to note that the requirement of low or moderate strength and high values of Young's modulus to minimize

the extent of dynamic crack propagation is exactly opposite to the requirement of a high value of fracture stress and low Young's modulus to prevent the onset of thermal stress fracture. These opposite requirements have created considerable confusion in the selection of materials for thermal stress applications and the interpretation of fracture data.

For thermal environments in which the thermal stress fracture for even the best material is likely to occur, attempts could be made to increase the thermal stress resistance by increasing strength. This frequently is the only possible alternative since such properties as coefficient to thermal expansion, Young's modulus, Poisson's ratio, thermal conductivity are not easily modified. This approach can have two effects. The strength improvements may be adequate such that the thermal stress failure is avoided, as desired. However, very severe thermal environments may require improvements in strength by an order of magnitude or so. Such improvements are not easily achieved with presently available materials and the current state of technology. In this case, any improvement in strength which can be obtained in practice will not be sufficient to prevent the onset of thermal stress fracture, but will only result in more extensive crack propagation and a further reduction in retained load-bearing ability. This latter phenomenon is of vital importance in the selection of materials for thermal environments in which thermal stress failure is likely to occur. In the view of the present writers, this may well be the case for the components of a solar receiver directly exposed to the incident solar radiation.

A considerable body of experimental evidence for this type of fracture behavior of brittle ceramics was obtained in a number of laboratory

studies (Hasselman 1970, Gupta 1972, 1973, Mai and Atkins 1975, 1976). Many of these studies concentrated on measuring both the severity of thermal shock required for the onset of fracture and the extent of crack propagation as it affected the retained tensile load-bearing ability of the ceramic following fracture. Many of these results are presented in a number of the appendices to this report. However, the implications of these results for the selection of brittle ceramics for severely thermally stressed solar receivers are sufficiently important that a brief overview and discussion of their significance will be included in the main body of this report.

For this purpose, fig. 4.6.3.1, indicates schematically the length of a crack and corresponding retained tensile strength as a function of severity of thermal shock. This latter quantity could include a temperature difference, the magnitude of incident heat flux, rate of heating, etc. Typically, in laboratory studies, the severity of thermal shock is measured by the temperature difference between the specimen and the quenching medium in a thermal quench experiment where the specimens at higher temperature are quenched in water, oil or similar other fluids at lower temperature.

For dynamic crack propagation at ΔT_c, the crack length and retained strength show a discontinuity. In contrast, for stable crack propagation no such discontinuity occurs, with crack length and retained strength, increasing and decreasing, respectively, in a monotonic manner at $\Delta T > \Delta T_c$.

Figure 4.6.3.2 compares the strength behavior of two different aluminum oxides subjected to a water quench, described in further detail in Appendix 4.6.3.A. It should be noted, that the alumina with the initially higher strength requires a higher quenching temperature difference for the

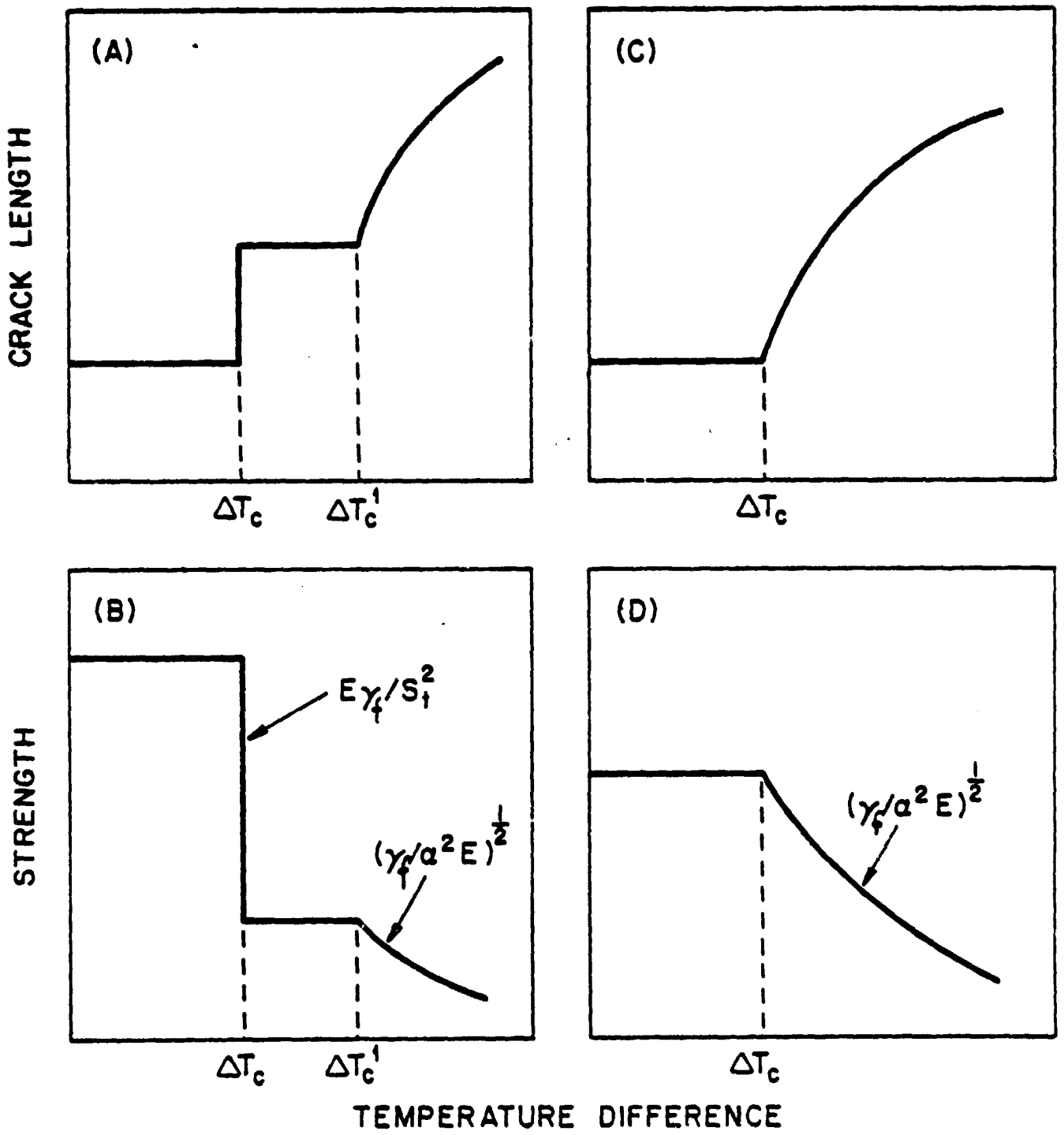

Fig. 4.6.3.1. Crack propagation and strength behavior for (A) and (B): Unstable and (C) and (D): stable mode of crack propagation under conditions of thermal shock (Larson et. al., 1974)

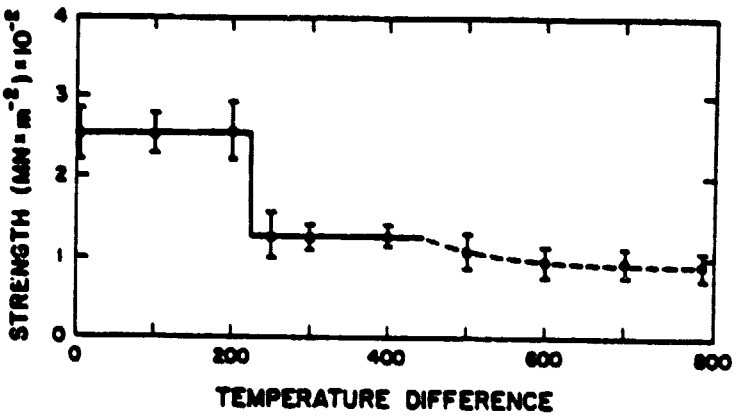

(a)

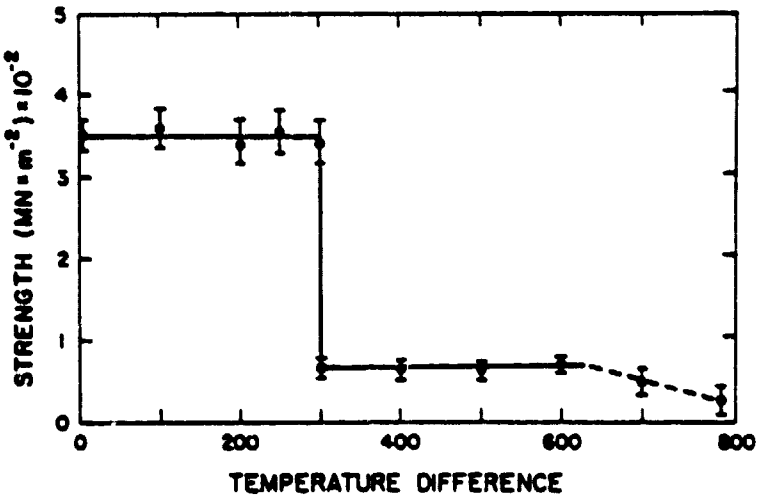

(b)

Fig. 4.6.3.2. Comparative strength behavior of two aluminas with differing initial strength subjected to thermal shock by quenching into water. a: AL-300, b: AD-96. (Experimental data from Hasselman, 1970)

onset of thermal stress fracture than the alumina with the lower value of initial strength. This observation is entirely in accordance with the selection rules presented earlier for avoiding thermal stress fracture altogether. On the other hand, if the relative thermal stress resistance is compared on the basis of tensile strength retained, the alumina with the initially lower strength has the greater thermal stress resistance. Clearly, for a severity of thermal shock corresponding to $\Delta T \leq 300^{\circ}C$ the alumina with the initial higher strength is obviously the material with the higher thermal stress resistance whereas, for a severity of thermal quench corresponding to $\Delta T > 300^{\circ}C$ which will cause the onset of fracture in both aluminas, the material with the lower initial strength should be the logical choice. These two sets of data are quite illustrative of the two different philosophies for defining thermal stress resistance. In general, material selection based on limited crack propagation is far more common in high-temperature technology than material selection based on the resistance to the onset of thermal stress fracture.

The differences in the two different philosophies for defining thermal stress resistance is illustrated further by the comparative strength behavior of polycrystalline alumina and beryllia subjected to a water quench shown in fig. 4.6.3.3 (Krchn, et al., 1973). From the point of view of avoiding thermal stress fracture, the beryllium oxide is the preferred material. However, the strength retention behavior of the beryllia is inferior to that of the alumina.

Glassy materials generally undergo extensive crack propagation with little or no strength retained following fracture as illustrated by the

data of Badaliance et. al. (1974) for a soda-lime-silica glass, shown in fig. 4.6.3.4. This effect can be attributed to a very small flaw size in the glass compared to the flaw size generally found in polycrystalline ceramics or in other words, a low fracture toughness and Young's modulus and comparatively high strength.

As indicated by the observations of Crandall and Ging (1955) for aluminum oxide and Hasselman and Shaffer for zirconium carbide (1962), unstable crack propagation can occur in an almost explosive manner with the resulting cracks extending completely through the sample. This, in effect, corresponds to zero retained strength. For this reason, for designs involving thermal shock of such severity that thermal stress fracture cannot be avoided, high-strength materials which fail in a highly unstable mode should not be selected. Instead, materials with only moderate strength (i.e. large flaw size) will be found to be far more suitable in view of their stable nature of crack propagation.

The advantage of the initially lower strength which results in relatively smaller strength loss accompanying stable crack propagation is indicated in fig. 4.6.3.5(a) which shows the retained strength of a high-alumina refractory subjected to a water quench as measured in a study by Larson et. al (1975), reproduced in Appendix 4.6.3B. The discontinuity in strength at ΔT_c, typical for unstable crack propagation is absent. In fact, it was found that the cracks formed even during the most severe quench were difficult to detect by optical or other means. This is due to the coarse and heterogeneous microstructure of these types of materials. It is evident that this type of crack propagation is preferred, since the material is still entirely capable of providing adequate service in its intended applications such as furnace linings, thermal insulation, etc.

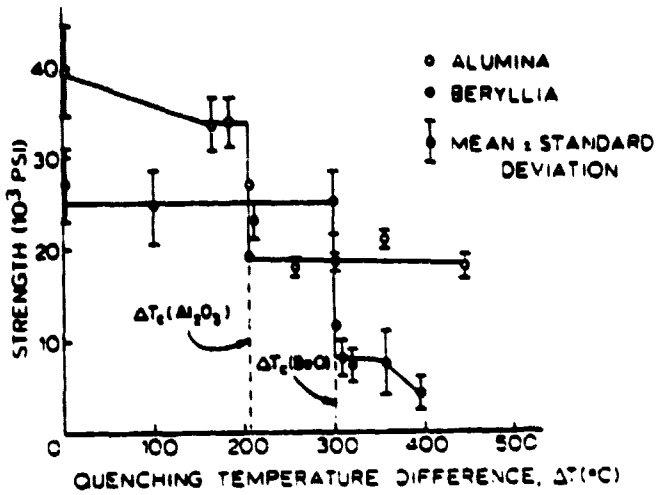

Fig. 4.6.3.3. Comparative strength behavior of polycrystalline beryllia and alumina following thermal shock by quenching into a water bath. (Krohn, et al., 1973)

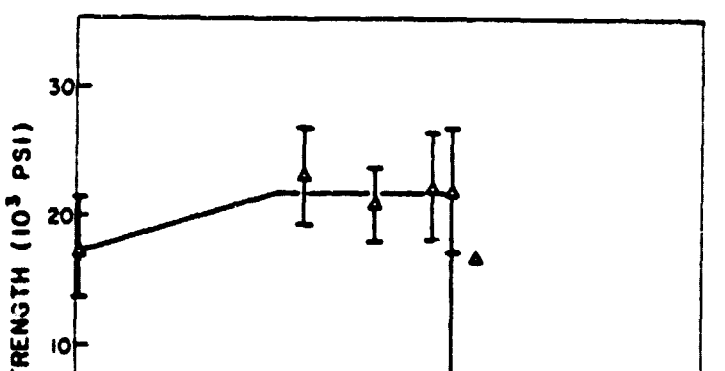

Fig. 4.6.3.4. Strength behavior of soda-lime-silica-glass rods following thermal shock by quenching into a water bath. (Badaliance et. al., 1974)

Similar results for a number of refractories showed that the strength retained was proportional to the value of the parameter $(\gamma_f/\alpha^2 E)^{1/2}$ as predicted by the analysis of the stability and propagation of cracks in thermal stress field, presented earlier.

It is important to note, however, that whether a brittle ceramic will fail in a stable or unstable manner depends on the nature of thermal shock, particularly in regard to the number of cracks which are nucleated during the thermal fracture. Briefly, as can be ascertained from fig. 4.6.2.1, a decrease in crack density for a given crack length can change the mode of fracture from a stable to an unstable one even in the same material. Evidence for the validity of this conclusion provided in the paper of Larson and Hasselman (Appendix 4.6.3B) is shown in fig. 4.6.3.5(b), which shows the strength behavior of the same alumina refractory of fig. 4.6.3.5(a), but subjected to radiation heating. As indicated by the discontinuity in the strength curve, failure occurred by unstable crack propagation.

This latter observation together with those of Crandall and Ging (1955) and Hasselman and Shaffer (1962) suggests that severe thermal shock on heating can be more damaging than thermal shock by cooling. This suggestion can be rationalized by noting that on cooling, such as in a quench, much, if not all, of the surface is placed in tension. This provides an opportunity for the nucleation of many cracks. On the other hand, in case of heating of spheres, cylinders or plates, only a point, line or plane within the material is placed in tension. Therefore, for a given geometry and volume of material, the number of cracks nucleated per unit volume is expected to be much less during transient heating than during cooling. Correspondingly, the extent of crack propagation is expected to be higher in heating than in cooling.

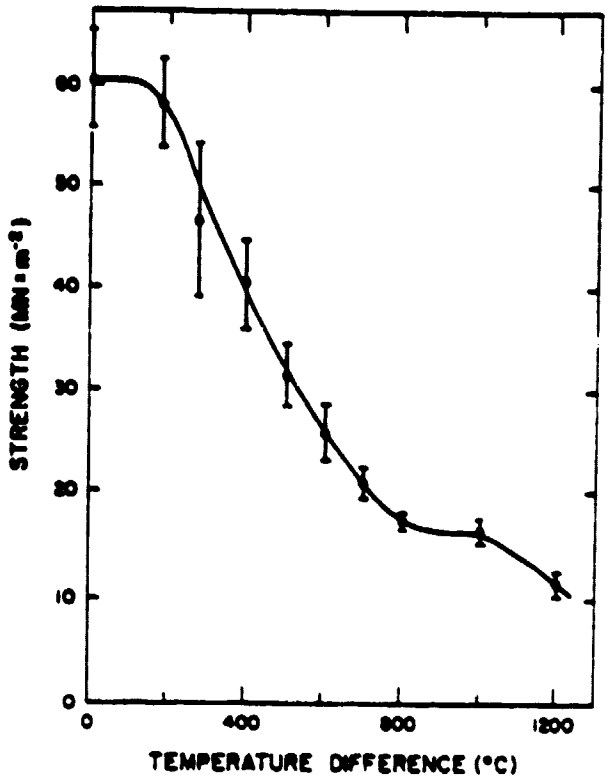

(a)

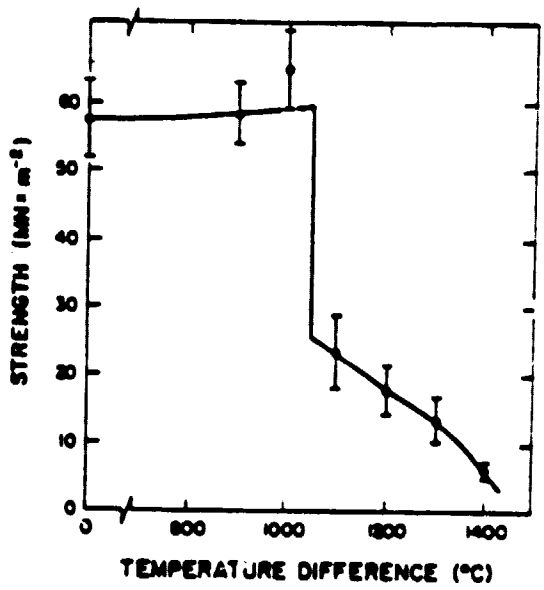

(b)

Fig. 4.6.3.5. Strength behavior of high-alumina refractory following thermal shock by: a, quench into water and b, radiation heating. (Larson et al., 1975)

For the same reasons, for a given type of thermal shock (heating or cooling) a size effect is expected. Large sized bodies are expected to exhibit more unstable and more extensive crack propagation than specimens of smaller size. It is anticipated that certain geometries may be less susceptible to such extensive crack propagation than other geometries. However, verification of this conclusion will require more experimental and theoretical work.

In summary, for thermal shock of such severity that the nucleation of thermal stress fracture cannot be avoided, material selection should be based on the criterion that the extent of crack propagation be kept to a minimum. This requires materials with moderate strength, high Young's modulus of elasticity, high surface fracture energy, low coefficient of thermal expansion and large number of cracks nucleated during fracture. A small component size is also preferred.

The above recommendations should be relevant to solar receivers. For these, it is anticipated that during sudden heating or cooling as the result of the passage of a cloud, the magnitude of the thermal stresses will approach or exceed the fracture stress. Depending on the material of construction, this could result in explosive, catastrophic failure. If so, the designer may be tempted to choose or develop a material with increased strength. As discussed, this attempt if not successful will only result in increasingly catastrophic crack propagation. The alternative, preferred approach is to search for a material with lower strength, high fracture toughness, high Young's modulus and low coefficient of thermal expansion such that failure will take place by stable crack propagation. For many materials, this can be achieved simply by incorporating a 15-20% pore phase.

Furthermore, large monolithic components should be avoided as well. Instead, an assembly of small, loosely interlocked sub-components also is recommended, whenever practical.

5. SUMMARY AND DISCUSSION OF THERMAL STRESS RESISTANCE PARAMETERS AND COMMENTS ON INDIVIDUAL PROPERTY DATA

5.1. Thermal Stress Resistance Parameters

Table II summarizes the thermal stress resistance parameters presented in the previous sections of this report. It should be noted that in presenting these parameters, redundancy has been avoided as much as possible. For example, the parameters for thermal buckling failure as listed in Table II are appropriate for slender columns with narrow width. Replacing E in these parameters by $E/(1-\nu^2)$ results in equivalent parameters, appropriate to plates. In many of the other parameters listed in Table II for steady-state or transient heat transfer, deletion of the term $(1-\nu)$ converts the parameter appropriate for a multi-axially stressed configuration to a corresponding uni-axial one. Furthermore, the parameters appropriate for radiation heating, by the addition or deletion of the exponent 1/4 can be converted to radiation temperature (t_{max}) or radiation heat flux (q_{max}), respectively. Even with these simplifications, Table II contains a total of twenty-seven non-redundant thermal stress resistance parameters. The two parameters, $S_t(1-\nu)/\alpha E$ and $S_t(1-\nu)K/\alpha E$ listed under steady-state and transient heat transfer, although dimensionally of the same form, nevertheless apply to completely different measures of thermal stress resistance.

It is critical to note that the role of the individual material properties which affect thermal stress resistance differs from one parameter to another. For this very reason no general statement can be made of the relative thermal stress resistance for a given set of different materials. Such relative thermal stress resistance can be

TABLE II. Summary of Thermal Stress Resistance Parameters for Brittle Ceramics

A. Steady-State Heat Flow or Isothermal Conditions:

$S_t(1-\nu)/\alpha E$; $S_t(1-\nu)K/\alpha E$; $S_c(1-\nu)/\alpha E$

$S_t(1-\nu)/\alpha\eta$; $S_t(1-\nu)K/\alpha\eta$; $\dfrac{S_t(1-\nu)}{E\Delta\alpha\Delta T}$

B. Transient Heat Transfer:

$S_t(1-\nu)/\alpha E$; $S_t(1-\nu)K/\alpha E$; $S_t(1-\nu)\kappa/\alpha E$

$\{S_t(1-\nu)K/\alpha E\varepsilon\}^{\frac{1}{2}}$; $\{S_t(1-\nu)K/(1-F_{\lambda_o})\alpha E\varepsilon\}^{\frac{1}{2}}$;

$\dfrac{S_t(1-\nu)K}{\alpha E\varepsilon\mu}$; $\dfrac{S_t(1-\nu)K}{\alpha E\varepsilon\mu^3}$

C. Thermal Buckling:

α^{-1} ; $S_t/\alpha E$; $S_t^2/\alpha E^2$; $(S_t/\alpha^2 E)^{\frac{1}{2}}$;

$S_t/\alpha^2 E$; $S_tK/\alpha^2 E$; $(S_t/\alpha^3 E)^{\frac{1}{2}}$; $S_t/\alpha^3 E$;

$S_tK/\alpha^3 E$

D. Crack Propagation

$(1-\nu)^2[\exp(Q/RT)]/\alpha^2E^2(n-2)A$

$(1-\nu)^2[\exp(Q/RT)]K^2/\alpha^2E^2(n-2)A$

$(\gamma_f/\alpha^2E)^{\frac{1}{2}}$; γ_fE/S_t^2

defined only if the heat transfer environment, failure mode, criterion of thermal stress resistance have been established.

Furthermore, it should be noted that these parameters consider thermal stress failure only, without considering other performance criteria, which will add a further complexity in the selection of materials. In fact, the criterion for high thermal stress resistance may well be incompatible with material requirement for other functional purposes. As an example, a material simultaneously may be required to exhibit high thermal stress resistance and good thermal insulating property. The first requirement demands a material with high thermal conductivity, whereas low thermal conductivity is essential to meet the second requirement. A similar contradiction exists for materials which may undergo catastrophic thermal stress failure, but which nevertheless may be subjected to mechanical stresses of high magnitude. The first requirement requires a low to moderate tensile strength in order to keep the extent of crack propagation to a minimum. In contrast, high tensile strength is required to meet the second requirement. Clearly trade-offs need to be made. Alternatively, major re-designs could be in order, if the material properties required for high thermal stress resistance are found to be incompatible with other functional requirements, to an extent that appropriate trade-offs cannot be made with the perhaps limited number of potential candidate materials.

5.2. Comments on Design Values and Selection of Property Data

For purpose of analytical convenience, the thermal stress resistance parameters presented above, were derived on the assumption that ceramic materials have well-defined values for their various properties. In practice, however, this assumption is far from the truth. In fact, for

a number of reasons, considerable variation in ceramic property values can be encountered.

A major reason for the variability in property values can be attributed to the lack of reproducibility of the manufacturing methods for ceramic materials, which generally are based on powder-metallurgical techniques. Such techniques are highly sensitive to even slight variation in powder characteristics such as particle size distribution, particle shape, impurities, pressure used in green-forming or hot-pressing, firing temperatures and times as well as heating and cooling rates. An extensive literature for these phenomena is available. Such lack of reproducibility in the processing variables results in variation in the microstructural and other variables which critically affect many of the material properties. Such microstructural variables include porosity (including pore amount, shape and size), grain size distributions, amount and distribution of second phase impurities and many others.

A second reason for major property variation is their time-dependent behavior resulting from environmental effects encountered during operation such as corrosion, erosion, sub-critical or catastrophic crack growth, pore-migration, grain-growth, micro-cracking and other effects.

A third, and not insignificant reason for the variability in ceramic property values is the uncertainty in establishing these values due to systematic, statistical and other effects. Property data frequently are found to depend on the technique (with inherent assumptions) as well as the environmental conditions including atmosphere, specimen geometry and size, and other variables, under which they are measured. Frequently,

significant variations in property values can be found by different investigators for the same material, measured by identical testing procedures.

Regardless of the reason for the variability in property data, the design engineer should be aware that such variability exists. Handbook values should be treated with a great deal of caution. The reliability of available property data should be assessed in terms of the sophistication and the assumptions inherent in the measurement technique, specimen quality and the statistical significance of the data. Property data obtained from materials made under closely controlled laboratory conditions can differ significantly from the property data for materials made by mass production methods. Special caution is advised with data for which the pertinent test conditions are not supplied. Frequently, such data are given in qualitative terms such as "excellent, good or poor." This latter statement applies particularly to data for thermal shock resistance, which neither provide information on the test method nor by which criterion such thermal shock resistance is defined.

Of the material properties which affect thermal stress resistance, some are more susceptible to variations than others. Only minor uncertainties are expected with data for the coefficient of thermal expansion. This property is measured easily with relatively simple, standard equipment. Furthermore, the coefficient of thermal expansion is not affected by micro-structural variation such as grain size or pore content. Unless excessive, impurity content has little or no effect on the value of coefficient of thermal expansion. Micro-cracking in brittle composites or polycrystalline materials can alter the values of the coefficient of thermal expansion significantly. But then, micro-cracking generally decreases the coefficient of thermal expansion, which from the point of view of thermal stress resistance, must be considered favorable.

Elastic properties, too, can be measured by a number of straight forward methods. Elastic property data obtained by acoustic methods should be considered highly reliable. Data obtained by measurements of strains or deflections, especially at high temperature, should be treated with somewhat greater caution. Some variation in elastic properties are expected as the result of variability in porosity or the presence of second phase. The pore morphology and distribution of second phases also affects elastic behavior. The relative influence of these effects will be governed by the control and the reproducibility of the manufacturing process. Mirco-cracking can have a profound effect on elastic behavior, generally favorable to thermal stress resistance. Such micro-cracking is a function of the grain size of the material which controls the size of the micro-crack pre-cursors, i.e. the pore at triple-points and grain boundaries. Growth of such pre-cursor micro-cracks could cause time-dependent elastic behavior due to the gradual growth of micro-cracks with time. Service conditions such as corrosive effects could cause considerable decreases in elastic property values. The elastic moduli of materials which have undergone thermal stress failure can be significantly below the values for the unfractured material at the time of installation.

Optical properties pertinent to thermal stress resistance (i.e., the reflectivity, emissivity and absorption coefficient) can be measured by straight-forward methods, although such measurements at high temperatures can be prone to experimental difficulties. Reflectivity is expected to be controlled by the nature of the surface roughness and can be affected considerably by the presence of foreign matter, such as dust on the surface. In practice, then, reflectivity may exhibit a strongly

time-dependent behavior, depending on the specific environmental conditions encountered in practice.

The absorption coefficient is expected to be time-dependent due to a possible pick-up and/or migration of impurities. Even for materials with very low absorption coefficient the transmission of radiation through a material can be strongly effected by scattering at such micro-structural features as a residual pore phase (with size being very critical) and grain-boundaries. Even slight differences in such features can create major differences in the optical transmissivity. Time-dependent pore migration or pore growth as well as grain growth would lead to a time-dependent optical transmission under service conditions.

The thermal conductivity and thermal diffusivity generally exhibit property value variations well in excess of the relative variations found in the coefficient of thermal expansion, elastic and optical behavior. Compilations of data for the thermal conductivity can show data scatter of an order of magnitude at a given temperature for nominally the same material. This excessive scatter in data can be attributed to differences in material quality as well as major experimental difficulty in obtaining reliable data especially at high temperature. Thermal conductivity as well as thermal diffusivity are very strongly affected by impurity levels as well as the presence and the morphology of a pore phase and/or second phase inclusions. The presence of cracks especially at the lower temperature levels can cause a major decrease in the ability of a material to conduct heat. Unknown or unaccounted for heat losses in the experimental measurement of the thermal conductivity and thermal diffusivity are a major contribution to the scatter in data.

The uncertainty in the data for the heat conduction properties introduces a corresponding uncertainty in the estimates of the temperature and thermal stresses and interpretation of experimental results for the performance of solar receivers. In fact, significant under- or overestimates of the efficiency can result from erroneous data for the thermal conductivity.

It is unfortunate that in spite of their variability and their absolute necessity, heat conduction data for candidate materials, especially ceramics, for high-temperature technology is relatively sparse. Such scarcity in part can be attributed to the relatively high cost and complexity of such measurements. Nevertheless, it is urgently recommended that a development and testing program of solar receivers be assisted by extensive measurements of heat conduction properties, preferably on the very same materials or components used in a test structure.

The phenomena related to the mechanical failure of brittle ceramic materials is expected to introduce major uncertainty in the design of structures for high-temperature technology in general and solar receivers in particular. A considerable body of literature (see for instance Fracture Mechanics of Ceramics, Vols. 1,2,3 and 4, 1974, 1978), indicates that the strength, fatigue and crack propagation behavior of brittle ceramics is controlled by a wide variety of factors. Ideally, a material should fail at a given stress level. Unfortunately, for brittle ceramics this statement is far from the truth.

Experimentally the failure stress of brittle materials has been found to be a function of the grain size as well as the presence of a

pore phase. The grain size distribution and orientation as well as the pore morphology are expected to be significant variables as well.

The method of surface preparation or surface damage occurred during service can have a profound negative effect on the magnitude of the failure stress. Environmental effects such as temperature and level of humidity or other surface-active molecules also can affect the magnitude of the strength and fatigue-life considerably.

Of significance is that the strength of brittle ceramics is a function of the method by which it is measured. It has been found experimentally that strength is affected by the stressing rate, the size and geometry of the test specimens, the method of loading as well as the distribution of stress within the specimen. Even for a given test method, strength data show a large degree of scatter with coefficients of variation as high as twenty-five percent for many high-strength brittle ceramics. Worse yet, significant difference in strength data have been found by different investigators for the identical material tested under presumably identical conditions.

Fatigue-life under steady-state or cyclic load even for a set of identical specimens may show variations of as much as three orders of magnitude for a given stress level. Such scatter in strength and fatigue-life can be attributed to differences in the size, geometry or orientation of the failure-initiating flaws.

Measurements of property data related to critical crack propagation such as fracture toughness (K_{IC}) or fracture energy indicate that microstructural effects such as grain size and porosity can play a significant role. Temperature also plays an important role especially at levels

where inelastic effects become prominent. In service, material degradation due to corrosion effects also is expected to modify crack propagation considerably.

Taking into account the collective uncertainties of all material properties discussed above, indicates that reliable predictions and/or quantitatively significant interpretations of experimental data of the thermal stress behavior of ceramic materials for solar receivers, is a relatively complex task. Quantitative data for all these effects should be established for all candidate materials. With this information, estimates of strength performance and fatigue behavior can be based on statistical theories such as those advanced by Weibull and many others (1951), coupled with failure prediction methodology and proof-testing based on fracture-mechanics principles (See Fracture Mechanics of Ceramics, Vols, 1, 2, 3 and 4).

In the absence of complete information, due to budgetary or other constraints, the design engineer can take a very conservative approach. This would require assumptions of design stresses of the order of no more than ten to twenty percent of the fracture stresses determined on laboratory specimens made and tested under closely controlled conditions. The same approach should be taken in the design, relying entirely on experimental thermal shock data obtained in appropriate test facilities. It is expected, however, that such a conservative approach may limit the indicent heat flux, potential efficiencies and power output of solar receivers to levels which are not economically justified. On the other hand, operation at higher flux levels may result in replacement of component at too frequent intervals.

For all the above reasons, it is recommended that in the construction of solar receivers, design configurations be selected with minimum levels of thermal stress, by careful selection of materials and by following design recommendations outlined in a subsequent section of this report.

6. EFFECT OF DIMENSIONAL AND GEOMETRIC VARIABLES AND NON-UNIFORM HEATING OR COOLING ON THERMAL STRESS RESISTANCE

A general survey of the results presented in section 4 of this report, indicates that a number of conclusions can be drawn in regard to the effect of dimensional and geometric effects on thermal stress resistance of brittle ceramic materials.

Firstly, for nearly all thermal environments as indicated, for example by representative equations 4.1.6.1, 4.3.2.1, 4.3.3.1, 4.3.3.10 etc, and the numerical results shown in fig. 4.3.1.1 for convective heat transfer (with the exception of thermal buckling instability), the magnitide of the thermal stress increases with increasing component size. The primary reason for this effect is that in larger structures heat flow occurs over larger distances.

The above effect is particularly pronounced for non-uniform heating (or cooling) of large structures, such as plates partially heated over much of its surface, as indicated by the recent study of Stahn et al. (1980).

These observations immediately suggest that if high thermal stress resistance is to be achieved, large monolithic ceramic structures should be avoided, whenever possible. Instead, the dimensions of the components should be kept as small as possible. Large structures, if required to meet other design objectives should consist of assemblies of smaller components. In case of non-uniform heating or cooling, the structures should be segmented, such that the size of each segment is no greater than the size of the region over which the non-uniform heating or cooling occurs. This will result in a uniform heating over each segment.

The same conclusion applies to the effect of size on the extent of crack propagation in severe thermal environments in which thermal stress fracture cannot be avoided. For a given number of cracks nucleated during failure, the extent of crack propagation is expected to be proportional to the volume of the component (Hasselman 1970; Gupta, 1972). Decreasing component size will reduce the extent of crack propagation and increase the load-bearing capability following thermal stress fracture.

Secondly, as indicated by the various expressions presented earlier, the geometry of a structure and/or component as well as the value of heat transfer also plays an important role in determining thermal stress resistance. No general rule can be given for the effect of geometry, but this effect allows the designer additional freedom in obtaining the maximum resistance to thermal stress failure. One specific example can be given. Radially outward heat flow through the walls of a concentric hollow cylinder will result in significantly lower values of the tensile thermal stresses than for radially inward heat flow. This is especially the case for cylinders, with wall thicknesses which are a significant fraction of the cylinder radii.

The above conclusions with regard to the effects of size and geometry, together with the effect of external constraints discussed previously, leads to the following design recommendation:

> "Structures operating in thermal environments with a high risk of thermal stress failure, whenever possible, should be constructed in the form of assemblies of components (or sub-components) of small size and simple geometry, to permit maximum free thermal expansion, minimum non-uniformity in heat transfer and minimum temperature non-uniformity within each component."

The above conclusion has a number of implications for the various designs proposed for point-focussing solar receivers, reviewed recently by Ewing and Zwissler, 1979. For instance, in the design proposed by M.I.T., it may be preferable to construct the dome-shaped heat-exchanger from a number of individual segments. The single monolithic dome of the current design may exhibit large tangential temperature non-uniformities, unless by careful design, the air-flow over the dome is distributed such that only the radial (through-the-thickness) temperature gradient exists.

The same conclusion applies to the honey-comb heat exchanger in the design advanced by Sanders Associates. It is recommended that this heat exchanger be constructed of a number of parallel thin plates, rather than the monolithic design currently envisioned. For spatially non-uniform heating, these plates could be further segmented.

Similar consideration may apply to other components and designs advanced by other organizations.

Clearly, these recommendations are based on considerations which emphasize thermal stress failure. Final designs should take into account all performance criteria. Nevertheless, it is important to note that thermal stress failure can be minimized by careful design based on dimensional and geometric factors coupled with the selection of materials with optimum thermal stress resistance on the basis of the parameters presented in earlier sections of this report.

7. RECOMMENDATIONS FOR MATERIALS FOR POINT-FOCUSSING SOLAR RECEIVERS

7.1. General

The selection of materials of construction for point-focussing solar receivers should be based on a number of criteria. First of all, the material properties should be such that all design and performance standards are met. This applies not only to thermal shock, but also to other load-bearing requirements, erosion, corrosion and optical properties. The relative importance of these criteria is expected to be governed by the final design.

Secondly, material selection should take into account availability and price. This criterion is critical to the timely development and demonstration of the technical and economic feasibility of point-focussing solar receivers. It is entirely conceivable that on the basis of handbook or preliminary laboratory data, a particular material may appear very attractive indeed. However, usually for newly developed materials insufficient manufacturing experience and facilities exist. Development programs for new ceramic materials are notorious for falling behind schedule due to unforeseen difficulties. In addition, development costs can exceed initial estimates by considerable margins. For this reason, it is strongly recommended that the construction of a point-focussing solar receiver not depend on the success or failure of new material development. Instead, it is urged that whenever possible, materials of construction be selected which are currently available, even if this would require receiver operation at less than optimum efficiencies. Once, feasibility is demonstrated, the performance standards can be improved further with a parallel or follow-up program of development of new materials.

These recommendations not only apply to the choice of materials, but also to geometry and dimension. Whenever possible, the final design of a point-focussing solar receiver should be based on components of a size and geometry for which extensive manufacturing experience exists. This recommendation implies that with few exceptions the component size is small and that their geometry is relatively simple. It is anticipated that such components can be manufactured at minimum cost.

7.2. Materials for Individual Components

In view of these authors, the components of point-focussing solar receivers most susceptible to thermal shock failure are:

a. window

b. heat exchanger

c. thermal insulators

d. down-stream tubing or manifolds

The material requirements for these four components are discussed below. The requirement of high melting point, oxidation resistance, erosion and corrosion resistance is common to all these components. The subsequent discussion will focus on the material requirements for fulfilling the basic function of the component as far as the operation of the solar receiver is concerned in combination with the requirements for thermal shock resistance.

7.2.1. The window

A number of anticipated designs for point focussing receivers rely on the window in order to transmit the incident solar radiation into the chamber containing the heat exchanger and working fluid. Since the working

fluid is under some pressure, the high temperature mechanical properties of the window material should be such that no creep or fracture will result under normal operating conditions.

In order to transmit the solar radiation at maximum efficiency, the window material should have low reflectivity and low absorption coefficient. High resistance to thermal shock failure requires a window material with high reflectivity and thermal conductivity in combination with low absorption coefficient, coefficient of thermal expansion, Young's modulus of elasticity and Poisson's ratio. It should be noted that high reflectivity for high thermal stress resistance is incompatible with the low reflectivity required for maximum transmission of the solar radiation. Also, all the above requirements may not be met within a single material. Nevertheless, in spite of these conflicting requirements, fused quartz, in view of its very low coefficient of thermal expansion should be considered a prime candidate for the window material. Thermal stress fracture, in view of these writers, is not likely to occur in this material. Its absorption coefficient at wavelength greater than 4 μm is greater than that for single crystal materials such as sapphire, rutile, magnesium oxide and other infrared transmitting materials developed for aerospace and other purposes. For this reason, the temperature levels which could be encountered in windows made of fused quartz could be high which could lead to creep, devitrification and corresponding loss of transmissivity. In that case, other materials such as sapphire or the other aforementioned material may provide superior service. On the other hand, the reflectivity of sapphire exceeds that of fused quartz, which is undesirable. Also, much higher value of the coefficient of thermal expansion of sapphire compared to quartz is not favorable from the point of view of thermal stress resis-

tance. However, the higher thermal conductivity of sapphire than for fused quartz, at lower temperature levels will compensate for this latter deficiency.

Fused quartz, however, is considerably cheaper than any other window material. Furthermore, excessive window temperatures can be reduced by flow patterns of the working fluid which will promote window cooling. External cooling may be used to advantage to reduce or eliminate the accumulation of dust which could adversely affect overall transmission of the incident radiation.

If fused quartz were found to be unsuitable for a window material, other materials should be considered. These could include single or polycrystals of alumina, titanium oxide, magnesium oxide, magnesium fluoride, calcium-alumina-germanate and similar materials currently being used or under investigation in aerospace industry. Most of these materials will transmit radiation over a wider range of wavelength than fused quartz. On the other hand, their coefficients of thermal expansion exceed the value for quartz by a considerable margin. For these reasons, it is recommended that fused quartz be given high priority even if this would involve design modification to keep the window temperature within reasonable limits.

Regardless of the choice of material, it is recommended that the window be supported by sliding seals in order to minimize in-plane and bending constraints. Nickel oxide has been used for sliding seals in turbine regenerators and may prove to be useful in solar receivers as well.

7.2.2. Heat exchanger and thermal insulator

The purpose of the heat-exchanger in a solar receiver is to absorb the solar radiation. The absorbed heat is removed from the heat-exchanger by the working-fluid by forced convection.

In order to fulfill its basic function, the heat exchanger material should have low reflectivity (high absorptivity) and high absorption coefficient. Furthermore, if the absorbed heat is to be conducted through the heat exchanger wall, high thermal conductivity is required in order to minimize the non-linearity of the temperature distribution and to keep the temperature of the irradiated face within reasonable limits.

For high thermal stress resistance, the material of the heat exchanger should have high reflectivity, thermal conductivity and tensile strength in combination with low absorption coefficient, coefficient of thermal expansion, Young's modulus and Poisson's ratio.

The requirement for low reflectivity and high absorption coefficient for high heat absorption is incompatible with the requirement for high reflectivity and low absorption coefficient required for good thermal shock resistance. Clearly, the requirement for low reflectivity and high absorption coefficient must be given priority in order to meet the performance criteria for the heat exchanger. Fortunately, high thermal conductivity is required for high thermal stress resistance and high heat conduction. This latter requirement is imperative for the MIT, NRL and Black and Veatch design.

Silicon carbide or silicon nitride probably are the best materials for consideration for these three designs. The relatively higher coefficient of thermal expansion and Young's modulus of silicon carbide is offset by its higher thermal conductivity compared to silicon nitride. The relatively low value for thermal conductivity for the cordierite ceramic considered for the exchanger in the NRL design may cause difficulty unless the wall thickness can be reduced appreciably. This may conflict with other structural

requirements. Because of the complex configuration of the NRL heat exchanger, substitution of silicon carbide or silicon nitride for the cordierite may lead to manufacturing difficulties. The same will be true for other refractory materials with high thermal conductivity such as other nitrides, carbides or borides.

As pointed out earlier, the writers of this report prefer a heat-exchanger design in which the heat is removed by the working fluid at the same surface on which the radiation is incident. For a given temperature level of the working fluid, this will involve much lower surface temperature than that in case where heat is removed on the opposite surface. This has the advantage that the requirement for melting-point and high temperature structural integrity are less stringent. Furthermore, heat losses by re-emitted radiation are also reduced. These advantages are incorporated in the heat exchanger design advanced by Sanders Associates, in which the working fluid is pumped through the heat-exchanger in the form of a honey-comb type structure. This type of configuration also will keep the reflectivity to a minimum. For this type of heat exchanger, cordierite of the type, identical or similar to that used for automotive exhaust catalyst support, appears to be an excellent candidate. Its temperature characteristics are deemed sufficient to withstand long-term operation at temperatures approaching 1000°C. Furthermore, its coefficient of thermal expansion and effective elastic behavior are such that the problem of thermal shock failure can be minimized or even eliminated by appropriate design. Also, because of its extremely low cost and easy availability, cordierite honey-comb heat exchangers can be readily replaced if some form of degradation should still occur. It should be noted that thermal shock failure of cordierite honey-comb structure is still a matter of concern in the automotive industry. However, in the latter application the thermal

shock problem is magnified because of uneven heating as the direct result of the differences in dimensions of the exhaust manifold and container for the catalyst support. In comparison, the radiation heat flux on the heat exchanger in the Sanders design is expected to be more uniform. Furthermore, as discussed earlier, by appropriate segmenting of the honey-comb receiver, the problem of thermal shock failure, if any, can be reduced even further.

If the cordierite would be found unsuitable due to loss of structural integrity at high temperature, honey-comb structures of reaction-sintered silicon nitride or silicon carbide should be considered. The technology for the manufacture of silicon nitride honey-comb material is well established. However, the thermal shock resistance of reaction sintered silicon nitride may well be less than for cordierite. If so, a change in geometry of the heat exchanger may be in order. The configuration of packed spheres, chosen by General Motors for its automotive catalyst system possibly may be used to advantage. Such a bed of packed spheres will permit easy passage of the working fluid. At the same time, thermal shock failure, due to the absence of mechanical constraints between spheres, will not be a problem. Thermal stress failure due to non-uniform temperatures within each sphere can be eliminated by appropriate selection of the sphere size. One half inch spheres (or less) should eliminate thermal stress failure in any ceramic which may be chosen. A similar configuration of spheres could be considered for the ceramic heat storage buffer incorporated in the Sanders design. Also, the use of small interlocking hexagonal ceramic blocks of alumina, magnesia and zirconia used in air-preheaters for wind-tunnels and MHD power systems should not be ruled out.

The relative thermal shock resistance of insulating refractory materials frequently is designated by the manufacturer as "poor", "good" or

"excellent". It should be noted that for such material with few exceptions, thermal shock resistance is based on the "crack arrest" concept, discussed in detail in an earlier section of this report.

Refractory fibrous silica or alumino-silicate insulating materials also can be used to advantage in some areas of solar receivers. Such materials in the form of sheet or rope can be used to reduce heat losses through gaps or spaces between components required for maximum free thermal expansion. Such fibrous materials are readily available at low cost from a number of suppliers.

7.2.3. Down-stream components

Components, down-stream from the heat exchanger, such as manifolds and piping required to transfer the working fluid to the turbine, will be subjected to transient as well as steady-state non-uniformity in temperature. Such non-uniform temperature could give rise to thermal stress of high magnitude to result in immediate failure or failure by thermal fatigue. Hopefully, the temperature levels and pressure encountered will permit refractory metals or alloys for their construction. If not, reaction sintered silicon nitride or silicon carbide appears to offer a combination of properties suitable for this purpose. Also, these materials can be manufactured in relatively complex shapes (manifolds or other) down-stream components are expected to take. Even then, it is strongly recommended that their geometry be kept as simple as possible and the size also be kept to a minimum.

7.3. Final Remarks

Much relevant information for the selection of materials can be obtained once a final design or designs are selected and detailed temperature and stress analyses have been carried out. The finite element modelling

should be of major benefit for this purpose. Also, rapid feed-back on material behavior will be provided by the experimental thermal shock testing program outlined later, which should pinpoint unforeseen difficulties and/or particular material requirements. With such data in hand, assessment can be made for the need for re-design, material modification or the development of novel material not available at this time.

8. THERMAL SHOCK TESTING AND ANALYSIS

8.1. General

Engineering design and selection of materials for high-temperatures in general and solar receivers in particular can benefit considerably from advance information on the performance of the components under conditions of thermal shock. Such information can be established by testing the thermal shock behavior by experimental techniques.

Many methods for testing the thermal shock response of ceramic materials have been developed. Thermal stress resistance under conditions of steady-state heat flow or controlled heating can be established by the internal heating of hollow cylinders (Coble and Kingery, 1955; Hummel, 1955; Gogotsi and Groushevsky, 1980). Thermal stress failure under conditions of transient convective heat transfer can be established by quenching specimens in the form of cylinder or other geometry, from higher temperature into fluid media at lower temperature, such as water, molten salts, liquid metals, oils or fluidized beds (Crandall and Ging, 1955; Hasselman, 1970; King and Webb, 1971; Kirchner et al, 1968, 1971, 1973 and Hasselman, et al., 1975). Rapid convective cooling can also be achieved by air-blasts, frequently used for studies of thermal fatigue behavior, (Ammann et al., 1976, Quinn et al., 1977). Thermal shock response to black-body radiation can be determined by "up-quenching" appropriate specimens at a low temperature into a black-body cavity (furnace) at high temperature (Crandall and Ging, 1955; Hasselman and Shaffer, 1962; Hasselman, 1963). Other methods for inducing thermal shock include plasma-heating, arc-discharge heating, laser-heating, induction heating and burner-rigs (Starret, 1977; Johnson, 1974; Sato, et al., 1980; Schwille, et al., 1980; Mecholsky, et al., 1980).

Numerous other testing methods have been developed for many special industrial and consumer products susceptible to thermal stress failure under the conditions of their intended application.

From the results presented in previous sections of this report, it should be clear to the reader that the material properties and other variables such as geometry and size, which affect thermal stress failure can vary significantly from one thermal environment to another. This conclusion also applies to the various methods for thermal shock testing. Results obtained under conditions of steady-state heat flow are not appropriate to transient heating. The results for tests which rely on radiation heat transfer are not expected to reflect results to be obtained for convective heat transfer. (In this respect it should be noted that convective heat transfer coefficients are highly variable, such that results of tests which rely on this mechanism of heat transfer, are difficult to interpret for quantitative purposes). Furthermore, results for thermal shock tests involving external constraints will not apply to thermal shock environments in which such constraints are absent. Even for the same test method results obtained for one level of average temperature may differ significantly from the results obtained at some other test temperature. This conclusion also applies to differences in geometry as well as specimen size. For these reasons, attempts to "infer" thermal shock behavior for a given thermal environment from test data obtained for some other environment is not expected to yield reliable results. In particular, this will be the case of major differences in mechanisms of heat transfer and complex geometries for which the magnitude and distribution of the temperatures and thermal stresses are not readily obtainable.

The above discussion is critical to the selection of the most appropriate test method for the thermal shock behavior of materials or components for solar receivers in order to yield quantitatively meaningful results for the designer. For this reason, such a test should simulate as closely as possible the thermal shock environment to be encountered in solar receivers. This applies not only to the magnitudes of temperatures and stresses but also to the combined radiation heating-convection cooling conditions and specimen size and geometry as well.

Specific recommendations for a thermal shock testing program for point-focus solar receivers must await final selection of the design expected to yield most efficient and reliable operation and for which estimates or data for the heat transfer characteristics are available. For these reasons, a number of general recommendations for the thermal shock test facilities and procedures will be made at this time.

8.2. Thermal Shock Test Facilities and Procedures

The following recommendations are made for the type and scope of the thermal shock test facilities and testing procedures.

1. The components of the solar receiver directly subjected to the incident solar radiation probably are most susceptible to thermal stress failure. The spectral distribution of solar radiation may be difficult to duplicate by radiation from lasers, plasma-torches or other intense light sources. Furthermore, each candidate material has its own unique spectral dependence of its pertinent material properties. For these reasons, it is recommended that a thermal shock test facility use solar radiation itself, concentrated by parabolic mirrors or by other techniques.

2. The solar-radiation thermal shock test facility should be designed to permit control over the intensity of the radiation incident on the component being tested. By varying the position of the component to be tested with respect to the focal plane, the radiation intensity is varied easily even for constant solar flux at the mirror surface. Lateral movement within the focal plane will permit testing the effect of spatially non-uniform incident radiation. Both these latter objectives can be achieved by partial screening, as well.

3. The thermal shock test facility should be designed such as to include capability for convective cooling in order to simulate the combination of radiation heating and convective cooling encountered within the solar receiver. The geometry of the manifold, air flow velocities and distribution should be such that the spatial variation in heat transfer coefficient found within the solar receiver are duplicated as closely as possible.

4. Control over the radiation should be such that variations in the radiation intensity expected during intermittent cloud cover or other conditions can be closely duplicated.

5. The convective cooling system should permit control over flow speeds and pressure in order to simulate unusual operating conditions such as loss of compressor power due to electrical or mechanical breakdown.

6. The thermal shock test facility should be instrumented as completely as possible to detect and record all pertinent operational variables such as radiation intensity, air flow speeds and pressures, as well as temperatures and deformations. Acoustic spectrometers will permit detection of the fatigue phenomena or the onset of failure.

7. The fixture which holds the component(s) to be tested, should permit testing of components, singly or in combination in order to establish thermal interactions and possible effects of mutual constraints. In this manner, a window or a receiver could be tested individually or in combination. This permits assessment of the effects of window absorption and reflection on the thermal shock behavior of the receiver and the effect of reflection of the incident radiation as well as thermal emission from the receiver plate on the thermal shock behavior of the window.

8. The radiation thermal shock test facility should permit thermal shock testing of down-stream components not directly subjected to the solar radiation, but subjected to thermal stresses during normal or special operating conditions of the solar receivers. If desired, a complete alternative test facility could be constructed for testing of down-stream components. However, the thermal conditions expected in practice, can be duplicated most easily and closely by the solar radiation thermal shock test facility itself.

9. All components to be tested should be subjected to a thorough quality control check, in order to detect defects or other irregularities which could affect the test results. Records of all such defects should be kept carefully in order to facilitate analysis of the test results.

10. First stages of the test program should concentrate on thermal shock tests duplicating conditions to be encountered in practice. Radiation levels required to initiate failure should be measured and compared to radiation levels to be expected in practice. A comparison of these values will allow assessing the direction of design modification such as

modification in radiation intensities and convection cooling rates, component geometry and size or selection and development of alternative materials with improved thermal shock behavior.

Later stages of the testing program should include unusual thermal shock conditions such as sudden incident radiation in the absence of air-flow or steady-state radiation with sudden loss of air-flow and similar emergency conditions.

11. After testing, each component should be examined as thoroughly as possible for possible failure. For some materials it is expected that failure is catastrophic, the component falling apart spontaneously on removal from the test facility. Cracks in brittle ceramics are not easily detected with unaided eye. For this reason any tested component should be examined in detail using dye-penetrant, ultrasonic or other non-destructive test methods for the presence of cracks. Macrophotography and microfractography of fractured samples will provide permanent records as well as the vital information on the mode of failure, the site of fracture initiation and the magnitude of stress at which failure occurred. This latter information will provide important feed-back information for the validity of the assumptions made for the calculations of the thermal stresses, as well as provide directions for design modification and selection or development of alternative materials of construction.

12. A final, but critical comment on thermal shock testing is in order. From the above recommendations, it is clear that the thermal shock test facility and program should be similar or even duplicate the design and testing programs for a prototype solar receiver. At first sight, such a test facility and program may be judged as too complex and uneconomical. For this reason, it could be tempting to resort to simplified testing

methods or even to rely on manufacturer's data for thermal shock behavior. This approach is not recommended. However, by means of technology of which these writers may not be aware, other radiation sources can be found which duplicates the nature and magnitude of the thermal shock environment encountered in a solar receiver. The design of such a test using other than solar radiation is expected to be difficult or impossible. Any other test methods may not yield data which are quantitatively meaningful for design purposes, but in fact may provide data that are erroneous and misleading for solar receivers. For these reasons, it is suggested that if the recommended test facility is not feasible on technical, economic or other grounds, the testing should be avoided altogether. Instead, thermal shock behavior should be calculated from the material property data and best estimates for the heat transfer environments.

8.3 Theoretical Analysis in Support of Experimental Thermal Shock Testing Program

As indicated in section 4 of this report, thermal stress failure of brittle ceramics is controlled by a large number of variables, including material properties, geometric, size and heat transfer effects. For this reason, the interpretation of experimental data for thermal shock can be quite complex. This is especially the case for complex geometries subjected to mixed-mode of heat transfer conditions for which the temperatures and thermal stresses are not easily established. Without this information, experimental data for thermal shock behavior may provide little or no guidance for the direction in which design or material improvements are to be made. Therefore, it is strongly recommended that the experimental program for the thermal shock behavior, be supported by a theoretical

effort of calculating magnitudes and distributions of the temperatures and thermal stresses by computer simulation. These calculations can be based on analytical methods, whenever practical. Preferably, such calculations should be based on finite difference or finite element principles, because of their much greater flexibility than analytical methods.

A number of benefits can be derived from an experimental and parallel analytical program on assessing thermal stress resistance. Comparisons of the experimental and theoretical data for the temperature distribution will provide valuable feed-back for the validity of the assumptions made with regard to heat transfer mechanisms and magnitudes of the heat transfer properties of the component being tested. The reliability of the thermal stress calculations and predicted failure mode will be improved accordingly.

A further major advantage is that computer simulation can provide rapid information on the degree of improvement obtained by changing the material, component size and shape, incident solar radiation intensity as well as pressure and flow rates of the working-fluid. Costly and time-consuming test programs can be avoided or reduced to a minimum. The effects of unusual operating conditions, not easily duplicated in a test facility, can also be assessed easily by computer simulation.

In general, such supporting theoretical analyses should reduce the cost of an experimental thermal shock testing program to a minimum. This should, consequently, lead to a reduction in the total cost and duration of the development program of solar receivers.

9. MATERIALS-RELATED COMMENTS AND RECOMMENDATIONS FOR SYSTEM DESIGN AND OPERATION

The conclusions obtained in this study have a number of implications for the design and operation of point-focussing solar receivers. Undoubtedly, these already have been considered in design studies carried in parallel with the present program. Although clearly beyond the scope of this report, these implications must be listed as they are related directly to materials performance.

First of all the design of the receiver and its control equipment must be such that under no condition the solar energy will be directed at the heat exchanger without adequate flow of the working fluid. If such flow and corresponding cooling is not provided, the heat exchanger will reach temperatures well in excess of the melting point of most, if not all, candidate materials of construction. This recommendation implies that an external power source be provided (not powered by solar energy) which can circulate the working fluid prior to the incidence of the solar radiation. It is anticipated that this may require rapidly acting sensing and control devices which govern the working-fluid flow and/or the orientation of the focussing mirror.

Secondly, the theoretical results for the thermal stresses in the semi-absorbing plates indicate that the transient stresses are an inverse function of the heat transfer coefficient. For this reason it is recommended that on start-up, the rate of circulation of the working-fluid be greater than required for steady-state operation. For the same reason it may be desirable to reduce the rate of flow on reduction in solar intensity in order to reduce the cooling rates and the magnitude of the

corresponding thermal stress. Here too, automatic sensing and control devices are expected to be useful.

A further highly speculative recommendation will be made aimed at elimination or reduction of excessive heating and cooling rates and the distribution difficulties encountered in the utility industry by rapid variations in power-output such as those expected for intermittent cloud-covers. Such variation may require stand-by power-generating units such as pumped-storage or other systems in order to assure an uninterrupted power supply. It is suggested here that such difficulties can be overcome by using a hybrid-system such as a combination of a solar receiver and a gas-turbine generator or other power generating systems. For instance, the Sanders design could be modified slightly to permit the introduction of natural gas into the cavity between the window and the heat exchanger. Combustion could be achieved within the heat exchanger with the aid of the appropriate catalyst. This latter technology is well developed. The amount of gas to be introduced would depend on the intensity of the incident radiation. In this manner, temperature levels could be maintained within prescribed tolerances. Furthermore variations in power output could be kept to a minimum. Such a hybrid system could be described as turbine-assisted solar receiver or a solar-augmented gas-turbine. Undoubtedly other such hybrid systems relying on other methods of power generation, depending on fuel availability and location, can be devised as well.

10. RECOMMENDATIONS FOR FUTURE ANALYTICAL WORK TO AID MATERIALS SELECTION FOR SOLAR RECEIVERS

This report has presented criteria for the selection of ceramic materials, which are currently available in the technical literature. However, for at least two conditions of possible thermal stress failure unique to solar receivers, analyses are required for purposes of material selection, design and possible failure prediction. These studies recommended for follow-on work are:

1. An extension of the thermal stress analysis of semi-absorbing ceramics to include the spectral dependence of the relevant optical properties to correspond to the spectral distribution of solar radiation.

2. Analysis of thermal stresses which occur in semi-absorbing ceramic materials, initially at thermal equilibrium under conditions of radiation heating and convection cooling, subjected to sudden loss of radiation, followed by rapid convection cooling. This type of thermal-shock is expected to occur frequently in solar receivers. It is essential that the role of the pertinent material properties must be established in order to properly assess the criteria for materials selection and interpretation of failure modes.

SUMMARY

An analysis was conducted of the possible modes of thermal stress failure of brittle ceramics for potential use in point-focussing solar receivers. The pertinent material properties which control thermal stress resistance were identified for conditions of steady-state and transient heat flow, convective and radiative heat transfer, thermal buckling and thermal fatigue as well as catastrophic crack propagation. Selection rules for materials with optimum thermal stress resistance for a particular thermal environment were identified. Recommendations for materials for particular components were made. The general requirements for a thermal shock testing program quantitatively meaningful for point-focussing solar receivers were outlined. Recommendations for follow-on theoretical analyses were made.

REFERENCES

C. L. Ammann, J. E. Doherty and C. G. Nessler, "Thermal Fatigue Behavior of Hot Pressed Silicon Nitride," Mat. Sc. and Engr., 22 [1], 15-22 (1976).

R. Badaliance, D. A. Krohn and D. P. H. Hasselman, "Effect of Slow Crack Growth on the Thermal-Stress Resistance of an Na_2O-CaO-SiO_2 Glass," J. Am. Ceram. Soc., 57 [10], 432-36 (1974).

Z. P. Bazant and A. B. Wahab, "Instability and Spacing of Cooling or Shrinkage Cracks," J. of the Engng. Mech. Div., Proc. Soc. of Civil Engr., 105, 873-89 (1979).

Bruno A. Boley and J. H. Weiner, Theory of Thermal Stresses, John Wiley & Sons, Inc., New York, 1960.

G. Buergermeister and H. Steup, Stability Theory (Stabilitaets Theorie). Akademie Verlag, Berlin, Federal Republic of Germany, 1957.

W. R. Buessem, "Resistance of Ceramic Bodies to Temperature Fluctuations," Sprechsaal Keram. Glas Email Silikate, 93 [6] 137-41 (1960).

R. L. Coble and W. D. Kingery, "Effect of Porosity on Thermal Stress Failure," J. Am. Ceram. Soc., 38 [1] 33-37 (1955).

W. B. Crandall and J. Ging, "Thermal Shock Analysis of Spherical Shapes," J. Am. Ceram. Soc., 38 [1] 44-54 (1955).

A. F. Emery, "Stress-Intensity Factors for Thermal Stresses in Thick Hollow Cylinders," Trans. ASME, J. Basic Eng., 88 [1], Ser. D, 45-52 (1966).

A. F. Emery, J. A. Williams and J. Avery, "Thermal-Stress Concentration Caused by Structural Discontinuities," Experimental Mechanics, 9 [12] 558-64 (1969)a.

A. F. Emery, G. E. Walker, Jr., and J. A. Williams, "A Greens Function for the Stress Intensity Factors of Edge Cracks and Its Application to Thermal Stresses," Trans. ASME, J. Basic Eng., 91 [4], Ser. D, 618-24 (1969)b.

J. D. Eshelby; pp. 89-139 in Progress in Solid Mechanics, Vol. II, eds. I. N. Sneddon and R. Hill, North-Holland Publishing Company, Amsterdam, 1961.

A. G. Evans, "A Method of Evaluating the Time-Dependent Failure Characteristics of Brittle Materials and Its Application to Polycrystalline Alumina," J. Mat. Sc., 7 [10] 1137-46 (1972).

J. Ewing and J. Zwissler, "Performance Prediction Evaluation of Ceramic Materials in Point-Focusing Solar Receivers," Jet Propulsion Laboratory Publication 79-58; DOE/JPL-1060-23, June 1, 1979.

A. F. Florence and J. N. Goodier, "Thermal Stress at Spherical Cavities and Circular Holes in Uniform Heat Flow," Trans. ASME, J. Appl. Mech., 81, Ser. E, 293-94 (1959).

Fracture Mechanics of Ceramics, Vol. I and II, eds. R. C. Bradt, D. P. H. Hasselman and F. F. Lange, Plenum Press, New York, 1974.

Fracture Mechanics of Ceramics, Vol. III and IV, eds. R. C. Bradt, D. P. H. Hasselman and F. F. Lange, Plenum Press, New York, 1978.

Ya. B. Fridman in Thermal Stability of Plates and Shells, ed. Ya. B. Fridman Consultants Bureau, New York, 1964.

M. S. Ganeeva, "Stability of a Rectangular Cylindrical Panel Rigidly Clamped at the Edges Located in a Nonuniform Temperature Field," Uch. Zap. Kazanskogo Univ., 116 [1] (1956).

E. Glenny and M. G. Royston "Transient Thermal Stresses Promoted by the Rapid Heating and Cooling of Brittle Circular Cylinders," Trans. Brit. Ceram. Soc., 57 [10] 645-77 (1958).

G. A. Gogotsi and Ya. L. Groushevsky, "Investigation of the Thermal Shock Resistance of Ceramics Under Programmed Heating," Proc. Intl. Conf. on Thermal Stresses in Materials and Structures in Severe Thermal Environments, eds. D. P. H. Hasselman and R. Heller, Plenum, New York (in press, 1980).

T. K. Gupta, "Strength Degradation and Crack Propagation in Thermally Shocked Al_2O_3," J. Am. Ceram. Soc., 55 [5] 249-53 (1972).

T. K. Gupta, "Resistance to Crack Propagation in Ceramics Subjected to Thermal Shock," J. Mat. Sc., 8 [9] 1283-86 (1973).

D. P. H. Hasselman and P. T. B. Shaffer, "Factors Affecting Thermal Shock Resistance of Polyphase Ceramic Bodies, Pt. II," Tech. Rept. WADD-TR-60-749; Contract AF 33(616)-6806, 155 pp.; April 1962.

D. P. H. Hasselman, "Thermal Shock by Radiation Heating," J. Am. Ceram. Soc., 46 [5] 229-34 (1963).

D. P. H. Hasselman and W. B. Crandall, "Thermal Shock Analysis of Spherical Shapes, II," J. Am. Ceram. Soc. 46 [11], 535-40 (1963).

D. P. H. Hasselman, "Theory of Thermal Shock Resistance of Semitransparent Ceramics Under Radiation Heating," J. Am. Ceram. Soc., 49 [2] 103-104 (1966).

D. P. H. Hasselman, "Approximate Theory of Thermal Stress Resistance of Brittle Ceramics Involving Creep," J. Am. Ceram. Soc., 50 [9] 454-57 (1967).

D. P. H. Hasselman, "Unified Theory of Thermal Shock Fracture Initiation and Crack Propagation in Brittle Materials," J. Am. Ceram. Soc., 52 [11] 600-604 (1969).

D. P. H. Hasselman, "Strength Behavior of Polycrystalline Alumina Subjected to Thermal Shock," J. Am. Ceram. Soc., 53 [9] 491-95 (1970).

D. P. H. Hasselman; pp. 89-103 in Materials Science Research, Vol. 5. Edited by W. Wurth and Hayne Palmour III, Plenum Press, New York, 1971.

D. P. H. Hasselman, "Crack Propagation Under Constant Deformation and Thermal Stress Fracture," Int. J. Fract. Mech., 7 [2] 157-61 (1971).

D. P. H. Hasselman, E. P. Chen, C. L. Ammann, J. E. Doherty and C. G. Nessler, "Failure Prediction of the Thermal Fatigue of Silicon Nitride," J. Am. Ceram. Soc., 58 [11-12] 513-16 (1975).

D. P. H. Hasselman, R. Badaliance, K. R. McKinney and C. H. Kim, "Failure Prediction of the Thermal Fatigue Resistance of Glass," J. Mat. Sc., 11 [3], 458-64 (1976).

D. P. H. Hasselman and G. E. Youngblood, "Enhanced Thermal Stress Resistance of Structural Ceramics with Thermal Conductivity Gradient," J. Am. Ceram. Soc., 61 [49] 49-52 (1978).

D. P. H. Hasselman and W. Zdaniewski, "Thermal Stress Resistance Parameters for Brittle Materials Subjected to Thermal Stress Fatigue," J. Am. Ceram. Soc., 61 [7-8] 375 (1978).

D. P. H. Hasselman, "Role of Physical Properties in the Resistance of Brittle Ceramics to Failure by Thermal Buckling," J. Am. Ceram. Soc., 62 [3-4] (1979).

D. P. H. Hasselman, J. R. Thomas, Jr., M. P. Kamat and K. Satyamurthy, "Thermal Stress Analysis of Partially Absorbing Brittle Ceramics Subjected to Symmetric Radiation Heating," J. Am. Ceram. Soc., 63 [1-2] 21-25 (1980).

F. A. Hummel, "Ceramic Materials for Thermal Shock Resistance," Ceramic Industry, 65 [6] 84-86 (1955).

J. C. Jaeger, "On Thermal Stresses in Circular Cylinders," Phil. Mag., 36 [7] 419-28 (1945).

C. F. Johnson and D. L. Hartsock, "Thermal Response of Ceramic Turbine Stators" in Ceramics for High Performance Applications, Eds. J. J. Burke, A. E. Gorum and R. N. Katz, Brook Hill Publishing Co., Chestnut Hill, MA., 1974.

C. H. Kent, "Thermal Stresses in Thin-Walled Cylinders," Trans. ASME, 53, 161-80 (1931).

C. Y. King and W. W. Webb,"Internal Fracture of Glass Under Triaxial Tension Induced by Thermal Shock", J. App. Phys., 42 [6] 2386-95 (1971).

H. P. Kirchner, R. M. Gruver and R. E. Walker, "Strengthening Alumina by Glazing and Quenching," Bull. Am. Ceram. Soc., 47 [9] 798-802 (1968).

H. P. Kirchner, R. E. Walker and D. R. Platts, "Strengthening Alumina by Quenching in Various Media," J. Appl. Phys., 42 [10] 3685-92 (1971).

H. P. Kirchner, R. M. Gruver and R. E. Walker, "Strengthening of Hot-Pressed Al_2O_3 by Quenching," J. Am. Ceram. Soc., 56 [1] 17-21 (1973).

D. A. Krohn, D. R. Larson and D. P. H. Hasselman, "Comparison of Thermal-Stress Resistance of Polycrystalline Al_2O_3 and BeO," J. Am. Ceram. Soc., 56 [9] 490-91 (1973).

D. R. Larson, J. A. Coppola and D. P. H. Hasselman, "Fracture Toughness and Spalling Behavior of High-Al_2O_3 Refractories," J. Am. Ceram. Soc., 57 [10] 417-21 (1974).

D. R. Larson and D. P. H. Hasselman, "Comparative Spalling Behavior of High-Alumina Refractories Subjected to Sudden Heating and Cooling," J. Am. Ceram. Soc., 74 [2] 59-65 (1975).

Y. W. Mai and A. G. Atkins, "Fracture Strength Behavior of Tool Carbides Subjected to Thermal Shock," J. Am. Ceram. Soc., 54 [6] 593 (1975).

Y. W. Mai, "Thermal Shock Resistance and Fracture Strength Behavior of Two Tool Carbides," J. Am. Ceram. Soc., 59 [11-12] 491-94 (1976).

J. J. Mecholosky, P. F. Becher, R. W. Rice, J. R. Spann and S. W. Freiman, "Laser Induced Thermal Stresses in Brittle Materials," Proc. Intl. Conf. on Thermal Stresses in Materials and Structures in Severe Thermal Environments, eds. D. P. H. Hasselman and R. Heller, Plenum, New York (in press, 1980).

H. Poritsky and F. A. Fend, "Relief of Thermal Stresses Through Creep," Trans. ASME, J. Appl. Mech., 25 [4] 589-97 (1958).

G. D. Quinn, R. N. Katz and E. M. Lenoe, "Thermal Cycling Effects, Stress Rupture and Tensile Creep in Hot-Pressed Silicon Nitride," 3rd Conf. Gas Turbine Matl's in Marine Environments, Castine, Maine, 1977.

S. Sato, H. Awaji, Y. Imamura, K. Kawamata and T. Oku, "Determination of the Thermal Shock Fracture Toughness of Reactor Graphite Subjected to Neutron Irradiation at High Temperature," Proc. Intl. Conf. on Thermal Stresses in Materials and Structures in Severe Thermal Environments, eds. D. P. H. Hasselman and R. Heller, Plenum, New York, (in press, 1980).

S. G. Schwille, R. A. Taxzilli and S. Musikant, "Thermal Stress Testing of Advanced Optical Ceramics by a Laser Technique," Proc. Intl. Conf. on Thermal Stresses in Materials and Structures in Severe Thermal Environments, eds. D. P. H. Hasselman and R. Heller, Plenum, New York, (in press, 1980)

J. Selsing, "Internal Stresses in Ceramics," J. Am. Ceram. Soc., 44 [8] 419 (1961).

L. A. Shapovalov in Thermal Stability of Plates and Shells, ed. Ya. B. Fridman Consultants Bureau, New York, 1964.

J. P. Singh, J. R. Thomas, Jr., and D. P. H. Hasselman, "Thermal Stresses in Partially Absorbing Flat Plate Symmetrically Heated by Thermal Radiation and Cooled by Convection," J. Thermal Stresses (in press, 1980)a.

J. P. Singh, K. Satyamurthy, J. R. Thomas, Jr., and D. P. H. Hasselman," Analysis of Thermal Stress Resistance of Partially Absorbing Ceramic Plate Subjected to Assymmetric Radiation, II: Convective Cooling at Front Surface", J. Am. Ceram. Soc., (in review, 1980)b.

D. Stahn and F. Kerkhof, "Danger of Thermal Stress Fracture of Glass Plates," Glastechnische Bezichte 50 [6] 121-28 (1977)a.

D. Stahn, "Thermal Stresses in Large Glass Plates," Glastechnische Berichte, 50 [7] 149-58 (1977)b.

D. Stahn and V. Seidelmann, "Thermal Stresses in Glass Plates with Special Respect to Tinted Glazing," Proc. Intl. Conf. on Thermal Stresses in Materials and Structures in Severe Thermal Environments, eds. D. P. H. Hasselman and R. Heller, Plenum, New York (in press, 1980).

H. S. Starrett, "Probable Values for the Mechanical and Thermal Properties of 994-2 Graphite," Air Force Materials Laboratory, Technical Report AFML-TR-76-117, February 1977.

Morris Stern, "The Numerical Calculation of Thermally Induced Stress Intensity Factors," J. Elasticity, 9 [1] 91-95 (1979).

T. R. Tauchert, "Thermal Stresses at Spherical Inclusions in Uniform Heat Flow," J. Compos. Mater., 2 [4] 478-86 (1968).

Thermal Stress Techniques in the Nuclear Industry, eds. Z. Zudans, T. C. Yen and W. H. Steigelmann, American Elsevier Publishing Company, New York, 1965.

J. R. Thomas, Jr., J. P. Singh and D. P. H. Hasselman, "Analysis of Thermal Stress Resistance of Partially Absorbing Ceramic Plate Subjected to Assymmetric Radiation, I: Convective Cooling at Rear Surface," J. Am. Ceram. Soc., (in press, 1980).

S. Timoshenko and J. N. Goodier, Theory of Elasticity, McGraw-Hill Book Company, New York, 1951.

S. P. Timoshenko and J. M. Gere, Theory of Elastic Stability, McGraw-Hill Book Company, Inc., New York, 1961.

W. Weibull, "Statistical Distribution Function of Wide Applicability," J. Appl. Mech., 18 [3] 293-97 (1951).